Plasmids

A FLAG epitope-tagged paxillin construct was generated by amplifying the coding sequence of human paxillin by PCR using the primers 5′-CGTACCTCGAGGCCATGGACGA CCTCGACGC-3′ and 5′-GGAATTCATTTGTCGTCGTC GTCCTTGTAGTCGCAGAAGAGCTTGAGGAAGC-3′. This resulted in a fragment with an *Xho*I site (underlined), a sequence encoding the FLAG epitope (DYKDDDDK), followed by a termination codon and an *Eco*RI site (underlined). This fragment was then digested with *Xho*I and *Eco*RI sequentially, and ligated into the mammalian expression vector pcDNA3.1(−)/ Myc-His B (Invitrogen).

GFP-paxillin is a kind gift from Dr Y Sawada (Department of Biological Sciences, Columbia University). Phenylalanine mutant at Tyr 31 and Tyr 118 was generated by amplifying GFP-paxillin with following primers. 5′-CGGCCTGTGT TCTTAAGCGAGGAGACCCCCTTCTCATACCCAAC-3′ and 5′-GTTGGGTATGAGAAGGGGGTCTCCTCGCTTA AGAACACAGGCCG-3′ were used for Tyr 31, and 5′-CCGTGCTCTAGAGTGGGAGAGGAGGAGCACGTGT TCAGCTTCCC-3′ and 5′-GGGAAGCTGAACACTGTC TCCTCCTCTCCCACTCTAGAGCACGG-3′ were used for Tyr 118.

A FLAG epitope-tagged Fyn construct was generated by amplifying the RT–PCR product of human colon cancer cell line, HCT116, by PCR using the primers 5′-GGATC CATGGGCTGTGTGCAATGTAAG-3′ and 5′-GTTAACT CACTTGTCGTCATCGTCCTTGTAGTCCAGGTTTTCA CCAGGTTG-3′. This PCR product was first inserted into pGEM-T Easy vector (Promega), followed by excision with *Eco*RI, and ligated into the mammalian expression vector pcDNA3.1(−)/Myc-His A (Invitrogen).

Cell culture and transfection

A human osteosarcoma cell line, HuO9, and its high-metastatic (M112, M132) and low-metastatic (L12, L13) sublines have been described previously (Nakano *et al*., 2003). Osteosarcoma cells were maintained in RPMI 1640 medium with 10% fetal bovine serum (FBS) at 37°C with 5% CO_2. Cos-7 cells were maintained in Dulbecco's modified Eagle's medium (DMEM) with 10% FBS at 37°C with 5% CO_2. Transfection was performed by using FuGENE 6 (Roche) according to the manufacturer's instruction. Selection of clones was performed by using geneticin (Sigma) at the concentration of 30 μg/ml.

Immunoblotting and immunoprecipitation

Before extracting cell lysates, osteosarcoma cells were cultured for at least 48 h to ensure complete cell adhesion to culture dishes unless otherwise indicated. Cells were lysed in 1% Triton X-100 buffer (50 mM HEPES, 150 mM NaCl, 10% glycerol, 1% Triton-X 100, 1.5 mM $MgCl_2$, 1 mM EGTA, 100 mM NaF, 1 mM Na_3VO_4, 10 μg/ml aprotinin, 10 μg/ml leupeptin, 1 mM phenylmethylsulfonyl fluoride), and insoluble materials were removed by centrifugation. To investigate the effect of PP2 treatment, cells were treated with 10 μM of PP2 or 10 μM of PP3 for 30 min prior to harvesting cells.

Protein concentration was measured by BCA Protein Assay (PIERCE) and the protein aliquots were separated by SDS–PAGE. Gels were transferred to a polyvinylidene difluoride membrane (Millipore) and subjected to immunoblotting. After blocking in 5% skim milk/TBST (100 mM Tris-HCl pH 8.0, 150 mM NaCl, 0.05% Tween 20) for 1 h, blots were incubated with appropriate primary antibodies. In case of 4G10 stain, blocking was performed with 5% bovine serum albumin (BSA) which was used instead of skim milk. Blots were then washed three times with TBST, incubated with HRP-conjugated secondary antibodies for 30 min, washed twice by TBST and twice with TBS (100 mM Tris-HCl pH 8.0, 150 mM NaCl), and visualized by autoradiography using chemiluminescence reagent (Western Lighting, Perkin Elmer).

The images were captured by molecular imager GS800 (BIO-RAD) and the density of each smear was quantified by Quantity One (BIO-RAD).

For immunoprecipitation, aliquots of protein were mixed with appropriate antibodies and incubated for 1 h on ice. Then, samples were rotated with protein A- or protein G-sepharose beads (Amersham Pharmacia) for 2–12 h at 4°C. After the beads were washed four times with 1% Triton-X 100 buffer, the samples were boiled in sample buffer (0.1 M Tris-HCl pH 6.8, 2% SDS, 0.1 M dithiothreitol, 10% glycerol, 0.01% bromophenol blue) for 5 min and analysed by SDS–PAGE.

Immunocytochemistry

Cells were grown on 12-mm circle cover glasses (Fisher) in 24-well plates, washed three times with phosphate-buffered saline (PBS), fixed with 4% paraformaldehyde/0.1 M phosphate buffer for 5 min at room temperature, washed once with PBS, and permeabilized with 0.2% Triton-X 100 in PBS for 10 min. After another washing step with PBS and blocking in 5% goat serum and 3% BSA/TBST for 30 min, cells were incubated with anti-paxillin antibody (1 : 2000) and anti-phospho-paxillin antibody (1 : 250) in 5% goat serum and 3% BSA/TBST for 1 h at room temperature. Cells were washed three times with PBS and incubated with appropriate second antibodies (Molecular Probe) (1 : 2000) in 5% goat serum and 3% BSA/TBST. When actin was stained with phalloidin, Alexa Fluor phalloidin was combined with second antibody at the concentration of 1 U/ml.

After cells were washed three times with PBS, cover glasses were mounted in 1.25% DABCO, 50% PBS, 50% glycerol and visualized using a Radiance 2100 confocal microscopic system (BIO-RAD).

In vitro *kinase assay*

For kinase assay, fresh cell lysate was prepared and mixed with the antibody of interest for 1 h on ice. Then, samples were rotated with protein A-sepharose or protein G-sepharose for 1 h at 4°C. The beads were consequently washed with 1% Triton-X 100 buffer and kinase buffer (50 mM Tris HCl, pH 7.4, 50 mM NaCl, 10 mM $MgCl_2$, 10 mM $MnCl_2$) three times, respectively. Kinase reaction was performed in 30 μl of kinase buffer with 10 μg of synthetic polypeptides poly[Glu-Tyr](4 : 1) (Sigma) as exogenous substrate and 5 μCi of [γ-32P]ATP (ICN) at room temperature for 1 h. Kinase reaction was stopped by the addition of SDS–PAGE sample buffer (0.1 M Tris-HCl pH 6.8, 2% SDS, 0.1 M dithiothreitol, 10% glycerol, 0.01% bromophenol blue). The samples were boiled for 5 min and analysed by SDS–PAGE using 8% polyacrylamide gel. The gels were then dried and exposed to autoradiography. The images were captured by molecular imager GS800 (BIO-RAD) and the density of each smear (area shown by a bracket) was quantified by Quantity One (BIO-RAD).

Cell migration assay

Cell migration assay was performed by using Cell Culture Insert with 8.0 μm pore size PET filter (Becton Dickinson). Prior to the assay, the lower surface of the filter was immersed for 30 min in 10 μg/ml fibronectin (Sigma) diluted with PBS. Next, 700 μl of RPMI 1640 medium with 10% FCS was added to the lower chamber. Then, 5×10^4 cells were suspended in 300 μl of RPMI 1640 medium with 10% FCS and added to the upper chamber.

After incubation for 24 h at 37°C in a humid 5% CO_2 atmosphere, the cells on the upper surface of the filter were completely removed by wiping with cotton swabs. The cells on the lower surface of the filter were fixed in methanol for 30 min, washed with PBS, and then stained with Giemsa's stain solution (Muto Pure Chemicals Co. Ltd.) for 30 s. After washing three times with PBS, the filters were mounted on a glass slide. The cells on the lower surface were counted from photographs taken of at least five fields at a magnification of ×200 under the microscope. Student's *t*-test was used to analyse data from these experiments. To investigate the effect of PP2 treatment, cells were allowed to migrate in the presence of 10 μM of PP2 or 10 μM of PP3.

RNAi analysis

siRNA of human paxillin and $p130^{Cas}$ was generated using BLOCK-iT RNAi TOPO Transcription Kit and BLOCK-iT Complete Dicer RNAi Kit (Invitrogen) according to the manufacturer's instructions. In the generation of siRNA for paxillin, 936 bp from the initiation codon of human paxillin were chosen as the target sequence, and amplified by PCR using the primers, 5′-ATGGACGACCTCGACGCC-3′ and 5′-GTTCAGGTCAGACTGCAGGC-3′. As for $p130^{Cas}$, 866 bp was chosen as the target sequence, and amplified with the primers, 5′-ACACCATGAACCACCTGAACGTG-3′ and 5′-ATACACCTCCAGCAACGGGT-3′.

siRNA of LacZ was generated in the same procedure as paxillin siRNA, and was used as a negative control. Transfection was performed with Lipofectamine 2000 (Invitrogen) and the effect was analysed 72 h after the transfection.

Abbreviations

BSA, bovine serum albumin; Cas, Crk-associated substrate; FAK, focal adhesion kinase; FBS, fetal bovine serum; PBS, phosphate-buffered saline; PP2, 4-amino-5-(4-chlorophenyl)-7-(t-butyl)pyrazolo[3,4-d]pyrimidine; PP3, 4-amino-7-phenylpyrazol [3,4-d]pyrimidine; RNAi, RNA interference; SH2, Src homology 2 domain; siRNA, short interfering RNA.

Acknowledgements

We are grateful to Dr Y Sawada (Department of Biological Sciences, Columbia University) for donating paxillin cDNA. KA is an awardee of the Research Resident Fellowship from the Foundation for Promoting of Cancer Research (Japan) for the 3rd Term Comprehensive 10-Year-Strategy for Cancer Control. This study was supported by the Program for Promotion of Fundamental Studies in Health Science of Pharmaceuticals and Medical Devices Agency (PMDA).

References

Batanian JR, Cavalli LR, Aldosari NM, Ma E, Sotelo-Avila C, Ramos MB, Rone JD, Thorpe CM and Haddad BR. (2002). *Mol. Pathol.*, **55**, 389–393.

Burnham MR, Bruce-Staskal PJ, Harte MT, Weidow CL, Ma A, Weed SA and Bouton AH. (2000). *Mol. Cell. Biol.*, **20**, 5865–5878.

Burridge K, Turner CE and Romer LH. (1992). *J. Cell. Biol.*, **119**, 893–903.

Huang J, Asawa T, Takato T and Sakai R. (2003). *J. Biol. Chem.*, **278**, 48367–48376.

Huth JF and Eilber FR. (1989). *Arch. Surg.*, **124**, 122–126.

Iwaya K, Ogawa H, Kuroda M, Izumi M, Ishida T and Mukai K. (2003). *Clin. Exp. Metast.*, **20**, 525–529.

Khanna C, Khan J, Nguyen P, Prehn J, Caylor J, Yeung C, Trepel J, Meltzer P and Helman L. (2001). *Cancer Res.*, **61**, 3750–3759.

Khanna C, Wan X, Bose S, Cassaday R, Olomu O, Mendoza A, Yeung C, Gorlick R, Hewitt SM and Helman LJ. (2004). *Nat. Med.*, **10**, 182–186.

Kimura K, Nakano T, Park YB, Tani M, Tsuda H, Beppu Y, Moriya H and Yokota J. (2002). *Clin. Exp. Metast.*, **19**, 477–485.

Kiyokawa E, Hashimoto Y, Kobayashi S, Sugimura H, Kurata T and Matsuda M. (1998). *Genes Dev.*, **12**, 3331–3336.

Klinghoffer RA, Sachsenmaier C, Cooper JA and Soriano P. (1999). *EMBO J.*, **18**, 2459–2471.

Lau CC, Harris CP, Lu XY, Perlaky L, Gogineni S, Chintagumpala M, Hicks J, Johnson ME, Davino NA, Huvos AG, Meyers PA, Healy JH, Görlick R and Rao PH. (2004). *Genes Chromosomes Cancer*, **39**, 11–21.

Lewis JM and Schwartz MA. (1998). *J. Biol. Chem.*, **273**, 14225–14230.

Marchetti D, Parikh N, Sudol M and Gallick GE. (1998). *Oncogene*, **16**, 3253–3260.

Meyers PA, Heller G, Healey JH, Huvos A, Applewhite A, Sun M and LaQuaglia M. (1993). *J. Clin. Oncol.*, **11**, 449–453.

Nakamoto T, Sakai R, Ozawa K, Yazaki Y and Hirai H. (1996). *J. Biol. Chem.*, **271**, 8959–8965.

Nakano T, Tani M, Ishibashi Y, Kimura K, Park YB, Imaizumi N, Tsuda H, Aoyagi K, Sasaki H, Ohwada S and Yokota J. (2003). *Clin. Exp. Metast.*, **20**, 665–674.

Pawson T. (2004). *Cell*, **116**, 191–203.

Petit V, Boyer B, Lentz D, Turner CE, Thiery JP and Valles AM. (2000). *J. Cell. Biol.*, **148**, 957–970.

Sakai R, Iwamatsu A, Hirano N, Ogawa S, Tanaka T, Mano H, Yazaki Y and Hirai H. (1994). *EMBO J.*, **13**, 3748–3756.

Schaller MD. (2001). *Oncogene*, **20**, 6459–6472.

Schaller MD, Hildebrand JD, Shannon JD, Fox JW, Vines RR and Parsons JT. (1994). *Mol. Cell. Biol.*, **14**, 1680–1688.

Schaller MD and Parsons JT. (1995). *Mol. Cell. Biol.*, **15**, 2635–2645.

Schlaepfer DD, Broome MA and Hunter T. (1997). *Mol. Cell. Biol.*, **17**, 1702–1713.

Squire JA, Pei J, Marrano P, Beheshti B, Bayani J, Lim G, Moldovan L and Zielenska M. (2003). *Genes Chromosomes Cancer*, **38**, 215–225.

Talamonti MS, Roh MS, Curley SA and Gallick GE. (1993). *J. Clin. Invest.*, **91**, 53–60.
Tsubouchi A, Sakakura J, Yagi R, Mazaki Y, Schaefer E, Yano H and Sabe H. (2002). *J. Cell. Biol.*, **159**, 673–683.
Tsuchiya H, Kanazawa Y, Abdel-Wanis ME, Asada N, Abe S, Isu K, Sugita T and Tomita K. (2002). *J. Clin. Oncol.*, **20**, 3470–3477.
Turner CE. (2000). *Nat. Cell. Biol.*, **2**, E231–E236.
Ward WG, Mikaelian K, Dorey F, Mirra JM, Sassoon A, Holmes EC, Eilber FR and Eckardt JJ. (1994). *J. Clin. Oncol.*, **12**, 1849–1858.
Yano H, Uchida H, Iwasaki T, Mukai M, Akedo H, Nakamura K, Hashimoto S and Sabe H. (2000). *Proc. Natl. Acad. Sci. USA*, **97**, 9076–9081.
Yeatman TJ. (2004). *Nat. Rev. Cancer*, **4**, 470–480.

Supplementary Information accompanies the paper on Oncogene website (http://www.nature.com/onc)

Available online at www.sciencedirect.com
SCIENCE DIRECT®
ELSEVIER
Biochemical and Biophysical Research Communications 339 (2006) 99–106
BBRC
www.elsevier.com/locate/ybbrc

Identification of novel steroid target genes through the combination of bioinformatics and functional analysis of hormone response elements

Kuniko Horie-Inoue [a], Kenichi Takayama [a,b], Hidemasa U. Bono [c], Yasuyoshi Ouchi [b], Yasushi Okazaki [c], Satoshi Inoue [a,b,*]

[a] *Division of Gene Regulation and Signal Transduction, Research Center for Genomic Medicine, Saitama Medical School, 1397-1 Yamane, Hidaka-shi, Saitama 350-1241, Japan*
[b] *Department of Geriatric Medicine, Graduate School of Medicine, The University of Tokyo, 7-3-1 Hongo, Bunkyo-ku, Tokyo 113-8655, Japan*
[c] *Division of Functional Genomics and Systems Medicine, Research Center for Genomic Medicine, Saitama Medical School, 1397-1 Yamane, Hidaka-shi, Saitama 350-1241, Japan*

Received 18 October 2005
Available online 8 November 2005

Abstract

Steroid hormone receptors including androgen receptor (AR), glucocorticoid receptor (GR), progesterone receptor (PR), and mineralocorticoid receptor (MR) recognize and bind to identical consensus hormone response elements (HREs), which consist of two hexameric half-sites (5′-AGAACA-3′) arranged as inverted repeats with a 3-bp spacer. Although only a few near-consensus HRE sequences have been identified in the transcriptional regulatory regions of known steroid target genes, it has been unclear whether the exact consensus sequences function as bona fide HREs in vivo. A genome-wide in silico screening of palindromic HREs identified 565 exact consensus sequences in human genome (NCBI 35 assembly). In this study, of 565 exact consensus elements, functional in vivo receptor binding was evaluated regarding 26 sequences located within 10 kb upstream to the 5′ end of annotated genes through chromatin immunoprecipitation (ChIP) assay using cells endogenously expressing steroid hormone receptors. Hormone responsiveness of proximal gene expression was examined through quantitative RT-PCR. As far as performing ChIP assay for AR, GR, and PR, 14 of 26 elements significantly recruited at least one of the receptors by hormone treatment (>2-fold enrichment versus vehicle). In terms of gene expression in the vicinity of the above 14 functional perfect HREs, four genes were upregulated by >2-fold with hormone treatment. The present data suggest that the combination of bioinformatics analysis and quantitative experimental evaluation is useful to identify novel functional HREs that may contribute to the transcriptional regulation of steroid target genes.

Keywords: Androgen receptor; Progesterone receptor; Glucocorticoid receptor; Steroid target gene; Hormone response element; Chromatin immunoprecipitation; Quantitative PCR; Transcriptional start site

Steroid hormone receptors are nuclear receptors that play essential roles in various physiological and pathophysiological states. Forming complexes with coactivators and general transcription factors, ligand-stimulated steroid hormone receptors including androgen receptor (AR), glucocorticoid receptor (GR), progesterone receptor (PR), and mineralocortitoid receptor (MR) recognize and bind to hormone response elements (HREs) in the regulatory regions of various hormone responsive genes, leading to the modulation of target gene transcription [1]. Despite the degeneracy of the nucleotide sequence of the HREs, steroid hormone receptors generate distinct hormone-specific responses. The palindromic 15-bp sequence (5′-AGAACA*nnn*TGTTCT-3′) that contains inverted repeats with a 3-bp spacer (IR3 sequence) has been identified as the consensus sequence for HRE [2], though only a few perfect consensus HREs have yet been identified in the regulatory regions of known hormone responsive genes. A question that continues to engage the steroid receptor field is

* Corresponding author. Fax: +81 42 985 7209.
E-mail address: s_inoue@saitama-med.ac.jp (S. Inoue).

0006-291X/$ - see front matter © 2005 Elsevier Inc. All rights reserved.
doi:10.1016/j.bbrc.2005.10.188

whether perfect HRE sequences function as hormone receptor binding sites in vivo, which regulate the transcription of steroid target genes.

Previously, we have identified perfect ARE sequences of IR3 type in silico in the human genome and characterized AR-binding ability of perfect AREs on chromosome X [3]. More than one-third of perfect ARE sequences (8 of 21) recruited more ARs compared with the proximal promoter region of prostate-specific antigen (PSA) containing a functional ARE. In the present study, we extend our study to a question whether perfect HRE sequences in silico situated in the proximal upstream regions of annotated genes function as bona fide functional binding sites for steroid hormone receptors in human cells derived from different tissues. Our combined approach of bioinformatics and experimental validation identified several perfect HRE sequences that could bind to steroid hormone receptors and some proximal downstream genes that were responsive to hormone treatment in the vicinity of the perfect HREs.

Materials and methods

Bioinformatics. Consensus HREs in the human genome (Ensembl version 34 based on the NCBI 35 assembly retrieved from Ensembl ftp site [4]) were screened by a 'pipeline' computational system called SayaMatcher [5], which utilizes in-house Perl script and a program for regular expression search of a nucleotide sequence (program name: dreg) in EMBOSS package [6]. The regular expression pattern for HRE was obtained from a recent literature by Nelson et al. [7], in which the palindromic 5′-AGAACAnnnTGTTCT-3′ sequence corresponding to the ARE sequence in TRANSFAC database [8] was used as a consensus sequence.

Cell culture. Human prostate cancer LNCaP cells and DU145 cells, breast cancer T47D cells, and osteosarcoma SaOS2 cells were purchased from American Type Culture Collection (Rockville, MD). LNCaP cells were maintained in RPMI 1640 supplemented with 4.5 g/dl glucose, 1 mM sodium pyruvate, 10 mM Hepes, and 10% fetal bovine serum (FBS). Other cells were maintained in DMEM supplemented with 10% fetal bovine serum (FBS). Prior to hormone addition, cells were cultured for 2 days in phenol red-free RPMI 1640 or DMEM supplemented with 5% dextran-charcoal stripped FBS (dcc-FBS) and 1 day in phenol red-free medium supplemented with 2.5% dcc-FBS.

Chromatin immunoprecipitation assay. Chromatin immunoprecipitation (ChIP) assay was performed as described previously [3]. LNCaP cells, T47D cells, and DU145 cells as well as SaOS2 cells after 72-h hormone depletion were treated with 10 nM R1881 (NEN Life Science Products, Boston, MA), progesterone (Sigma), or dexamethasone (Sigma), respectively, for indicated times. Control cells were treated with 0.1% ethanol as a vehicle. Cells were fixed in 1% formaldehyde for 5 min at room temperature. Chromatin was sheared to an average size of 500 bp by sonication using a Bioruptor ultrasonicator (Cosmo-Bio, Tokyo, Japan). Lysates corresponding to 2×10^7 cells were rotated at 4 °C for overnight with 3 μg of polyclonal antibodies against AR (H-280, Santa Cruz Biotechnology, Santa Cruz, CA), PR (H-190, Santa Cruz Biotechnology), or GR (H-300, Santa Cruz Biotechnology). Salmon sperm DNA/protein A–agarose (Upstate Biotechnology, Lake Placid, NY) was added and incubated for 1 h. Washing and reversal of cross-links was performed as described [9]. Precipitated DNA fragments were quantified by quantitative real-time PCR using the Applied Biosystems 7000 sequence detector (Foster City, CA) based on SYBR Green I fluorescence. Primer pairs were designed by Primer Express ver. 2.0 software (Applied Biosystems), generating perfect ARE-containing fragments with the requirements of primer T_m temperature at basically 58–60 °C and the requirements of amplicon length for 50–150 bp. The protocol of PCR was 2 min at 50 °C, 10 min at 95 °C, and 40 cycles of 15 s at 95 °C and 1 min at 60 °C. To determine relative differences among the treatment groups for the ChIP assays, we used the $\Delta\Delta C_T$ method as outlined in the Applied Biosystems protocol for reverse transcriptase-PCR (http://www.appliedbiosystems.com/). The threshold cycle C_T was defined as the cycle at which the fluorescence signal was statistically significant over background. The reciprocal of 2^{C_T} (used C_T as an exponent for the base 2) for each target element was normalized by that for an external control of the genomic fragment GAPDH and subsequently normalized by input DNAs obtained from either steroid or vehicle-treated cells. Fold enrichment in steroid-treated cells was obtained through the division by the values in vehicle-treated cells. Genomic fragments containing proximal or distal ARE in the promoter region of prostate-specific antigen (PSA) [−250 to −39 bp and −4170 to −3978 bp from the transcriptional initiation site (TSS), respectively] [3,9] were used as positive controls for AR binding. The proximal promoter region of α subunit of amiloride-sensitive epithelial sodium channel (ENaCα) (−867 to −761 bp from the TSS, containing the GRE sequence as previously described [10]) was used as a positive control for GR binding. We also used a genomic fragment on the intron 1 of FK506 binding protein 51 (FKBP51) (+359 to +426 bp from the TSS of the long isoform ENST00000357266) as a positive control for GR and PR binding, which was newly identified in our ChIP assay scanning the gene regulatory region of FKBP51. The quality of precipitated DNA was analyzed by PCR amplification of positive controls and 8% polyacrylamide electrophoresis prior to quantitative analyses and the batches of ChIP samples with maximal responses were selected for quantitative PCR. The sequences of the primers used in ChIP assays (synthesized by Sigma Genosys, Japan) are described in Table 1.

Quantitative reverse transcription-PCR. Total RNA was extracted from hormone-treated or 0.1% ethanol-treated cells for indicated times using ISOGEN reagent (Nippon Gene, Tokyo, Japan). First strand cDNA was generated from RNase-free DNase I-treated total RNA by using SuperScript II Reverse Transcriptase (Invitrogen, Carlsbad, CA) and pdT_{12-18} primer (Amersham Biosciences, Piscataway, NJ). Hormone responsiveness of the proximal genes located downstream to the 26 perfect HRE sequences was analyzed by quantitative reverse transcription-PCR (RT-PCR) using the Applied Biosystems 7000 sequence detector based on SYBR Green I fluorescence. Primer design and PCR protocol were as described above. The evaluation of relative differences of PCR product amounts among the treatment groups was carried out using the $\Delta\Delta C_T$ method. The reciprocal of 2^{C_T} (used C_T as an exponent for the base 2) for each target gene was normalized by that for GAPDH coding region, followed by the comparison with the relative value in vehicle-treated cells. PSA was served as a positive control for androgen responsiveness, while FKBP51 was used for both progesterone and glucocorticoid responsiveness. ENaCα was another positive control for the glucocorticoid response and the progesterone-dependent change of ENaCα mRNA level was also evaluated. The primer sequences for the amplifications are described in Table 2.

Results

In silico identification of perfect palindromic HRE sequences in the human genome

In terms of palindromic HRE sequences composed of two AGAACA sequences separated by a 3-bp spacer, only a few near-consensus sequences have been identified in the vicinity of human genes that are responsive to steroid hormones including androgen, progesterone, glucocorticoid, and mineralocorticoid. In order to answer the question of whether perfect palindromic HRE sequences do function as in vivo binding sites for steroid hormone receptors, we computationally searched for all the consensus HRE sequences in the human genome utilizing in-house Perl script and a program for regular expression pattern search of a nucleotide sequence in the EMBOSS package (program name: dreg) as previously described [3,5]. The screening defined 563 sequences on the NCBI 34 assembly of the human genome [3] and additional two sites on the NCBI 35 assembly. The two new sequences were located on chromosomes 1 and 14. The number of HRE sites was larger than the expected frequency in random DNA sequences as calculated by the total number of base pairs in the genome devided by the frequency of a sequence with specific base pairs at 12 positions ($3272\ \text{Mb}/4^{12} = 195$). The distribution of consensus sequences among the chromosomes is generally consistent with chromosomal size [3]. The highest frequency of HRE was 28.0 sites per 100 Mb on chromosome 8 and the lowest frequency was 6.9 sites per 100 Mb on chromosome Y, the average being 17.4 ± 4.4 sites per 100 Mb.

Table 1
Primers for quantitative ChIP assay

Target	Forward primer	Reverse primer
HRE sites		
HRE1	5′-CCAAATATGTCCATTCATCCAACA-3′	5′-GGAAACATACGCATTGCCTAGAA-3′
HRE2	5′-CCAACAAACACTAGCAGAACATTATG-3′	5′-AGAGGGCATCTGAACAATAGAAGA-3′
HRE3	5′-CAAGGCCTGGGGACATTTAA-3′	5′-CGAAGCTGCTGGGAGGTATC-3′
HRE4	5′-TCAAAGGTGGTGCTTATCAT-3′	5′-GAACTGAGTTCCAGGAAATATG-3′
HRE5	5′-AAGGGAAAAGATCTCATATTGCA-3′	5′-CACGGCAATTTTAATACTCATCA-3′
HRE6	5′-GACCATACCTTGGTATGACCCCTT-3′	5′-TCTGTGGTTATCCTGCAAGTCAGT-3′
HRE7	5′-AAGAAACCATTTTGAAATGTGCC-3′	5′-CAGGTCAGTTAGGCTCTGATAAAACC-3′
HRE8	5′-TACTTACCCAGTGCTTCCCAATC-3′	5′-GAGCACCTGAGGTGTTTTTTTT-3′
HRE9	5′-AGCGAGACTCCGTCTTAAA-3′	5′-GGAGGAGTTACTGTTACAATTAT-3′
HRE10	5′-ACACTGTGGTGGGCAGGATT-3′	5′-GCTCAAACAAACAGGCTAAGACA-3′
HRE11	5′-TGTCCTTCTGAAGACTTCCATTCC-3′	5′-TACAGGCACACACCACCAGATTG-3′
HRE12	5′-CTTGCAGTGAGCCGAGATC-3′	5′-TTCTGGAGGAGTTACTGTTACAATTA-3′
HRE13	5′-CCTGCTCTTTGATTTTCGTAAGA-3′	5′-TGAAGCCAAATGCTGAAGTG-3′
HRE14	5′-TTGACAGTATATTTAGAGCGTGTTATCT-3′	5′-GTTAATTCTCTTTCCCTATGGTAGAAT-3′
HRE15	5′-TGTGCAAGAAATGCCATCCT-3′	5′-CATCATAGCTGCATGGGTGTT-3′
HRE16	5′-TGAAAATAATTTCACTTATCCTTTAAGC-3′	5′-AATGACTTGCTGACCAAATCC-3′
HRE17	5′-GGCCTATTTTAATCAGCATTTCAGA-3′	5′-ATCCTCATTCCTACCCAGCATCT-3′
HRE18	5′-ACATCAGTGGCTCTTAAGCACTG-3′	5′-CAGAGAGAATAAAAAAACTAGCCCAAA-3′
HRE19	5′-AATGCTGCTCAAAGAAATCAGA-3′	5′-TTTAATTCCAAATGCATTTTAGAAC-3′
HRE20	5′-CTCCATGTTTGAGGCGGAGA-3′	5′-CATCCCACTTTGTGCGTAACTTT-3′
HRE21	5′-CTCCAGGGCTGTACTGGTATCTG-3′	5′-CAGGTGTGGGCCCTCTGT-3′
HRE22	5′-TCTTAAGCAAAAGGCCAACAA-3′	5′-TCTATCATTACAAGAAAAGTTGGTTATCTG-3′
HRE23	5′-GCCAGCACTCACGTGGCTAT-3′	5′-CTGCGGTGCCGTGACA-3′
HRE24	5′-TGTACACACAAAAACTGCTAGAACACTCT-3′	5′-GCTCAGCCATGGGTTGGT-3′
HRE25	5′-GGGAGCTGGCTAGAACACTCA-3′	5′-CATGCTGGGCTAAAGCAGAAC-3′
HRE26	5′-TGTGTGCTCAAAGAGTAGATTGG-3′	5′-TCATCACTTATTGCCTGAACTATCA-3′
FKBP51 intron 1	5′-TGCAAGAGCGGTTGATCTG-3′	5′-GCGAGAACAGCCTGACTCA-3′
ENaCα promoter	5′-CCTCTGGTTGCCCACATTC-3′	5′-GGGCCCTAGGACATTCTGTT-3′
PSA proximal promoter	5′-TCTGCCTTTGTCCCCTAGAT-3′	5′-AACCTTCATTCCCCAGGACT-3′
PSA distal promoter	5′-ACAGACCTACTCTGGAGGAAC-3′	5′-AAGACAGCAACACCTTTTT-3′

To investigate whether the computationally identified perfect HRE sequences located in the canonical proximal promoters of annotated genes particularly function as steroid hormone receptor binding sites, we selected perfect HREs lying within 10 kb upstream to the transcriptional start sites (TSSs) of known human genes on the Ensembl Genome Browser [4]. We obtained 26 of 565 perfect HRE sequences (4.6%) in the proximal promoter regions of annotated genes (Table 3). The distribution of 26 perfect HREs in the proximal promoter elements was limited to 14 of 24 chromosomes and rather independent of chromosomal size. The longest chromosome 1 contained 5 sequences, while 4 sequences were found in both chromosomes 6 and 11.

Perfect HREs located in the proximal upstream regions of annotated genes

In vivo recruitment of steroid hormone receptors to perfect HREs located 5′ to annotated genes

To assess whether these perfect HREs situated within 10 kb of the 5′ ends of known genes (5′ HREs) do recruit steroid hormone receptors in vivo, we performed ChIP assay in human cells endogenously expressing receptors. Hormone-depleted cells were treated for 24 h (also 2 h in T47D cells) with either 10 nM of steroids or 0.1% ethanol as a vehicle, cross-linked by formaldehyde, sonicated, and immunoprecipitated by specific polyclonal antibodies against steroid receptors. LNCaP cells were treated with R1881 (or vehicle) and immunoprecipitated by AR antibody; T47D cells were treated with progesterone and immunoprecipitated by PR antibody; and DU145 cells as well as SaOS cells were treated with dexamethasone and

Table 2
Primers for quantitative RT-PCR

Target	Adjacent HRE	Forward primer	Reverse primer
IQSEC2	HRE1	5′-ACATCACAGAACTTGAGGACTCCTT-3′	5′-AGGGCTTCGTCGATGGATTC-3′
MELL1	HRE2	5′-GAGATCACGCACGGCTTTG-3′	5′-CCAATCCATCATGTTGCCATT-3′
HS163_HUMAN	HRE3	5′-GATGGAGGCGGTGGTGTTC-3′	5′-GTAATTATGAAGTAGACCGAGAGGAAGAT-3′
DISP1	HRE4	5′-CATGGAGCTGGAAAGGAGTACAG-3′	5′-CACCACTGCCCTGATAGTATCATT-3′
EXTL2	HRE5	5′-AGGCAGCCACGTGTTCTATTG-3′	5′-TTAACGCAGCAAAACGATCACT-3′
NP_689710.1	HRE6	5′-GAGGGCAGTGGCGTGATC-3′	5′-CAGTAGAATGGCGTGAACTCAGA-3′
B3GALT3	HRE7	5′-TGCAGCCCATGGCTTTTC-3′	5′-GGCATGTGGTGTTCCTTAGCA-3′
SLC36A1	HRE8	5′-CGGAAGGCCTCAACAACCT-3′	5′-CCATGTTGTGCTATTGCTTTGAC-3′
DAXX	HRE9	5′-GCCCTTCACCACTGTCTTAGAGA-3′	5′-GAGACGCCTCCATTGAAGGA-3′
ULBP3	HRE10	5′-CGGACTGACCACCTTCTTCAA-3′	5′-TGCATCAGGAAGTCCCTAAGC-3′
KIF13A	HRE11	5′-GCTGCTATGGAGTTAGTATTACGAAAAC-3′	5′-CTTCAAACTCTGCGTGAAACTCTGT-3′
ZNF297	HRE12	5′-CCTCTCAAGGATGCGCTCTT-3′	5′-GGGAATTTCCACGGGAAGTC-3′
GIMAP5	HRE13	5′-CAGGTGAAAACAGGAACATGGA-3′	5′-GGCCTGTGACTCAAAGATGGA-3′
ZNF398	HRE14	5′-GAGCTTCCGCTACAAACAGACA-3′	5′-ACCCCCACAGCCTCCATT-3′
NP_055096.2	HRE15	5′-CAGTGACCTCTCTGCGTGACA-3′	5′-AACCCAGAGGAAACAAGGAACA-3′
Q9C0D7_HUMAN	HRE16	5′-CCAGCTGTCCTGGCGACTAC-3′	5′-AGTCGAGAGTCAGAGATGCTGTCTATT-3′
OR8D4	HRE17	5′-GCTTTTATCCTCACCAGCATCCT-3′	5′-GAGCTACAGGTGCTAAACGCTTT
ENSG00000182203	HRE18	5′-ACACCAACAGGATACACTGAAAGC-3′	5′-GCACATTTAACTTGCAGGTTTTTG-3′
ENSG00000185439	HRE19	5′-TGCCTTCATGGTGGACAATG-3′	5′-GGATGCTCGATGTCCAGGTT-3′
CV106_HUMAN	HRE20	5′-CACAATTTAACTTACGAACTTCCAACTC-3′	5′-GCCAACTGAGCTCTAGTTAATGTCTTG-3′
SRP14	HRE21	5′-GTTGTTGGAGAGCGAGCAGTT-3′	5′-CCGACGTCCGGCACTTC-3′
NP_874362.2	HRE22	5′-TGCAGCGACTTGTGGACATC-3′	5′-CGAATGCAGGGCAGTCAGA-3′
MVD	HRE23	5′-TGGCGGCAGTCACTTGTACA-3′	5′-CGCGCTTGCCCCAGTA-3′
ENSG00000189289	HRE24	5′-GCCTGCTCCACCCAGAGAA-3′	5′-AACAGGTTCCAGCAGCTCAGA-3′
NP_775751.1	HRE25	5′-CACCAAGTGCAGGACAGTCTTC-3′	5′-GGTGCTTTTCGTCCACAGTGA-3′
NP_689725.2	HRE26	5′-CTTTACTAGCAACACCTCCTTCCAT-3′	5′-TGCACCCGAAAGATTACAAACTT-3′
FKBP51 coding		5′-CTGCAGACGATGTGGCATTCACT-3′	5′-TCCAGAGCTTTGTCAATTCCAA-3′
ENaCα coding		5′-CGCATGAAGACGGCCTTCT-3′	5′-CGCATGAAGACGGCCTTCT-3′
PSA coding		5′-GCCCTGCCCGAAAGG-3′	5′-GATCCACTTCCGGTAATGCA-3′
GAPDH coding		5′-GGTGGTCTCCTCTGACTTCAACA-3′	5′-GTGGTCGTTGAGGGCAATG-3′

Table 3
Perfect HRE sites that locate upstream to annotated genes at a distance within 10 kb

HRE ID	Chr. location	Start position	Stop position	HRE sequence	Proximal gene	Ensembl ID	Distance (kb)
HRE1	Xp11.22	53237415	53237429	AGAACAttaTGTTCT	IQSEC2	ENSG00000124313	3.9
HRE2	1p36.32	2603985	2603999	AGAACAagcTGTTCT	MELL1	ENSG00000142606	7.4
HRE3	1q42.12	220841360	220841374	AGAACAgttTGTTCT	HS163_HUMAN	ENSG00000143771	9.9
HRE4	1q41	219495172	219495186	AGAACAgtaTGTTCT	DISP1	ENSG00000154309	9.4
HRE5	1p21.1	101079768	101079782	AGAACAtaaTGTTCT	EXTL2	ENSG00000162694	6.2
HRE6	1p36.11	25913162	25913176	AGAACAgctTGTTCT	NP_689710.1	ENSG00000177493	9.9
HRE7	3q26.1	162310806	162310820	AGAACAttcTGTTCT	B3GALT3	ENSG00000169255	5.0
HRE8	5q33.1	150798127	150798141	AGAACAggcTGTTCT	SLC36A1	ENSG00000123643	9.2
HRE9	6p21.32	33401650	33401664	AGAACAttcTGTTCT	DAXX	ENSG00000007565	3.0
HRE10	6q25.1	150487454	150487468	AGAACAataTGTTCT	ULBP3	ENSG00000131019	5.1
HRE11	6p22.3	18101058	18101072	AGAACAtgcTGTTCT	KIF13A	ENSG00000137177	5.4
HRE12	6p21.32	33401650	33401664	AGAACAttcTGTTCT	ZNF297	ENSG00000168351	8.2
HRE13	7q36.1	149868965	149868979	AGAACAcaaTGTTCT	GIMAP5	ENSG00000196329	3.2
HRE14	7q36.1	148274989	148275003	AGAACAttaTGTTCT	ZNF398	ENSG00000197024	7.5
HRE15	8q24.3	144987498	144987512	AGAACAccgTGTTCT	NP_055096.2	ENSG00000179950	8.9
HRE16	11q22.3	109509863	109509877	AGAACAtttTGTTCT	Q9C0D7_HUMAN	ENSG00000149289	1.9
HRE17	11q24.1	123276891	123276905	AGAACAaagTGTTCT	OR8D4	ENSG00000181518	5.5
HRE18	11q24.2	125433385	125433399	AGAACAaaaTGTTCT	ENSG00000182203	ENSG00000182203	9.3
HRE19	11q12.3	62569237	62569251	AGAACAaatTGTTCT	ENSG00000185439	ENSG00000185439	1.8
HRE20	14q21.2	44792647	44792661	AGAACAtttTGTTCT	CV106_HUMAN	ENSG00000129534	0.5
HRE21	15q15.1	38128202	38128216	AGAACAaacTGTTCT	SRP14	ENSG00000140319	9.5
HRE22	15q22.3	62987265	62987279	AGAACAgatTGTTCT	NP_874362.2	ENSG00000166839	3.9
HRE23	16q24.3	87266241	87266255	AGAACAactTGTTCT	MVD	ENSG00000167508	9.2
HRE24	17q21.32	44836359	44836373	AGAACActcTGTTCT	ENSG00000189289	ENSG00000189289	3.2
HRE25	19p13.3	2844818	2844832	AGAACAggaTGTTCT	NP_775751.1	ENSG00000171970	7.1
HRE26	22q13.1	38616692	38616706	AGAACAgaaTGTTCT	NP_689725.2	ENSG00000176177	2.4

immunoprecipitated by GR antibody. We performed quantitative PCR using the genomic DNA obtained from each cell line (Fig. 1). The proximal and distal promoter regions of PSA including ARE sequences were used as positive controls for the AR association [3], and the proximal promoter of ENaCα including HRE sequences [10] was used as a positive control for the GR. The proximal promoter fragment of ENaCα was also found to recruit PR in the present study, as the PR recruitment to the fragment was ~9.5- and ~20-fold versus vehicle by 2 and 24-h treatments, respectively (Fig. 1B). FKBP51 has been previously described as a glucocorticoid or progesterone-inducible gene [11,12], however, functional HREs in the gene regulatory region have not been well characterized. We newly identified a functional HRE in the intron 1 of FKBP51 through scanning the gene regulatory region by ChIP assay. The intronic HRE of FKBP51 recruited PR in T47D cells as well as GR in DU145 cells and SaOS2 cells (Figs. 1B–D).

Of 26 genomic fragments containing perfect 5′ HRE sequences, 14 fragments recruited either one of the three steroid receptors by >2-fold enrichment in steroid-treated cells versus vehicle-treated cells (Fig. 1). HRE20 recruited three different receptors while HRE1, HRE15, and HRE24 recruited two different receptors by >2-fold enrichment. Other HRE sequences preferentially bound to only one steroid receptor. There seems to be no particular specificity of 3-bp spacer sequences for the receptor recruitment among the 14 functional HRE sequences.

Potential transcriptional regulation of proximal genes located downstream to perfect HREs

To examine whether the functional perfect 5′ HREs regulate transcriptional activity of their downstream proximal genes, we next performed quantitative RT-PCR for the downstream genes in the vicinity of the functional perfect 5′ HRE sequences. Of 7 proximal genes in the vicinity of functional perfect 5′ HRE sequences that recruited AR by >2-fold enrichment in LNCaP cells, OR8D4 (olfactory receptor family 8, subfamily D, member 4) adjacent to HRE17 exhibited a >2-fold increase in the mRNA level androgen-dependently (Fig. 2A). Of nine proximal genes in the vicinity of functional perfect 5′ HREs in T47D cells, MELL1 (mel transforming oncogene-like 1) and NP_775751.1 adjacent to HRE2 and HRE25, respectively, were upregulated by >2-fold at the mRNA level by progesterone treatment (Fig. 2B). Neither gene adjacent to the 2 functional perfect 5′ HREs in DU145 cells exhibited >2-fold increase in mRNA level, whereas Q9C0D7 adjacent to HRE16 in SaOS2 cells was upregulated by >2-fold at mRNA level glucocorticoid-dependently (Figs. 2C and D).

Discussion

A genome-wide in silico screening of palindromic perfect HREs identified 565 exact consensus sequences in the NCBI 35 assembly of the human genome. Of 565 perfect HRE sequences, 26 sites were situated within 10 kb upstream to the TSS of annotated genes. We investigated whether these perfect 5′ HRE sequences functioned as bona fide binding sites for steroid hormone receptors in different cell lines, and demonstrated that 14 of 26 perfect HREs significantly (>2-fold) recruited some of the receptors by performing ChIP assay for AR, GR, and PR binding. Hormone-dependent upregulation of mRNA level by >2-fold was shown in the four proximal genes adjacent to the functional perfect 5′ HREs. The average distance between 5′ HREs and the TSS of their proximal genes was not significantly smaller among these four proximal genes compared with the all 26 proximal genes in the vicinity of perfect 5′ HREs; the former and latter values were 4.5 ± 2.4 and 6.0 ± 3.0 kb, respectively.

The four hormone-responsive proximal genes adjacent to functional 5′ HRE sequences were upregulated by only either one of the three steroid hormone receptors and not by two or three other receptors. OR8D4 (HRE17) was identified as an AR target gene in LNCaP cells, MELL1 (HRE2) and NP_775751.1 (HRE25) were identified as PR target genes in T47D cells, and Q9C0D7 (HRE 16) was identified as a GR target gene in SaOS2 cells. Although a single IR3 type consensus HRE may be a potential binding site for various steroid hormone receptors, no common target gene for AR, PR, and GR was identified among the proximal genes close to the functional perfect 5′ HREs by the functional criteria used in this study. It is also notable that no significant GR target gene was shown in DU145 cells up to 24-h dexamethasone treatment, though the mRNA level of NP_055096.2 (HRE15) was increased >2-fold by 48-h treatment (data not shown). The results of DU145 and SaOS2 cells suggest that target genes for even a single steroid hormone receptor may be varied in different cell systems. Future studies including such as the chromosomal accessibility, the receptor recognition mechanism, and the coactivator recruitment in the surroundings of consensus HREs may reveal the specificity and the similarity of the transcription factor binding sites.

Besides the functions of the above four perfect HRE sequences adjacent to the steroid target genes, other near-consensus HRE sequences may participate in the regulation of gene expression. Using the SayaMatcher system [5] that enables us to visualize the genomic position for HREs on the Ensembl browser, we found several other near-consensus HRE sequences (>80% relative profile score threshold) based on the position-specific scoring matrix for ARE (MA0007) on the Jaspar database (http://jaspar.cgb.ki.se/), which is a collection of transcription factor DNA-binding preferences [13]. For instance, there is a near-consensus HRE at ~8-kb downstream to the 3′-end of MELL1. In the vicinity of Q9C0D7, one near-consensus HRE is in the intron 1 and the other is situated at 40-kb downstream to the 3′-end. OR8D4 contains a near-consensus HRE in its only exon. Although no particular high score position for the ARE matrix is found in the vicinity of NP_775751.1, there are a number of nuclear

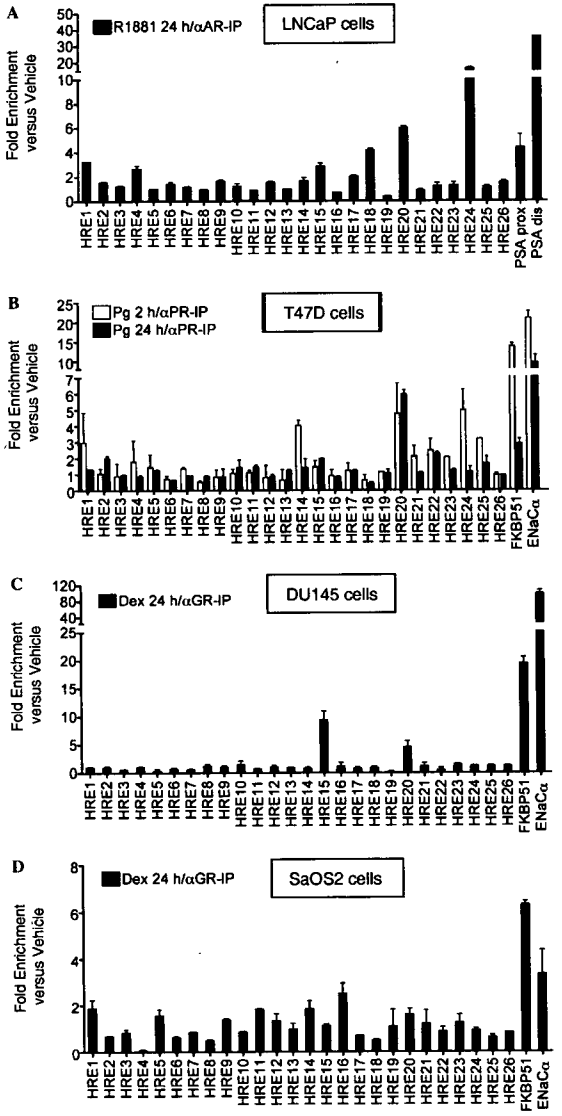

Fig. 1. In vivo recruitment of steroid hormone receptors to perfect HREs in the proximal upstream region of annotated genes. LNCaP, T47D, DU145, and SaOS2 cells after 72-h hormone depletion were treated with indicated hormones (10 nM each) or vehicle (0.1% EtOH) for indicated times. Immunoprecipitated DNA fragments were quantified by quantitative real-time PCR. In each case, fold enrichment values in hormone-treated samples precipitated by specific antibodies against receptors were normalized by those in vehicle-treated samples precipitated by the identical antibodies. Each result is the mean ± SD of two independent experiments in duplication (four determinants). Prostate-specific antigen (PSA) proximal (prox) and distal (dis) promoter regions including HREs were used as positive controls for AR binding. FK506-binding protein, 51-kDa (FKBP51) intron 1, and epithelial sodium channel α subunit (ENaCα) proximal promoter regions were used as positive controls for PR and GR binding. (A) AR recruitment in prostate cancer LNCaP cells. (B) PR recruitment in breast cancer T47D cells. (C) GR recruitment in prostate cancer DU145 cells. (D) GR recruitment in osteosarcoma SaOS2 cells.

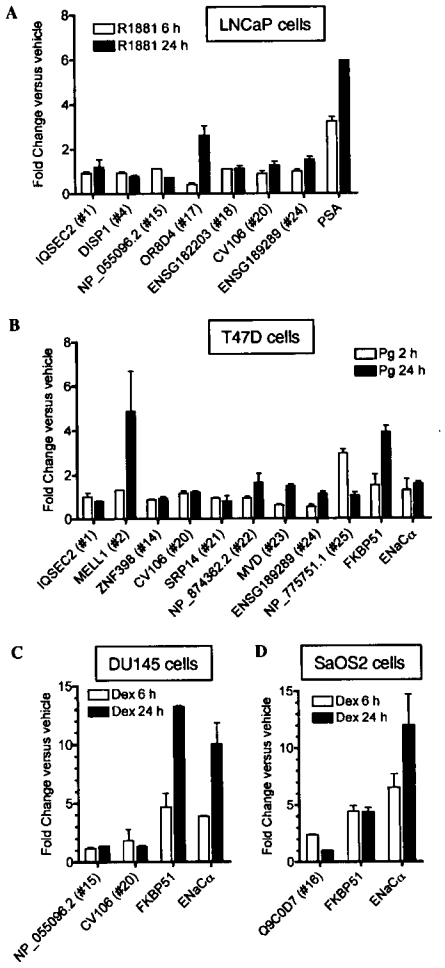

Fig. 2. Quantitative RT-PCR of proximal genes downstream to perfect HREs. LNCaP, T47D, DU145, and SaOS2 cells after 72-h hormone depletion were treated with indicated hormones (10 nM each) or vehicle (0.1% EtOH) for indicated times. Real-time PCR was conducted using the first strand cDNAs generated from the total RNAs of these cells. Each result is the mean ± SD of two independent experiments in duplication (four determinants). PSA was served as a positive control for androgen responsiveness. FKBP51 and ENaCα were served as positive controls for progesterone and glucocorticoid responsiveness. The numbers in parentheses after annotations correspond to the HRE ID in the vicinity of target genes. (A) R1881-dependent gene expression in LNCaP cells. (B) Progesterone-dependent gene expression in T47D cells. (C) Dexamethasone-dependent gene expression in DU145 cells. (D) Dexamethasone-dependent gene expression in SaOS2 cells.

receptor binding sites in the surroundings of the gene, suggesting that the region may be active for transcriptional regulation. Future studies will reveal whether these near-consensus HRE sequences coordinately function with the perfect HRE in the transcriptional regulation of the proximal genes.

Regarding the new steroid target genes identified in the present study, none of the genes has been characterized in connection with steroid hormones. The AR target gene OR8D4 (UniGene Hs. 449688) encodes a putative G protein-coupled receptor that belongs to the olfactory receptor superfamily, which is the largest gene family in the mammal genomes. In the mouse genomes, ~1300 genes were identified, whereas the number of olfactory receptors is expected ~500–750 genes in human [14]. Although ligands for most of the olfactory receptors have not been identified, it is plausible that certain receptors for odors or pheromones may be regulated by sex steroid hormones including androgen. The PR target gene MELL1 (UniGene Hs. 546429) is a membrane-bound zinc metalloprotease. It has been recently shown that mouse ortholog NL1 is expressed mainly in the testis as a secreted protein and male mice deficient in the NL1 exhibited reduced fertility [15]. It seems to be an interesting question whether human MELL1 may also play a role in reproductive tissues, particularly in the organs regulated by the progesterone-mediated gene network.

Another PR target gene NP_775751.1 encodes a putative KRAB domain-containing zinc finger protein. KRAB-containing zinc finger proteins are characterized to participate in the regulation of cell differentiation and development through transcriptional repression of RNA polymerase promoters, RNA binding, and RNA splicing [16]. Although many of these proteins have been identified, little is known about their structure and function. Since NP_775751.1 is clustered with a number of KRAB-containing zinc finger proteins on 19p13.3, these KRAB-containing zinc finger proteins might have arisen from a divergence event during evolution and may function coordinately in the various developmental and differentiation stages of organs. The GR target gene Q9C0D7 in SaOS2 cells is also annotated as zinc finger CCCH-type containing 12C (UniGene Hs. 376289). The CCCH-type zinc finger proteins such as tristetraprolin has been known as a binding protein to AU-rich element containing RNA transcripts [17], though no particular function of Q9C0D7 has yet been characterized.

In the present study, we focused on the perfect HRE sequences in the proximal upstream regions of annotated genes and found some of the elements were functional binding sites for steroid hormone receptors. It has been recently revealed, however, that transcription factor binding sites in intronic regions or in the 3′ downstream regions are also important for transcriptional regulation. Indeed, half of the perfect intronic ARE sequences on chromosome X (5 of 10) recruited more ARs compared with the proximal ARE on the PSA promoter in our

previous study [3]. In this study, we found that the FKBP51 intronic HRE sequence exhibited a significant binding ability for GR and PR. In the case of transcription factor binding sites on chromosomes 21 and 22, 36% of these regions are situated within known genes or proximal to the 3′ most exon of a gene and the frequency was also higher than that of binding sites within 5′ to known genes (22%) [18]. Thus, the further characterization of HRE sequences in introns as well as 3′ downstream regions will be required to reveal the whole entity of the transcriptional regulation mechanism mediated through steroid hormone receptors.

In summary, we have presented an integrated strategy for exploring novel steroid target genes that possess a functional perfect HRE sequence in their proximal upstream regions. Our results have shown that more than half of the perfect HREs identified by in silico analysis were functional binding sites for some of the steroid receptors including AR, PR, and GR. Potential steroid target genes were identified in the vicinity of perfect HRE sequences. We expect our strategy will be useful for further studies of gene regulation and the elucidation of the steroid hormone receptor-mediated gene network that exerts distinct physiological and pathophysiological functions.

Acknowledgments

We thank Y. Suzuki and R. Nozawa for their technical assistance. This work was supported in part by Grants-in-Aid from the Ministry of Health, Labor and Welfare; from the Japan Society for the Promotion of Science. This work was supported in part by a grant of the Genome Network Project from the Ministry of Education, Culture, Sports, Science and Technology of Japan and for Development of New Technology from The Promotion and Mutual Aid Corporation for Private Schools of Japan.

References

[1] D.J. Mangelsdorf, C. Thummel, M. Beato, P. Herrlich, G. Schutz, K. Umesono, B. Blumberg, P. Kastner, M. Mark, P. Chambon, R.M. Evans, The nuclear receptor superfamily: the second decade, Cell 83 (1995) 835–839.
[2] M. Beato, P. Herrlich, G. Schutz, Steroid hormone receptors: many actors in search of a plot, Cell 83 (1995) 851–857.
[3] K. Horie-Inoue, H. Bono, Y. Okazaki, S. Inoue, Identification and functional analysis of consensus androgen response elements in human prostate cancer cells, Biochem. Biophys. Res. Commun. 325 (2004) 1312–1317.
[4] T. Hubbard, D. Andrews, M. Caccamo, G. Cameron, Y. Chen, M. Clamp, L. Clarke, G. Coates, T. Cox, F. Cunningham, et al., Ensembl 2005, Nucleic Acids Res. 33 (2005) D447–D453.
[5] H.U. Bono, SayaMatcher: Genome scale organization and systematic analysis of nuclear receptor response elements, Gene (2005). Available online August 24.
[6] P. Rice, I. Longden, A. Bleasby, EMBOSS: the European Molecular Biology Open Software Suite, Trends Genet. 16 (2000) 276–277.
[7] P.S. Nelson, N. Clegg, H. Arnold, C. Ferguson, M. Bonham, J. White, L. Hood, B. Lin, The program of androgen-responsive genes in neoplastic prostate epithelium, Proc. Natl. Acad. Sci. USA 99 (2002) 11890–11895.
[8] V. Matys, E. Fricke, R. Geffers, E. Gossling, M. Haubrock, R. Hehl, K. Hornischer, D. Karas, A.E. Kel, O.V. Kel-Margoulis, D.U. Kloos, S. Land, B. Lewicki-Potapov, H. Michael, R. Munch, I. Reuter, S. Rotert, H. Saxel, M. Scheer, S. Thiele, E. Wingender, TRANSFAC: transcriptional regulation, from patterns to profiles, Nucleic Acids Res. 31 (2003) 374–378.
[9] Y. Shang, M. Myers, M. Brown, Formation of the androgen receptor transcription complex, Mol. Cell 9 (2002) 601–610.
[10] V.E. Mick, O.A. Itani, R.W. Loftus, R.F. Husted, T.J. Schmidt, C.P. Thomas, The alpha-subunit of the epithelial sodium channel is an aldosterone-induced transcript in mammalian collecting ducts, and this transcriptional response is mediated via distinct cis-elements in the 5′-flanking region of the gene, Mol. Endocrinol. 15 (2001) 575–588.
[11] H. Vermeer, B.I. Hendriks-Stegeman, B. van der Burg, S.C. van Buul-Offers, M. Jansen, Glucocorticoid-induced increase in lymphocytic FKBP51 messenger ribonucleic acid expression: a potential marker for glucocorticoid sensitivity, potency, and bioavailability, J. Clin. Endocrinol. Metab. 88 (2003) 277–284.
[12] T.R. Hubler, W.B. Denny, D.L. Valentine, J. Cheung-Flynn, D.F. Smith, J.G. Scammell, The FK506-binding immunophilin FKBP51 is transcriptionally regulated by progestin and attenuates progestin responsiveness, Endocrinology 144 (2003) 2380–2387.
[13] A. Sandelin, W. Alkema, P. Engstrom, W.W. Wasserman, B. Lenhard, JASPAR: an open-access database for eukaryotic transcription factor binding profiles, Nucleic Acids Res. 32 (2004) D91–D94.
[14] X. Zhang, S. Firestein, The olfactory receptor gene superfamily of the mouse, Nat. Neurosci. 5 (2002) 124–133.
[15] M. Carpentier, C. Guillemette, J.L. Bailey, G. Boileau, L. Jeannotte, L. DesGroseillers, J. Charron, Reduced fertility in male mice deficient in the zinc metallopeptidase NL1, Mol. Cell. Biol. 24 (2004) 4428–4437.
[16] R. Urrutia, KRAB-containing zinc-finger repressor proteins, Genome Biol. 4 (2003) 231.1–231.8.
[17] E. Carballo, W.S. Lai, P.J. Blackshear, Feedback inhibition of macrophage tumor necrosis factor-alpha production by tristetraprolin, Science 281 (1998) 1001–1005.
[18] S. Cawley, S. Bekiranov, H.H. Ng, P. Kapranov, E.A. Sekinger, D. Kampa, A. Piccolboni, V. Sementchenko, J. Cheng, A.J. Williams, R. Wheeler, B. Wong, J. Drenkow, M. Yamanaka, S. Patel, S. Brubaker, H. Tammana, G. Helt, K. Struhl, T.R. Gingeras, Unbiased mapping of transcription factor binding sites along human chromosomes 21 and 22 points to widespread regulation of noncoding RNAs, Cell 116 (2004) 499–509.

ELSEVIER

Seminars in Cancer Biology 16 (2006) 235–239

seminars in CANCER BIOLOGY

www.elsevier.com/locate/semcancer

Review

Epigenetic and proteolytic inactivation of 14-3-3σ in breast and prostate cancers

Kuniko Horie-Inoue [a], Satoshi Inoue [a,b,*]

[a] *Research Center for Genomic Medicine and Department of Molecular Biology, Saitama Medical School, 1397-1 Yamane, Hidaka-shi, Saitama 350-1241, Japan*
[b] *Department of Geriatric Medicine, Graduate School of Medicine, The University of Tokyo, 7-3-1 Hongo, Bunkyo-ku, Tokyo 113-8655, Japan*

Abstract

14-3-3σ is an epithelial marker whose expression is induced by DNA damage through a p53-dependent pathway. 14-3-3σ functions sequesters cyclin B1-CDC2 complexes outside the nucleus and thereby contributes to a G2 arrest. Down-regulation or lack of 14-3-3σ is a frequent event in breast and prostate cancers. Epigenetic silencing by CpG methylation, p53 inactivation, and proteasome-dependent proteolysis leads to loss of 14-3-3σ. Hypermethylation of the *14-3-3σ* gene is often observed in precancerous lesions and likely to be causally linked to the onset of cancer. Proteolytic inactivation of 14-3-3σ has been recently found in breast and prostate cancers. In breast cancer, the estrogen-responsive E3 ubiquitin ligase Efp specifically targets 14-3-3σ for degradation. The E2 ubiquitin conjugating enzyme UBC8 and Efp also mediates ISG15 modification of 14-3-3σ. Detection of 14-3-3σ inactivation on the protein or DNA methylation level may be used for cancer prognosis. Furthermore, 14-3-3σ may be a potential therapeutic target in breast and prostate cancer.

Keywords: 14-3-3σ; Breast cancer; Prostate cancer; CpG methylation; Proteasome-dependent proteolysis; ISG15 modification

Contents

1. Introduction

Breast and prostate cancer are common malignancies diagnosed in Western countries as well as in Japan, and the incidence of these endocrine tumors is steadily increasing. Despite recent advances of steroid hormone research in endocrine-dependent tumors, the molecular basis of these neoplastic transformations is still largely unknown. Loss of function in tumor suppressor genes as well as gain of function in proto-oncogenes accounts for the genetic defects in tumor development. *p53* is one of the key tumor suppressor genes which is frequently mutated in cancers. The p53 protein is a transcription factor that inhibits cell growth and stimulates cell death when induced by cellular stressors, as for example DNA damage [1]. Various biological effects of p53 are mediated through p53 target genes. After DNA damage *14-3-3σ*, or *stratifin*, is induced by p53 [2]. 14-3-3σ expression is lost or reduced in a number of carcinomas. This review focuses on the contribution of proteolysis of 14-3-3σ protein and CpG-methylation its promoter to tumor formation and progression, particularly in breast and prostate cancers.

* Corresponding author. Tel.: +81 3 5800 8652; fax: +81 3 5800 6530.
E-mail address: INOUE-GER@h.u-tokyo.ac.jp (S. Inoue).

1044-579X/$ – see front matter © 2006 Elsevier Ltd. All rights reserved.
doi:10.1016/j.semcancer.2006.03.006

2. Genetic and epigenetic inactivation of 14-3-3σ in malignancies

14-3-3σ is a member of a family of highly conserved, acidic dimeric 14-3-3 proteins. Among seven distinct *14-3-3* genes, *14-3-3σ* is the only gene that is induced by p53 and has been directly implicated in the etiology of human cancer [3]. 14-3-3σ sequesters cyclin B1-CDC2 complexes outside the nucleus and thereby helps to maintain a stable G2 block after DNA damage [4,5]. *14-3-3σ* has been originally cloned from human mammary epithelial cells [6] as well as from keratinocytes [7] and its expression seems to be restricted in epithelial cells. The *14-3-3σ* gene localizes to chromosome 1p36.11, which is involved in the 1p32–36 region where loss of heterozygosity (LOH) has been often observed in breast cancer [2,8]. LOH, however, seems to be not a primary mechanism for loss of 14-3-3σ expression as LOH was observed only for 5% (1/20) of primary breast cancer samples from patients with heterozygosity in their normal DNAs [9]. Genetic alterations within the coding region of *14-3-3σ* have not been observed even in breast cancer cells [9].

Epigenetic silencing of the *14-3-3σ* gene by CpG methylation has been detected at a high frequency in breast carcinoma [9], particularly in invasive tumors during early stages [10]. The *14-3-3σ* gene has a CpG-rich region within its first and only exon that begins near the transcription initiation site and ends ~800 bp downstream, including 27 CpG dinucleotides [9]. Epigenetic silencing of *14-3-3σ* has been also detected in carcinomas of the prostate [11–15], endometrium [15], ovary [15–17], lung [18], liver [19], oral epithelia [20], and skin [21]. Silencing of tumor suppressive genes by CpG methylation is presumably of equal importance for tumor development as functional inactivation by point mutation or allelic loss [22].

Inactivation of p53 is another mechanism for the cancer-specific loss of *14-3-3σ* expression, as mutations of p53 are frequent events in various types of carcinoma. It is unclear at present whether *p53* mutation and *14-3-3σ* methylation are mutually exclusive in human cancers [3]. Nevertheless, mutations in p53 may be late events during tumor formation and not a direct cause for *14-3-3σ* methylation, as several different *p53* mutations as well as CpG methylation of *14-3-3σ* have been observed in normal epidermis adjacent to basal cell carcinoma [23]. As keratinocytes may be immortalized by inactivation of *14-3-3σ* [24], *14-3-3σ* methylation may play a significant role in the escape from replicative senescence of precancerous epithelial cells. Cells with silenced *14-3-3σ* present in premalignant lesions may subsequently acquire p53 inactivation and then progress to full-blown malignancy.

3. Proteasome-mediated proteolysis of 14-3-3σ by Efp

In addition to epigenetic silencing and p53 inactivation, the expression of 14-3-3σ is also down-regulated by ubiquitin-dependent proteolysis. Using a yeast two-hybrid approach and the estrogen-responsive RING finger protein Efp as a bait, we identified an interaction between 14-3-3σ and Efp [25]. The RING finger features a set of cysteine and histidine residues that have a distinct spacing owing to their roles as the ligands of two zinc ions that stabilize a characteristic globular conformation [26]. RING finger proteins often function as E3 ubiquitin ligases, acting as scaffolds to promote ubiquitin transfer form E2 ubiquitin-conjugating enzymes to substrates [27,28]. Efp is indeed a specific E3 ligase for 14-3-3σ, preferentially recruiting UbcH8/UBC8 as the E2 conjugating enzyme [25]. Recently, proteins that contains three zinc-binding domains, a RING finger, types 1 and 2 B-boxes, and a coiled-coil region have been designated as members of the tripartite motif (TRIM) family [29]. Efp is also referred as TRIM25. Transfection experiments showed that the B-box-coiled-coil domain in Efp was essential for the binding to 14-3-3σ, while the RING finger in Efp was critical for the interaction with UbcH8/UBC8 [25] (Fig. 1).

Efp is predominantly expressed in estrogen responsive tissues including mammary glands, uteri, and osteoblasts [30,31]. Efp is robustly expressed in breast cancers and its transcription is positively regulated by estrogen in human breast cancer cell MCF7 [32]. The estrogen-response element situated in the 3′-untranslated region of Efp was identified to be responsible for the transcription of the gene [32]. The Efp gene is localized on chromosome 17q23.2, a region commonly amplified in breast tumors, especially those with poor prognosis [33]. Efp is essential for growth of female organs, as mice deficient in Efp gene show a defect in development of uteri [34]. Loss-of-function studies of Efp in MCF7 cells inoculated in nude mice revealed that Efp was a critical gene for tumor growth [25]. Whereas MCF7 cells form tumors in mice in an estrogen-dependent manner, MCF7 cells with overexpression of Efp (Efp-Mcf7) form tumors in ovariectomized mice [25]. In Efp-MCF7 cells, the expression of 14-3-3σ protein was markedly reduced and cell proliferation was significantly increased when compared with control MCF7 cells transfected with vector alone.

Efp immunoreactivity is a significant prognostic factor in breast cancer patients as shown by multivariate analyses of disease-free survival and overall survival for 151 Japanese patients [35]. Despite of previous reports regarding high frequency of hypermethylation at 14-3-3σ locus in breast cancer (91%) [9], a relatively high percentage of breast tumors that express 14-3-3σ immunoreactivity (38%) was detected in another study [35]. This discrepancy may suggest that CpG methylation is not the only determinant of 14-3-3σ expression.

4. Efp as an ISG15 E3 ligase for 14-3-3σ

Recently, it has been shown that Efp also functions as an ISG15 (15 kDa protein encoded by an interferon-stimulated gene) E3 ligase for 14-3-3σ [36]. Efp is up-regulated by type I interferon (IFN) treatment and the promoter region of Efp contains an IFN-stimulated response element (ISRE) like other genes related to ISG15 modification. ISG15 is a ubiquitin-like modification and it forms covalent conjugates with cellular proteins upon IFN treatment. Similar to ubiquitinylation, there are a series of enzymes including E1, E2, and E3 involved in the process of protein modification by ISG15 (ISGylation). The E1 enzyme of the ISG-conjugating system is the E1-like protein UBE1L [37]. UBE1L shows high homology to the ubiquitin-activating enzyme UBE1. Interestingly, the ubiquitin

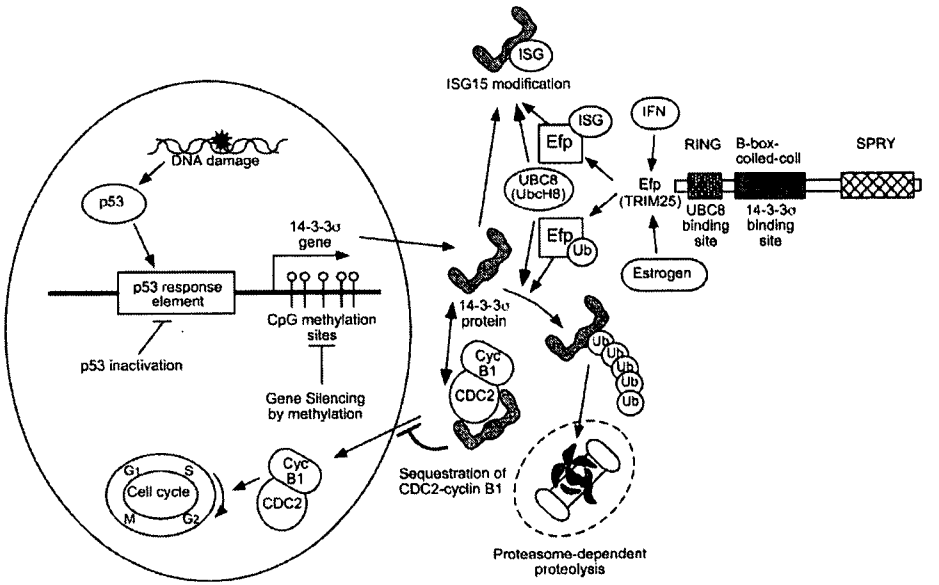

Fig. 1. 14-3-3σ regulation and function in cancer cells. *14-3-3σ* is a p53 target gene that has a p53 response element in the promoter region. DNA damage generated by such as telomere attrition and genotoxic stress by ROS production in mitogenic signaling pathways in cancer cells activate the p53 damage response. *14-3-3σ* gene expression is down-regulated by CpG methylation or by p53 inactivation. 14-3-3σ associates with cyclin B/CDC2 complexes and inhibits their nuclear translocation, which is required for cell cycle progression into G2 phase. 14-3-3σ expression is also regulated through proteasome-dependent proteolysis, which is mediated by the E3 ubiquitin ligase Efp (TRIM25) and the E2 ubiquitin conjugating enzyme UBC8 (UbcH8). Efp and UBC8 are also common components for ISG15 modification of 14-3-3σ, which can be activated by type I interferon stimulation. Efp has a structure of TRIM protein, containing RING finger, B-box-coiled-coil, and SPRY domains. UBC8 interacts with the RING finger whereas 14-3-3σ interacts with the B-box-coiled-coil domain of Efp. Repression or lack of 14-3-3σ expression through cancer-associated mechanisms leads to deregulated cell cycle progression and promotes tumor growth.

E2 UBC8 also functions as the ISG15 E2 conjugating enzyme [38,39]. So far, Efp is the only UBC8-interacting enzyme that functions as a dual E3 ligase for both ISG15 and ubiquitin [36].

Unlike ubiquitin modification, the role of ISG modification has not been well defined although ISG15 has been identified more than 25 years ago. ISG modification has been implicated in reproduction and innate immunity [37] and it has been found exclusively in vertebrates. However, it has been reported that generation and analysis of ISG15-deficient mice [40] and ISG15-conjugation deficient Ube 1L knockout mice [36] did not reveal any significant developmental abnormalities. Thus, the physiological relevance of ISG15 modification of 14-3-3σ and the spatio-temporal availability of ubiquitination or ISG15 modification of 14-3-3σ by Efp and UBC8 remain to be elucidated.

5. Regulation of 14-3-3σ expression in prostate cancer

In prostate cancer, epigenetic inactivation and proteolytic regulation of 14-3-3σ may be involved in tumorigenesis but the specificity of either mechanism may vary according to androgen responsiveness or tumor stages. Immunohistochemical studies showed high expression of 14-3-3σ in normal prostate epithelial and benign prostate hyperplasia cells, whereas prostate cancer cells displayed low expression or lack of 14-3-3σ [11,13]. Methylation-specific PCR analysis showed CpG methylation of *14-3-3σ* in all 41 primary prostate cancer samples [11]. A prototypical androgen receptor (AR)-positive prostate cancer cell line LNCaP also exhibited CpG methylation of *14-3-3σ* [11,13], whereas AR-negative human prostate cancer PC3 and DU145 cells did not exhibit CpG methylation of *14-3-3σ* [11,13]. In PC3 and DU145 cells, however, protein expression of 14-3-3σ was reduced compared with primary prostate epithelial cells and the protein expression was increased by the proteasome inhibitor MG132, indicating that proteasome-mediated proteolysis is responsible for the down-regulation of 14-3-3σ protein in these cell lines [13]. Interestingly, 14-3-3σ expression in PC3 and DU145 cells was also induced by tumor necrosis factor-related apoptosis-inducing ligand (TRAIL) [13], a member of the TNFα superfamily that induces apoptosis in a variety of transformed cells including PC3 and DU145 cells by engaging and activating death receptors [41]. TRAIL induces apoptosis in cancer cells with minimal cytotoxicity to normal cells. TRAIL also causes cell cycle arrest through the up-regulation of 14-3-3σ levels in TRAIL-sensitive cancer cells. TRAIL may therefore

have a therapeutic potential against advanced cancers regardless their p53 status.

6. Conclusions

14-3-3σ plays a role as a tumor suppressor gene whose expression is frequently reduced or diminished in breast and prostate cancers. Epigenetic silencing by CpG methylation, p53 inactivation, and proteasome-dependent proteolysis are responsible for loss of 14-3-3σ expression. The attenuation of checkpoint functions by loss of 14-3-3σ promotes cell cycle into G2/M transition and stimulates cell growth. Cancer cells lacking 14-3-3σ are further susceptible for genotoxic stress and exhibit genetic instability. The methylation status of *14-3-3σ* as well as the protein expression levels of 14-3-3σ may be useful markers for the determination of cancer prognosis, and reagents that induce the demethylation of *14-3-3σ* gene or inhibit of proteasome-dependent 14-3-3σ proteolysis and thereby lead to elevation of 14-3-3σ protein levels could be potential therapeutic options for cancers, especially those in advanced stages.

Acknowledgements

This work was supported in part by grants-in-aid from the Ministry of Health, Labor and Welfare, the Japan Society for the Promotion of Science and the Genome Network Project from the Ministry of Education, Culture, Sports, Science and Technology of Japan.

References

[1] Hermeking H, Lengauer C, Polyak K, He TC, Zhang L, Thiagalingam S, et al. 14-3-3σ is a p53-regulated inhibitor of G2/M progression. Mol Cell 1997;1:3–11.
[2] Vogelstein B, Kinzler KW. Cancer genes and the pathways they control. Nat Med 2004;10:789–99.
[3] Hermeking H. The 14-3-3 cancer connection. Nat Rev Cancer 2003;3:931–43.
[4] Chan TA, Hermeking H, Lengauer C, Kinzler KW, Vogelstein B. 14-3-3σ is required to prevent mitotic catastrophe after DNA damage. Nature 1999;401:616–20.
[5] Laronga C, Yang HY, Neal C, Lee MH. Association of the cyclin-dependent kinases and 14-3-3σ negatively regulates cell cycle progression. J Biol Chem 2000;275:23106–12.
[6] Prasad GL, Valverius EM, McDuffie E, Cooper HL. Complementary DNA cloning of a novel epithelial cell marker protein, HME1, that may be down-regulated in neoplastic mammary cells. Cell Growth Differ 1992;3:507–13.
[7] Leffers H, Madsen P, Rasmussen HH, Honore B, Andersen AH, Walbum E, et al. Molecular cloning and expression of the transformation sensitive epithelial marker stratifin. A member of a protein family that has been involved in the protein kinase C signalling pathway. J Mol Biol 1993;231:982–98.
[8] Bieche I, Lidereau R. Genetic alterations in breast cancer. Genes Chromosomes Cancer 1995;14:227–51.
[9] Ferguson AT, Evron E, Umbricht CB, Pandita TK, Chan TA, Hermeking H, et al. High frequency of hypermethylation at the 14-3-3σ locus leads to gene silencing in breast cancer. Proc Natl Acad Sci USA 2000;97:6049–54.
[10] Umbricht CB, Evron E, Gabrielson E, Ferguson A, Marks J, Sukumar S. Hypermethylation of 14-3-3σ (stratifin) is an early event in breast cancer. Oncogene 2001;20:3348–53.
[11] Lodygin D, Diebold J, Hermeking H. Prostate cancer is characterized by epigenetic silencing of 14-3-3σ expression. Oncogene 2004;23:9034–41.
[12] Cheng L, Pan CX, Zhang JT, Zhang S, Kinch MS, Li L, et al. Loss of 14-3-3σ in prostate cancer and its precursors. Clin Cancer Res 2004;10:3064–8.
[13] Urano T, Takahashi S, Suzuki T, Fujimura T, Fujita M, Kumagai J, et al. 14-3-3σ is down-regulated in human prostate cancer. Biochem Biophys Res Commun 2004;319:795–800.
[14] Henrique R, Jeronimo C, Hoque MO, Carvalho AL, Oliveira J, Teixeira MR, et al. Frequent 14-3-3σ promoter methylation in benign and malignant prostate lesions. DNA Cell Biol 2005;24:264–9.
[15] Mhawech P, Benz A, Cerato C, Greloz V, Assaly M, Desmond JC, et al. Downregulation of 14-3-3σ in ovary, prostate and endometrial carcinomas is associated with CpG island methylation. Mod Pathol 2005;18:340–8.
[16] Suzuki H, Itoh F, Toyota M, Kikuchi T, Kakiuchi H, Imai K. Inactivation of the 14-3-3σ gene is associated with 5′ CpG island hypermethylation in human cancers. Cancer Res 2000;60:4353–7.
[17] Akahira J, Sugihashi Y, Suzuki T, Ito K, Niikura H, Moriya T, et al. Decreased expression of 14-3-3σ is associated with advanced disease in human epithelial ovarian cancer: its correlation with aberrant DNA methylation. Clin Cancer Res 2004;10:2687–93.
[18] Osada H, Tatematsu Y, Yatabe Y, Nakagawa T, Konishi H, Harano T, et al. Frequent and histological type-specific inactivation of 14-3-3σ in human lung cancers. Oncogene 2002;21:2418–24.
[19] Iwata N, Yamamoto H, Sasaki S, Itoh F, Suzuki H, Kikuchi T, et al. Frequent hypermethylation of CpG islands and loss of expression of the 14-3-3σ gene in human hepatocellular carcinoma. Oncogene 2000;19:5298–302.
[20] Gasco M, Bell AK, Heath V, Sullivan A, Smith P, Hiller L, et al. Epigenetic inactivation of 14-3-3σ in oral carcinoma: association with p16(INK4a) silencing and human papillomavirus negativity. Cancer Res 2002;62:2072–6.
[21] Lodygin D, Yazdi AS, Sander CA, Herzinger T, Hermeking H. Analysis of 14-3-3σ expression in hyperproliferative skin diseases reveals selective loss associated with CpG-methylation in basal cell carcinoma. Oncogene 2003;22:5519–24.
[22] Lodygin D, Hermeking H. The role of epigenetic inactivation of 14-3-3σ in human cancer. Cell Res 2005;15:237–46.
[23] Ling G, Persson A, Berne B, Uhlen M, Lundeberg J, Ponten F. Persistent p53 mutations in single cells from normal human skin. Am J Pathol 2001;159:1247–53.
[24] Dellambra E, Golisano O, Bondanza S, Siviero E, Lacal P, Molinari M, et al. Downregulation of 14-3-3σ prevents clonal evolution and leads to immortalization of primary human keratinocytes. J Cell Biol 2000;149:1117–30.
[25] Urano T, Saito T, Tsukui T, Fujita M, Hosoi T, Muramatsu M, et al. Efp targets 14-3-3σ for proteolysis and promotes breast tumour growth. Nature 2002;417:871–5.
[26] Pickart CM. Mechanisms underlying ubiquitination. Annu Rev Biochem 2001;70:503–33.
[27] Zheng N, Schulman BA, Song L, Miller JJ, Jeffrey PD, Wang P, et al. Structure of the Cul1-Rbx1-Skp1-F boxSkp2 SCF ubiquitin ligase complex. Nature 2002;416:703–9.
[28] Orticky S, Tang X, Willems A, Tyers M, Sicheri F. Structural basis for phosphodependent substrate selection and orientation by the SCFCdc4 ubiquitin ligase. Cell 2003;112:243–56.
[29] Peng H, Feldman I, Rauscher 3rd FJ. Hetero-oligomerization among the TIF family of RBCC/TRIM domain-containing nuclear cofactors: a potential mechanism for regulating the switch between coactivation and corepression. J Mol Biol 2002;320:629–44.
[30] Orimo A, Inoue S, Ikeda K, Noji S, Muramatsu M. Molecular cloning, structure, and expression of mouse estrogen-responsive finger protein Efp. Co-localization with estrogen receptor mRNA in target organs. J Biol Chem 1995;270:24406–13.
[31] Inoue S, Urano T, Ogawa S, Saito T, Orimo A, Hosoi T, et al. Molecular cloning of rat efp: expression and regulation in primary osteoblasts. Biochem Biophys Res Commun 1999;261:412–8.

[32] Ikeda K, Orimo A, Higashi Y, Muramatsu M, Inoue S. Efp as a primary estrogen-responsive gene in human breast cancer. FEBS Lett 2000;472:9–13.
[33] Andersen CL, Monni O, Wagner U, Kononen J, Barlund M, Bucher C, et al. High-throughput copy number analysis of 17q23 in 3520 tissue specimens by fluorescence in situ hybridization to tissue microarrays. Am J Pathol 2002;161:73–9.
[34] Orimo A, Inoue S, Minowa O, Tominaga N, Tomioka Y, Sato M, et al. Underdeveloped uterus and reduced estrogen responsiveness in mice with disruption of the estrogen-responsive finger protein gene, which is a direct target of estrogen receptor alpha. Proc Natl Acad Sci USA 1999;96:12027–32.
[35] Suzuki T, Urano T, Tsukui T, Horie-Inoue K, Moriya T, Ishida T, et al. Estrogen-responsive finger protein as a new potential biomarker for breast cancer. Clin Cancer Res 2005;11:6148–54.
[36] Zou W, Zhang DE. Interferon-inducible ubiqitin E3 ligase efp also functions as an ISG15 E3 ligase.
[37] Ritchie KJ, Zhang DE. ISG15: the immunological kin of ubiquitin. Semin Cell Dev Biol 2004;15:237–46.
[38] Kim KI, Giannakopoulos NV, Virgin HW, Zhang DE. Interferon-inducible ubiquitin E2, Ubc8, is a conjugating enzyme for protein ISGylation. Mol Cell Biol 2004;24:9592–600.
[39] Zhao C, Beaudenon SL, Kelley ML, Waddell MB, Yuan W, Schulman BA, et al. The UbcH8 ubiquitin E2 enzyme is also the E2 enzyme for ISG15, an IFN-alpha/beta-induced ubiquitin-like protein. Proc Natl Acad Sci USA 2004;101:7578–82. Epub 2004 May 6.
[40] Osiak A, Utermohlen O, Niendorf S, Horak I, Knobeloch KP. ISG15, an interferon-stimulated ubiquitin-like protein, is not essential for STAT1 signaling and responses against vesicular stomatitis and lymphocytic choriomeningitis virus. Mol Cell Biol 2005;25:6338–45.
[41] Yu R, Mandlekar S, Ruben S, Ni J, Kong AN. Tumor necrosis factor-related apoptosis-inducing ligand-mediated apoptosis in androgen-independent prostate cancer cells. Cancer Res 2000;60:2384–9.

THE JOURNAL OF BIOLOGICAL CHEMISTRY VOL. 281, NO. 19, pp. 13092–13102, May 12, 2006

17β-Estradiol Protects against Oxidative Stress-induced Cell Death through the Glutathione/Glutaredoxin-dependent Redox Regulation of Akt in Myocardiac H9c2 Cells*

Received for publication, March 1, 2006 Published, JBC Papers in Press, March 20, 2006, DOI 10.1074/jbc.M601984200

Yoshishige Urata[‡1,2], Yoshito Ihara[‡1], Hiroaki Murata[‡], Shinji Goto[‡], Takehiko Koji[§], Junji Yodoi[¶], Satoshi Inoue[‖], and Takahito Kondo[‡]

From the [‡]Department of Biochemistry and Molecular Biology in Disease, Atomic Bomb Disease Institute, Nagasaki University Graduate School of Biomedical Sciences, 1-12-4 Sakamoto, Nagasaki 852-8523, Japan, the [§]Department of Histology and Cell Biology, Nagasaki University Graduate School of Biomedical Sciences, 1-12-4 Sakamoto, Nagasaki 852-8523, Japan, the [¶]Department of Biological Responses, Institute for Viral Research, Graduate School of Medicine, Kyoto University, 53 Shogoin, Kawahara-cho, Sakyo-ku, Kyoto 606-8397, Japan, and the [‖]Department of Geriatric Medicine, Graduate School of Medicine, University of Tokyo, 7-3-1 Hongo, Bunkyo-ku, Tokyo 113-8655, Japan

The GSH/glutaredoxin (GRX) system is involved in the redox regulation of certain enzyme activities, and this system protects cells from H_2O_2-induced apoptosis by regulating the redox state of Akt (Murata, H., Ihara, Y., Nakamura, H., Yodoi, J., Sumikawa, K., and Kondo, T. (2003) *J. Biol. Chem.* 278, 50226–50233). Estrogens, such as 17β-estradiol (E_2), play an important role in development, growth, and differentiation and appear to have protective effects on oxidative stress mediated by estrogen receptor α (ERα). However, the role of the ERβ-mediated pathway in this cytoprotection and the involvement of E_2 in the redox regulation are not well understood. In the present study, we demonstrated that E_2 protected cardiac H9c2 cells, expressing ERβ from H_2O_2-induced apoptosis concomitant with an increase in the activity of Akt. E_2 induced the expression of glutaredoxin (GRX) as well as γ-glutamylcysteine synthetase, a rate-limiting enzyme for the synthesis of GSH. Inhibitors for both γ-glutamylcysteine synthetase and GRX and ICI182,780, a specific inhibitor of ERs, abolished the protective effect of E_2 on cell survival as well as the activity of Akt, suggesting that ERβ is involved in the cytoprotection and redox regulation by E_2. Transcription of the GRX gene was enhanced by E_2. The promoter activity of GRX was up-regulated by an ERβ-dependent element. These results suggest that the GRX/GSH system is involved in the cytoprotective and genomic effects of E_2 on the redox state of Akt, a pathway that is mediated, at least in part, by ERβ. This mechanism may also play an antiapoptotic role in cancer cells during carcinogenesis or chemotherapy.

Oxidative stress is a principle cause of the development of aging and diseases such as inflammation, infection, cancer, and cardiovascular disorders (1, 2). Exogenous or endogenous sources of oxidative stress and weakened antioxidative defenses can damage macromolecules such as DNA, lipids, and proteins.

Estrogens play an important role in development, growth, and the differentiation of both female and male secondary sex characteristics (3). Protective effects of estrogen, such as 17β-estradiol (E_2),[3] on oxidative stress have been indicated (4). E_2 regulates longevity signals to enhance resistance to oxidative stress in mice. Inhibitory effects of E_2 on atherosclerosis are mediated by COX-2-derived prostacyclin (5). E_2 induces production of antioxidative enzymes, such as superoxide dismutase (6), γ-glutamylcysteine synthetase (γ-GCS), and glutathione *S*-transferase (7). The effects of E_2 are mediated mostly through ERα, which functions as a ligand-induced transcription factor and belongs to the nuclear receptor superfamily (8). ERα binds to a variety of ligands and displays tissue-specific effects through estrogen-response element (ERE). When estrogen-responsive genes do not contain EREs, ERα can up-regulate gene expression through AP-1 and Sp1 sites (9). Another ER, ERβ, is expressed in cells targeted by E_2, including cardiomyocytes (10). However, the role of ERβ in protection against oxidative stress has not been well studied.

Protein thiols act as redox-sensitive switches and are believed to be a key element in maintaining the cellular redox balance. The redox state of protein thiols is regulated by oxidative stress and redox signaling and important to cellular functions. To maintain the cellular thiol-disulfide redox status, living cells possess two major systems, the thioredoxin (TRX)/TRX reductase system and the glutathione (γ-glutamylcysteinyl glycine, GSH)/glutaredoxin (GRX) system (11). GSH is synthesized in two sequential enzymatic reactions that are each catalyzed by a rate-limiting enzyme, γ-GCS, and GSH synthetase (12). GRX, also known as thioltransferase, was first discovered as a GSH-dependent hydrogen donor for ribonucleotide reductase in *Escherichia coli* mutants lacking TRX (13). Oxidized GRX is recycled to the reduced form by GSH with the formation of glutathione disulfide and regeneration of GSH by coupling with NADPH and glutathione disulfide reductase (14). GRX functions via a disulfide exchange reaction by utilizing the active site, Cys-Pro-Tyr-Cys, which specifically and efficiently catalyzes the reduction of protein-SSG mixed disulfide (15). GRX also partially shares its function as a redox sensor with TRX (16, 17). Recently, we have found that GRX protects against oxidative stress-induced cell death from apoptosis by regulating the redox state of Akt (18).

Akt/protein kinase B is a pleckstrin homology domain-containing serine/threonine kinase and a critical component of an intracellular signaling pathway that exerts effects on survival and apoptosis (19). Akt has been found to be responsive to extracellular signaling factors, oxidative and osmotic stress, irradiation, and ischemic stress (20). Akt can phosphorylate Bad, caspase-9, and forkhead-related transcription factors, leading to an inhibition of apoptosis (21). The unphosphorylated form of Akt is virtually inactive, and phosphorylation at Thr^{308} and Ser^{473} stimulates its activity. Inactivation of Akt also occurs via dephosphorylation of the two phosphorylation sites by protein phosphatase 2A (PP2A) (22, 23). The activation of Akt contributes to the survival of H_2O_2-treated cells (24).

It has been reported that the function of ER-mediated transcriptional activity is regulated by redox (25). However, the precise mechanisms of redox regulation in the E_2-mediated signal pathways have not been clarified. Here we describe a mechanism for the antiapoptotic effect of E_2 through the regulation of the redox state of Akt under oxidative stress. Treatment of cardiac H9c2 cells with E_2 for 18 h protected against H_2O_2-induced apoptosis. E_2 induced the expression of GRX and γ-GCS, at least in part, through ERβ-mediated regulation. Elevated GSH and GRX levels potentiated the redox of Akt on the exposure of cells to H_2O_2.

MATERIALS AND METHODS

Reagents—Anti-PP2A scaffolding A subunit (PR65) antibody was obtained from Santa Cruz Biotechnology. Antibodies against human ERα (clone ER88) and ERβ (polyclonal) were from Kyowa Medex (Tokyo, Japan). Horseradish peroxidase (HRP)-conjugated goat anti-rabbit IgG F was purchased from MBL (Nagoya, Japan). HRP-goat anti-mouse IgG F was from Chemicon International (Temocula, CA). Normal goat IgG, normal rabbit IgG, and normal mouse IgG were from Sigma. Anti-Akt and anti-phospho-(Ser^{473})-Akt antibodies were from Cell Signaling Technology. Anti-PP2A catalytic C subunit antibody was from BD Transduction Laboratories. 3-(4,5-dimethyl-thiazole-2-yl)-2,5-diphenyltetrazolium bromide (MTT) was from Sigma. 4-Acetamido-4′-maleimidylstilbene-2,2′-disulfonic acid (AMS) was purchased from Molecular Probes, Inc. (Eugene, OR). H_2O_2 and $CdCl_2$ were from Wako Pure Chemicals (Osaka, Japan). ICI182,780 and propylpyrazoletriol (PPT) were from Tocris (Ballwin, MO).

Cell Culture—H9c2 cells, a clonal line derived from embryonic rat heart, and human breast cancer SK-BR-3 (SKB3) cells, and MDA-MB-231 (MDA) cells, were obtained from the American Type Culture Collection (CRL-1446). Human breast cancer MCF7 cells were from The Cell Resource Center for Biomedical Research Institute of Development, Aging, and Cancer, Tohoku University (Sendai, Japan). H9c2 cells were routinely maintained in Dulbecco's modified Eagle's medium, or MDA and SKB3 cells were maintained in RPMI1640 medium. The cells were supplied with 10% fetal calf serum in a humidified atmosphere of 95% air and 5% CO_2 at 37 °C (23).

Cell Viability—Cell viability was determined by a MTT assay as described (26). Briefly, cells (1500–5000) were placed in 100 μl of medium per well in 96-well plates. Four hours after treatment with various concentrations of H_2O_2, the cells were incubated for 4 h at 37 °C with 3-(4,5-dimethylthiazol-e-yl)-2,5-diphenyltetrazolium bromide (652 μg/ml) and lysed with 100 μl of 20% SDS, 50% *N*,*N*-dimethylformamide (pH 4.7) in each well. After an overnight incubation at 37 °C, the absorbance at 570 nm was measured. Wells without cells served as blanks.

Nuclear Condensation—For the histochemical analysis, cells were maintained in a four-well Lab Tec Chamber (Nalge Nunc International, Naperville, IL). After treatment with H_2O_2, cells were treated with 10 μM Hoechst 33342 for 30 min to estimate the extent of nuclear condensation. They were then washed again with PBS. Fluorescence intensity was examined using an Axioskop2 fluorescence microscope (Carl Zeiss, Jena, Germany), and the findings were analyzed using a charge-coupled device camera (Axio-Cam) and AxioVision software.

Morphological Staining—The immunohistochemical analysis to examine the expression of ERα and ERβ was performed as described previously (27). Briefly, cells were fixed with 4% paraformaldehyde in PBS and then preincubated with blocking solution for 1 h at room temperature. For ERβ 10% normal goat serum and 1% bovine serum albumin in PBS and for ERα 500 μg/ml of normal goat IgG and 1% bovine serum albumin in PBS were used, respectively. Next, the samples were incubated with the primary antibodies overnight and washed three times with 0.075% Brij 35 in PBS. Then samples were reacted with HRP-goat anti-mouse IgG or HRP-goat anti-rabbit IgG for 1 h at room temperature and washed three times with 0.075% Brij 35 in PBS. HRP sites were visualized with H_2O_2 and DAB solution or H_2O_2 and DAB in the presence of nickel and cobalt ions. As a negative control, normal rabbit IgG and normal mouse IgG were used instead of the primary antibodies. The results of immunohistochemistry for ERs were graded as positive or negative, compared with the staining with IgG or serum of a normal rabbit or mouse.

Immunoblot Analysis—Cultured cells were harvested and lysed for 20 min at 4 °C in lysis buffer as described previously (17). The supernatants obtained by centrifugation of the lysates at 8000 × *g* for 15 min were used in subsequent experiments. Protein concentrations were determined using a BCA assay kit (Pierce). Protein samples were electrophoresed on 10, 12.5, or 15% SDS-polyacrylamide gels under reducing conditions, except for thiol-modified protein samples. The proteins in the gels were transferred onto nitrocellulose membranes. The membranes were blocked in Tris-buffered saline (10 mM Tris-HCl (pH 7.5) and 0.15 M NaCl; TBS) containing 0.05% Tween 20 (v/v) (TBST) and 5% (w/v) nonfat dry milk and then reacted with primary antibodies in TBST containing 3% (w/v) bovine serum albumin overnight with constant agitation at 4 °C. After several washes with TBST, the membranes were incubated with horseradish peroxidase-conjugated anti-IgG antibodies. Proteins in the membranes were then visualized using the enhanced chemiluminescence detection kit (Amersham Biosciences) according to the manufacturer's instructions.

Akt Activity Assay—Akt activity was assayed using an Akt assay kit (Cell Signaling Technology) according to the manufacturer's directions with GSK3α/β fusion protein (GSK3α/β) as a substrate. Phosphorylation of GSK3α/β was assessed by immunoblot analysis using a specific antibody. Briefly, Akt was immunoprecipitated from cell lysates using the anti-Akt antibody, and then the immunoprecipitates were incubated at 30 °C for 30 min in an assay mixture containing GSK3α/β. Phosphorylated proteins were separated by 12.5% SDS-PAGE and then transferred to nitrocellulose membranes to detect phosphorylated GSK3α/β using an anti-phosphorylated GSK3α/β antibody.

Protein Phosphatase Assay—PP2A activity was assayed spectrophotometrically using a Ser/Thr phosphatase assay kit 1 (Upstate Biotechnology, Inc.) according to the manufacturer's instructions. The phosphopeptide RKpTIRR and *p*-nitrophenyl phosphate were used as phosphatase substrates.

Determination of Redox States—The redox states of proteins were assessed by modifying free thiol with AMS (28). Briefly, after incubation with or without H_2O_2, cell lysates or proteins were treated with trichloroacetic acid at a final concentration of 7.5% to denature and precipitate

* This work was supported in part by grants-in-aid for scientific research from the Ministry of Health, Labor, and Welfare of Japan (H15-Choju-015), by the Technology through the 21st Century Center of Excellence program, and by a research grant for health sciences from the Japanese Ministry of Health and Welfare. The costs of publication of this article were defrayed in part by the payment of page charges. This article must therefore be hereby marked "*advertisement*" in accordance with 18 U.S.C. Section 1734 solely to indicate this fact.

The nucleotide sequence(s) reported in this paper has been submitted to the GenBank™/EBI Data Bank with accession number(s) AF167981, BC063166, NM_001101.2, AY280663.1, U57439, NM_000125.2, and NM_001437.1.

[1] These authors contributed equally to this work.

[2] To whom correspondence should be addressed: Dept. of Biochemistry and Molecular Biology in Disease, Atomic Bomb Disease Institute, Nagasaki University Graduate School of Biomedical Sciences, 1-12-4 Sakamoto, Nagasaki 852-8523, Japan. Tel.: 81-95-849-7099; Fax: 81-95-849-7100; E-mail: urata@net.nagasaki-u.ac.jp.

[3] The abbreviations used are: E_2, 17β-estradiol; ER, estrogen receptor; ERE, estrogen-response element; GRX, glutaredoxin; γ-GCS, γ-glutamylcysteine synthetase; PP2A, protein phosphatase 2A; MTT, 3-(4,5-dimethyl-thiazole-2-yl)-2,5-diphenyltetrazolium bromide; HRP, horseradish peroxidase; PPT, propylpyrazoletriol; TBS, Tris-buffered saline; PDK1, 3-phosphoinositide-dependent protein kinase-1; TRX, thioredoxin; AMS, 4-acetamido-4′-maleimidylstilbene-2,2′-disulfonic acid; PBS, phosphate-buffered saline; RT, reverse transcription; BSO, buthionine sulfoximine; EpRE, electrophoretic response element.

the proteins as well as to avoid any subsequent redox reactions. The protein precipitates were collected by centrifugation at 12,000 × *g* for 10 min at 4 °C. The pellets were rinsed in acetone and centrifuged twice and then dissolved in a buffer containing 50 mM Tris-HCl (pH 7.4), 1% SDS, and 15 mM AMS. Proteins were then separated by 10% SDS-PAGE without using any reducing agents and blotted to nitrocellulose membranes. Proteins in the membranes were visualized by immunoblotting as described above.

Northern Blot Analysis—A 764-bp DNA fragment (bp 865–1628) of full-length γ-GCS heavy subunit cDNA was obtained by digestion with PstI (29). The probes were radiolabeled with ^{32}P using a random primer labeling kit (Takara Biomedicals, Shiga, Japan). The isolation of cytoplasmic RNA and Northern blotting were essentially performed as described by Sambrook *et al.* (30). Isolated RNAs (30 μg) were electrophoresed on a 1% agarose gel containing 0.6 M formaldehyde, transferred to a nylon membrane, and then hybridized with ^{32}P-labeled probes. Autoradiographed membranes were analyzed using a BAS5000 bioimage analyzer (Fuji Photo Film). A specific system for the amplification of mRNA was also used: an mRNA-selective PCR kit (Takara-Biomedicals; distributed by BioWhittaker, Europe). It had a total volume of 25 μl, comprising 12.5 μl of 2× buffer II, 5 mM $MgCl_2$, 0.5 μM PE1 and PE2, 1 mM each dNTP, 0.4 units of RNAsin (40 units/μl), 0.5 units of Rtase XL (5 units/μl), and 0.5 units of optimized Taq. As material, 1 μg of total RNA extracted from the cells was used. The 330-bp oligonucleotides for GRX (rat GRX sequence, accession number AF167981) were obtained using as a sense primer 5′-GCA TGG CTC AGG AGT TTG TGA ACT GCA AGA TTC AG-3′ and, as an antisense primer, 5′-CCT TTC ATA ACT GCA GAG CTC CAA TCT GCT TCA GC-3′. The 410-bp oligonucleotides for β-actin (rat β-actin sequence, accession number BC063166) were obtained using 5′-GAG CTA TGA GCT GCC TGA CG-3′ and 5′-AGC ATT TGC GGT GCA CGA TG-3′. The 410-bp oligonucleotides for β-actin (human β-actin sequence, accession number NM_001101.2) were obtained using 5′-GAG CTA CGA GCT GCC TGA CG-3′ and 5′-AGC ATT TGC GGT GCA CGA TG-3′. The 325-β oligonucleotides for ERα (rat ERα sequence, accession number AY280663.1) and 280-bp oligonucleotides for ERβ (rat ERβ sequence, accession number U57439) were obtained using 5′-GCT CTT GAC AAA CCC A-3′ and 5′-GCG GCG TTG AAC TCG TAG-3′ and 5′-GGC TGA GGA AAG CAC CTG TC-3′ and 5′-GCG GCG TTG AAC TCG TAG-3′, respectively. Similarly, the sense and antisense primers for the oligonucleotides for human ERα (accession number NM_000125.2) were 5′-GAC TAT GCT TCA GGC TAC C-5′ and 5′-GGT TCC TGT CCA AGA GCA AG-3′, whereas those for human ERβ (accession number NM_001437.1) were 5′-GTG GTC CAT CGC CAG TTA TC-3′ and 5′-GCA CTT CTC TGT CTC CGC AC-3′, respectively. The RT-amplification was carried out as follows: 30 min at 50 °C for the reverse transcription, denaturation for 5 min at 95 °C, and then a succession of 23 (35 for ERs) cycles as follows: 30 s at 95 °C, 40 s at 65 °C (55 °C for ERs), and 90 s at 72 °C. Amplification took place after 5 min at 72 °C.

Determination of Cellular Glutathione Levels—Total GSH and GSSG levels were measured using a total glutathione quantification kit (Dojindo Molecular Technologies, Inc.) according to the manufacturer's directions. Briefly, 5,5′-dithiobis-(2-nitrobenzoic acid) and GSH react to generate 2-nitro-5-thiobenzoic acid. The concentration of GSH in the sample solution was determined by measuring absorbance at 412 nm. For quantification of GSSG, cell lysates were treated with 2-vinylpyridine and triethanolamine to block the sulfhydryl residue of GSH. GSSG in the sample solution was reduced to GSH using a reducing mixture containing GSSG reductase and NADPH, and the levels of GSSG were determined photometrically as for GSH.

3-Phosphoinositide-dependent Protein Kinase-1 Activity—3-Phosphoinositide-dependent protein kinase-1 (PDK1) activity was estimated using an assay kit according to the manufacturer's instructions (Upstate Biotechnology). Briefly, recombinant human active PDK1 (Upstate Biotechnology) protein was incubated first with inhibitors for 30 min at 30 °C and then with inactive glucocorticoid-inducible kinase 1 (SGK1) for 30 min at 30 °C. Next, the PDK1-dependent SGK1 kinase activity was estimated by incubating the reaction mixture with glycogen synthase kinase 3 (GSK3) peptide as a substrate for 10 min at 30 °C in the presence of [γ-^{32}P]ATP.

Generation of Luciferase Reporter Constructs—A 2.0-kb fragment of the human GRX gene promoter (−2023 to −22) (31) was amplified by PCR using *Pfu* turbo DNA polymerase (Stratagene). The primers used were as follows: a forward primer (5′-GGA CTG AGT GAG AGG CAG ACA ATA GTC TCC-3′) and a reverse primer (5′-CGG GAA GAA TCC TCA GTT GCA GGT ATT GCT TGG-3′). The PCR product was subcloned into pUC18 to obtain pUC18-pro-GRX. PUC18-pro-GRX was digested with HindIII, and the resulting fragment containing the promoter region from −2023 to −22 was inserted into the HindIII site of the reporter vector pGL3-Basic (Stratogene) to give pGL3-pro-GRX. To generate a deleted version of the luciferase reporter construct (pGL3-pro-GRX-del), pGL3-pro-GRX was digested with KpnI and PvuII (Takara Biomedicals). Site-directed mutagenesis for luciferase vectors was performed with pGL3-pro-GRX (−2023 to −22) as a template by using a QuikChange site-directed mutagenesis kit (Stratagene). The oligonucleotides used were as follows: electrophoretic response element (EpRE)-like 1 forward (5′-GCT CCC CCT CCG GGA CTC AGA ATC TGG-3′) and EpRE-like 1 reverse (5′-CCA GAT TCT GAG TCC CGG AGG GGG AGC-3′). The nucleotide sequence was confirmed by sequencing with an ALFexpress II system (Amersham Biosciences).

Luciferase Activity Assay—Each vector was introduced into H9c2 cells by using Lipofectamine 2000 (Invitrogen) according to the manufacturer's instructions. After 12 h of transfection, cells were harvested for 24 h and then treated with E_2 (100 nM) or left untreated for 18 h. Then luciferase activity was assayed with cellular extracts by using a dual luciferase reporter assay system (Promega).

Electrophoretic Mobility Shift Assay—The electrophoretic mobility shift assay for the GC box and EpRE-like 1 element was performed as described (32). Briefly, oligonucleotides were annealed to double-stranded oligonucleotides and then labeled with [γ-^{32}P]ATP using T4 polynucleotide kinase. Oligonucleotides specific for the GC box and EpRE-like 1 element were prepared according to the nucleotide sequence of the human GRX promoter region. Oligonucleotides used were as follows: EpRE-like 1 element, 5′-CCC TCC GTG ACT CAG AAT CTG GCT TTC-3′; mutated EpRE-like 1 element, 5′-CCC TCC GGG ACT GTA AGC ACT TTA TGC TTC-3′. Binding reactions were performed in 15 μl of reaction mixture (25 mM Tris, pH 7.0, 6.25 mM $MgCl_2$, 0.5 mM EDTA, 0.5 mM dithiothreitol, 50 mM KCl, and 10% glycerol) containing 10 μg of nuclear extract and 25 ng of labeled oligonucleotide. For the supershift assay, specific antibodies were added to the reaction mixture during the binding reaction for 30 min.

Statistical Analysis—Data were presented as means ± S.D. Differences were examined by using Student's *t* test. A value of $p < 0.05$ was considered significant.

RESULTS

Expression of ERs—The expression of ERs in H9c2 cells was estimated immunohistochemically and genetically. Fig. 1 shows the results of the immunohistochemical analysis. Unlike MCF7 cells, which are known to express both ERα (Fig. 1*A*) and ERβ (Fig. 1*B*), H9c2 cells expressed ERβ (Fig. 1*F*) but not ERα (Fig. 1*E*). Fig. 1*I* shows the results of the RT-PCR

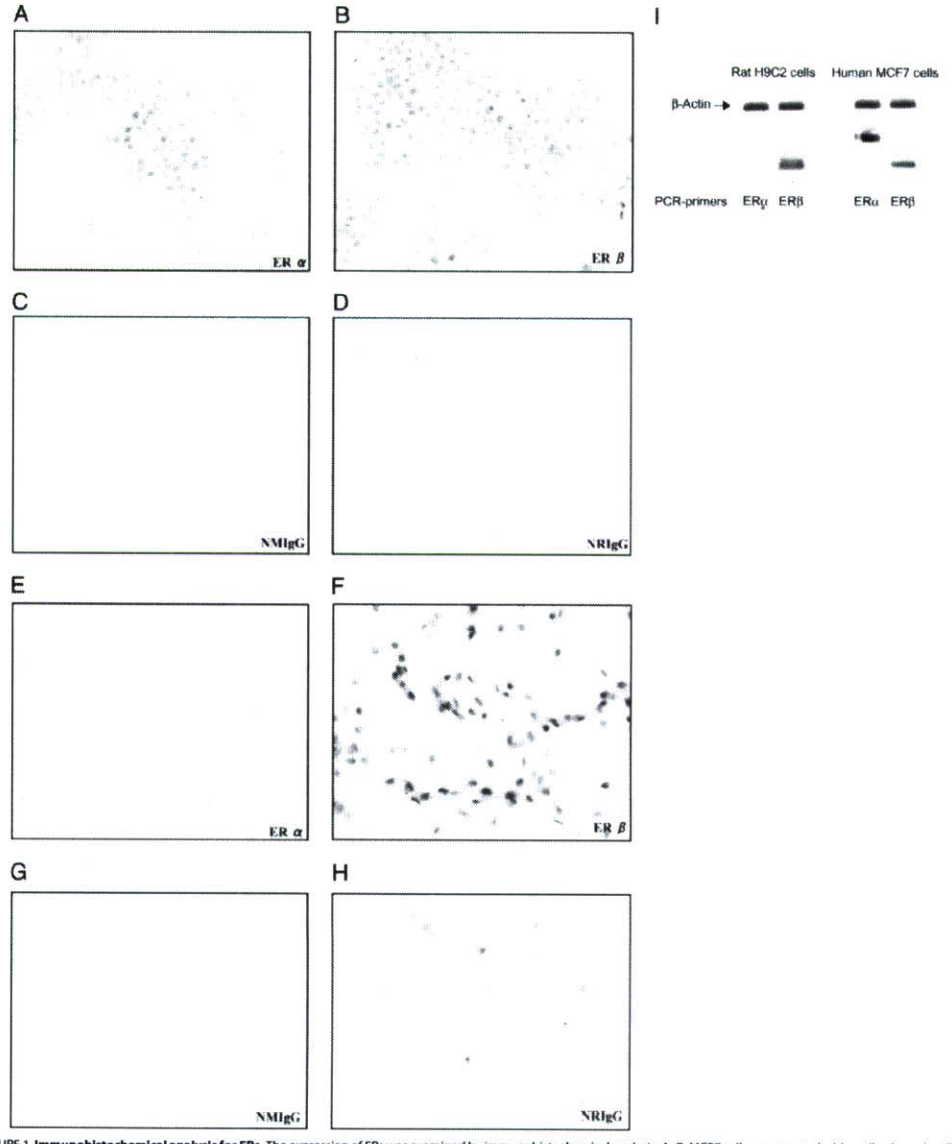

FIGURE 1. **Immunohistochemical analysis for ERs.** The expression of ERs was examined by immunohistochemical analysis. *A–D*, MCF7 cells were treated with antibody against ERα (*A*) and ERβ (*B*). *E–H*, H9c2 cells were treated with antibody against ERα (*E*) and ERβ (*F*). As a negative control, normal mouse IgG (*C* and *G*) or normal rabbit IgG (*D* and *H*) was used. The gene expression of ERs was examined by RT-PCR analysis (*I*) using sense-primers for rat ERα and -β mRNAs in H9c2 cells and those for human mRNA in MCF7 cells.

analysis. ERβ mRNA but not ERα mRNA was detected in H9c2 cells. On the other hand, both ER mRNAs were detected in MCF7 cells.

Cytoprotective Effect of E_2 on Oxidative Stress—We tested the cytoprotective effect of E_2 on oxidative stress-induced apoptosis in H9c2 cells. Hydrogen peroxide induces apoptosis or early mitochondrial dysfunction in cardiac H9c2 cells (32, 33). Since 10% fetal calf serum, required for maintaining cultured cells, reduces oxidative stress modification of cells, in order to observe the effect of E_2 on H_2O_2-induced oxidative stress, the concentration of fetal calf serum in the medium was changed from 10 to 0.5% in the experiments that followed. As shown in

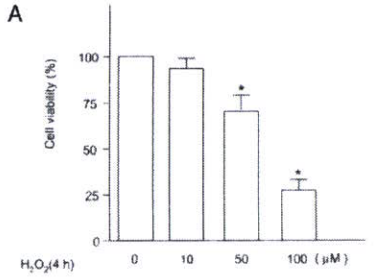

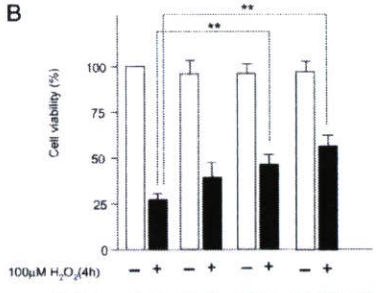

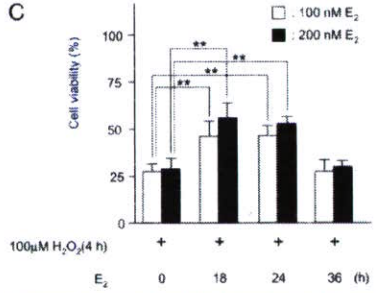

FIGURE 2. **Cytoprotective effect of E_2 on H_2O_2-induced apoptosis.** *A*, viability of H9c2 cells exposed to H_2O_2. Cells were treated with H_2O_2 (0–100 mM) for 4 h, and viability was estimated by the MTT assay. *B*, effect of E_2 on H_2O_2-induced apoptosis. Cells were treated with various concentrations (0–200 nM) of E_2 for 18 h and then with 100 mM H_2O_2 for 4 h. *C*, time course of the cytoprotective effect of E_2. Cells were treated with 100 nM E_2 for 0–36 h and then with 100 mM H_2O_2 for 4 h. The bars express viability (percentage) compared with the cells without H_2O_2. The data are mean ± S.D. of three independent analyses. *, $p < 0.05$ compared with untreated cells; **, $p < 0.05$ compared with cells with H_2O_2 without E_2.

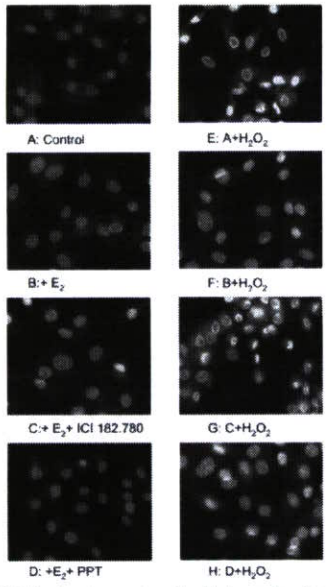

FIGURE 3. **H_2O_2-induced nuclear condensation.** Nuclear condensation was estimated from the PI staining. Cells were treated with 100 nM E_2 for 18 h with or without ICI182,780 (1 μM), a specific inhibitor of ERs, or 0.5 μM PPT (ERα agonist) and then with 100 μM H_2O_2 for 4 h. *A–D*, control cells; *B*, E_2; *C*, E_2 and ICI182,780; *D*, E_2 and PPT. *E–H*, cells treated with H_2O_2; *F*, E_2; *G*, E_2 and ICI182,780; *H*, E_2 and PPT.

Fig. 2*A*, the cell viability decreased by H_2O_2, as assessed photometrically with the MTT assay. The cell viability upon treatment with 100 μM H_2O_2 for 4 h was ~27% of the control. Prior treatment of the cells with 100 and 200 nM E_2 for 18 h prevented the H_2O_2 (100 μM)-induced cell damage by 1.4-fold and 1.8-fold of the control level, respectively (Fig. 2*B*). The increase in cell viability caused by E_2 observed in 18 h continued until 24 h and then declined until 36 h (Fig. 2*C*). Morphologically, H_2O_2-induced DNA condensation was observed (Fig. 3, *A versus E*). E_2 protected against DNA condensation (Fig. 3, *B versus F*). ICI182,780, an ER antagonist, abolished the protective effect of E_2 (Fig. 3, *C versus G*). PPT (0.5 mM), a specific inhibitor of ERα, had no apparent influence on the protective effect of E_2 (Fig. 3, *D versus H*). These results suggest that the protective effect against oxidative stress observed on treatment of the cells with E_2 for 18 h involves transcriptional regulation mediated by ERβ through a genomic pathway in this cell line. Unless otherwise indicated, subsequent experiments on the effect of E_2 were done by incubating the cells with 100 nM E_2 for 18 h.

E_2 Stimulated the Activity of Akt in Response to H_2O_2—The Akt cascade is known to mediate the survival function. The Akt signal is involved in both the genomic (34) and the nongenomic pathway of E_2 (35). We tested the involvement of Akt in the cytoprotective effect of E_2 in ERβ-positive H9c2 cells. Phosphorylation of Akt (Ser^{473}) was promoted by H_2O_2 in 10 min by 1.7-fold, and the control level was reached in 60 min (Fig. 4, *A* and *B*). Prior treatment with E_2 for 18 h resulted in a further increase in the H_2O_2-induced phosphorylation of Akt in 10 min by 4.1-fold, and the phosphorylation continued until 30 min (Fig. 4, *A* and *B*, *lanes 6 versus lanes 2* and *lanes 7 versus lanes 3*, respectively). ICI182,780 abolished the effect of E_2 (Fig. 4, *C* and *D*, *lanes 6 versus lanes 4*). The H_2O_2-induced enhancement of Akt activity estimated using GSK3α/β as a substrate was increased by E_2 (Fig. 4, *E* and *F*, *lanes 5 versus lanes 2* and *lanes 6 versus lanes 3*, respectively), concomitant with the increase in the phosphorylation of Akt. The activity of PDK1, upstream of Akt, was stimulated by H_2O_2; however, E_2 had no apparent effect on the activity of PDK1 (Fig. 4*G*). The phosphorylation of Akt is regulated by PP2A (18). The activity of PP2A assayed spectrophotometrically using RKpTIRR and *p*-nitrophenylphosphate as substrates was not affected by H_2O_2 and E_2 (Fig. 4*H*). The data suggest that the change in the activity of PP2A

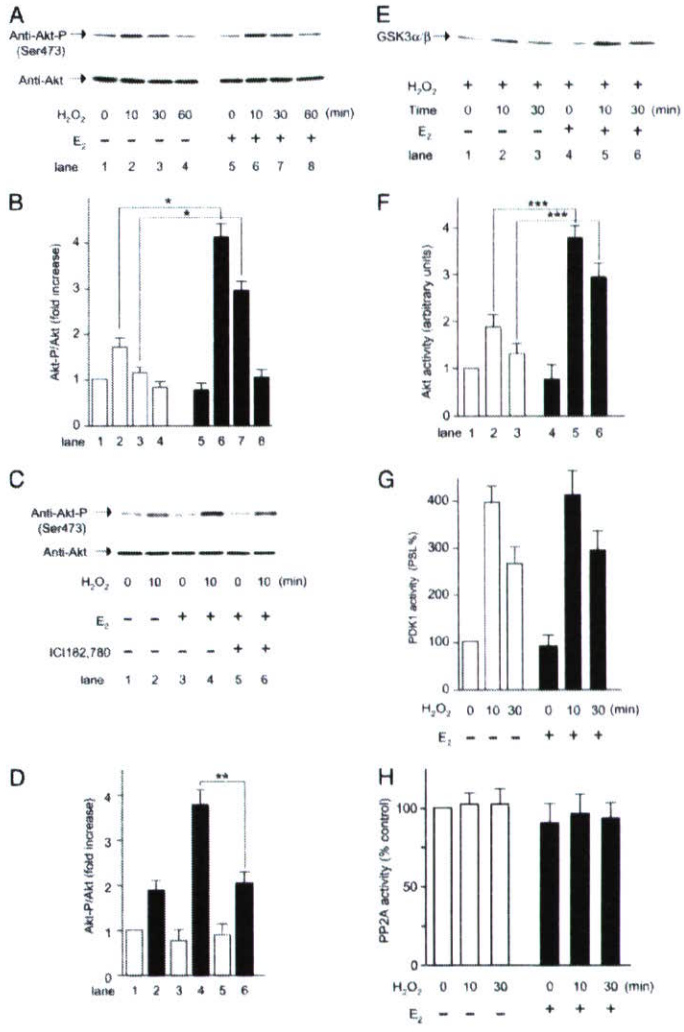

FIGURE 4. **Involvement of phosphorylation of Akt in the cytoprotective effect of E_2 against H_2O_2-induced apoptosis.** *A*, time course of Akt phosphorylation in H9c2 cells under oxidative stress. *C*, cells were treated with 100 nM E_2 in the presence or absence of 1 μM ICI182,780 for 18 h and then with 100 μM H_2O_2 for the period indicated. Phosphorylation of Akt was detected by immunoblot analysis using specific antibodies as described under "Materials and Methods." *B* and *D*, band intensity was estimated densitometrically, and the phosphorylation rates are expressed as the intensity of phosphorylated Akt relative to total Akt (*Akt-p/Akt*). *E*, activity of GSK3α/β. The kinase activity of Akt was measured based on the phosphorylation of GSK3α/β as described under "Materials and Methods." *F*, band intensity was estimated densitometrically, and the phosphorylation rates are expressed as arbitrary units. *G*, the activity of PDK1. The experimental conditions are the same as in *E*. *H*, the activity of PP2A. The activity of PP2A was measured as described under "Materials and Methods." The data are the mean ± S.D. of three independent analyses (*B*, *D*, and *F*). *, $p < 0.05$ compared with cells without E_2 at each time point; **, $p < 0.05$ compared with cells with H_2O_2 and E_2 without ICI182,780; ***, $p < 0.05$ compared with cells with H_2O_2 without E_2 at each time point.

is not involved in the up-regulation of the phosphorylation of Akt by E_2.

It has been reported that inactive Akt develops a redox-sensitive intramolecular disulfide bond close to its activation loop (18), and recently we found that the redox state of Akt is modulated by H_2O_2 (19). Fig. 5*A* shows the redox state of Akt assessed by modifying free thiol with AMS. In control cells, Akt existed mostly in an oxidized form (*lane 1*). Treatment of cells with H_2O_2 resulted in a further increase in an oxidized form of Akt (*lanes 2* and *3*). In the cells treated with E_2 for 18 h, Akt existed more in a reduced form (*lane 4*). The reduced form of Akt, once decreased by H_2O_2 for 30 min, was restored again in 60 min (*lanes 5* and *6*). The data suggested that E_2 maintains Akt in a reduced form under oxidative stress. The redox state of Akt is regulated by the GSH/GRX system, and this system protects cells against H_2O_2-induced apoptosis by preventing the association of Akt with PP2A (19). Then we estimated the effect of E_2 on the phosphorylation of Akt in the presence of buthionine sulfoximine (BSO), a specific inhibitor of γ-GCS, or cadmium, an inhibitor of GRX. γ-GCS is a rate-limiting enzyme of GSH synthesis. The effect of E_2 on the phosphorylation was abolished both by BSO (Fig. 5*B*) and by cadmium (Fig. 5*C*). These results suggest that E_2 increases the levels of GSH/GRX to protect cells against oxidative stress.

E_2 Induces the Expression of γ-GCS and GRX—We tested if E_2 increases the levels of GSH and GRX. E_2 increased the levels of GSH

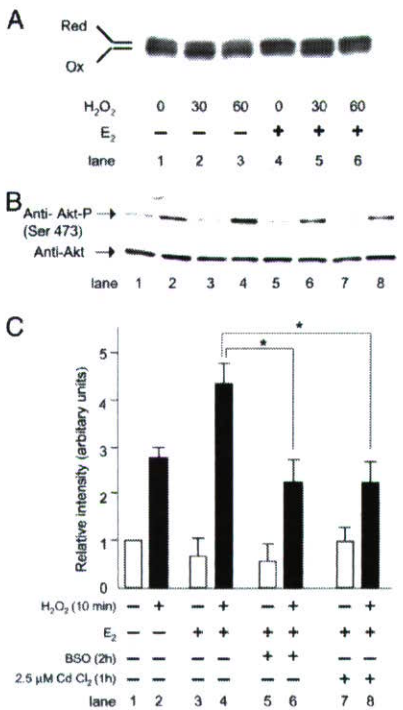

FIGURE 5. **E_2 retains the redox state of Akt.** *A*, the redox state of Akt was assessed based on mobility shifts of these proteins in an immunoblot analysis as described under "Materials and Methods." The positions of reduced (*Red*) and oxidized (*Ox*) proteins are indicated. The data are from a typical analysis. *B*, effect of modification of the redox on the phosphorylation of Akt was estimated, using 200 μM BSO, a specific inhibitor of γ-GCS (*lanes 5* and *6*), and 2.5 μM cadmium, an inhibitor of GRX (*lanes 7* and *8*). *C*, the activity of Akt phosphorylation is shown as relative intensity in the absence (*open bar*) and presence of H_2O_2 (*closed bar*). The data are the mean ± S.D. of three independent analyses. *, $p < 0.05$ compared with cells with H_2O_2 and E_2 without inhibitors.

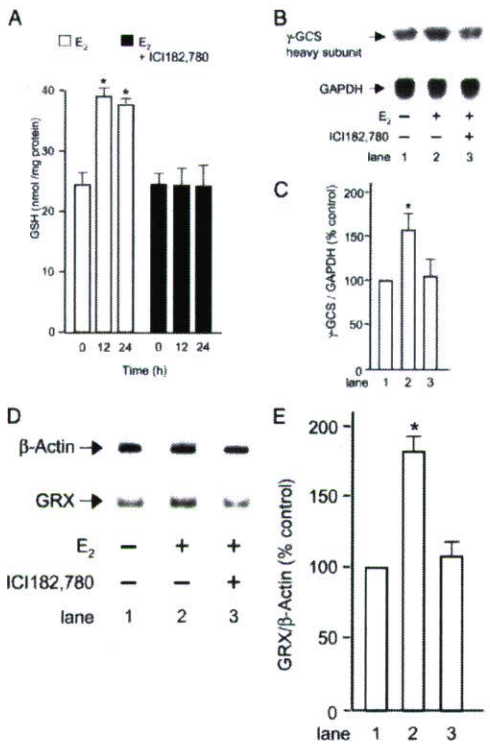

FIGURE 6. **GSH synthesis and GRX.** Effects of E_2 on levels of GSH, the γ-GCS heavy subunit, and GRX were estimated in the presence or absence of ICI182,780, as described under "Materials and Methods." *A*, cells were treated with 100 nM E_2 for 0–24 h, and the levels of GSH in the cell lysates were estimated. Cells were incubated with 100 nM E_2 for 6 h for the analysis of the expression of the γ-GCS heavy subunit by Northern blotting (*B*) and that of GRX by RT-PCR (*D*). The expression of γ-GCS was expressed as relative intensity (percentage of control) (*C*), and that of GRX was expressed as the intensity of GRX/β-actin (*E*). Each datum is a mean ± S.D. of three independent analyses. *, $p < 0.05$ compared with untreated cells.

(Fig. 6*A*). The level of GSH was 24.8 ± 4.0 nmol/10^6 cells in control cells and 38.5 ± 5.2 nmol/10^6 cells in cells treated with 100 nM E_2 for 18 h. The level of GSSG in the control cells was ~2 nmol/10^6 cells and was not changed by E_2 treatment (data not shown). The expression of γ-GCS was up-regulated by 100 nM E_2 by 1.6-fold in 18 h (Fig. 6, *B* and *C*). Similarly, 100 nM E_2 increased the expression of GRX by 1.8-fold in 18 h (Fig. 6, *D* and *E*). ICI182,780 abolished the E_2-dependent up-regulation of GSH synthesis as well as GRX synthesis (Fig. 6, *A–E*). It is suggested that the redox state of Akt is regulated by an E_2-dependent enhancement of the GRX/GSH system.

The Gene Promoter Activity of GRX Is Regulated by E_2 via an EpRE-like Element—As reported by Montano *et al.* (7), the expression of the γ-GCS heavy (catalytic) subunit is up-regulated by E_2 via an EpRE (5′-(G/A)TGACNNNGC(G/A)-3′), not by an ERE. To investigate the mechanism of the transcriptional regulation of GRX by E_2, we used a 2.0-kb genomic fragment containing the promoter region of GRX inserted into a luciferase vector, pGL3 Basic. The promoter region contains no apparent ERE or EpRE. There were two EpRE-like sites (EpRE-like 1 (−1380 to −1370; GTGACTCAGAA) and EpRE-like 2 (−347 to −337; GTGAGTAAGCA)) and Sp1 (−1217 to −1208, GCCCCGCCTC). The luciferase activity of the cells previously treated with E_2 for 18 h was almost lost when the EpRE-like 1 site was deleted or mutated (Fig. 7). Deletion of EpRE-like 2 or Sp1 had no apparent effect on the E_2-induced up-regulation of the luciferase activity.

E_2 Up-regulated the ERβ-EpRE-like 1 Complex Formation—To investigate the importance of the EpRE-like elements in the E_2-induced expression of GRX, an electrophoretic mobility shift assay was performed with nuclear extracts from the cells treated with E_2 for 18 h using ^{32}P-labeled oligonucleotides designed for EpRE-like 1. As shown in Fig. 8, a protein-DNA complex of EpRE-like 1 (*lane 2*) increased by E_2 (*lane 3*) and appeared in the presence of an excess of unlabeled probe (*lane 4*), or ^{32}P-labeled probe with the disabled mutant for EpRE-like 1 (*lane 5*). The addition of the anti-ERβ antibody caused the ERβ-DNA-binding complex to disappear (*lane 12*), indicating the involvement of ERβ as a transcription factor that bound to the EpRE-like 1 site. The EpRE-like 1 of GRX did not bind with Nrf2, Sp1, c-Jun, or c-Fos (*lanes 9–11*), different from the EpRE site of the γ-GCS heavy subunit (7). On the other hand, neither EpRE-like 2 site nor the Sp1 site was stimulated by E_2 (data not shown).

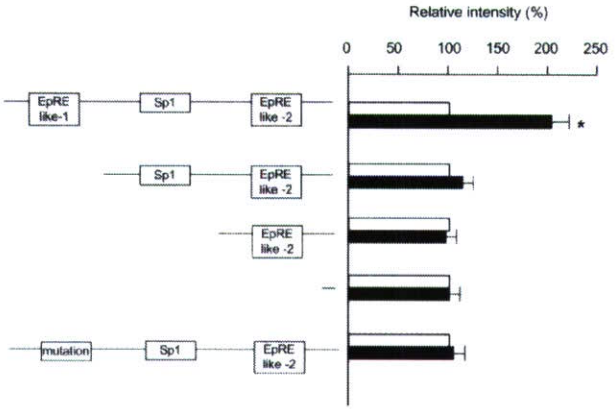

FIGURE 7. **The EpRE-like element is important for the E_2-dependent induction of the GRX promoter in H9c2 cells.** *Left*, schematic representation of luciferase vector constructs for the human GRX promoter. Each luciferase vector construct was generated as described under "Materials and Methods." *Right*, luciferase activity of the vector constructs for the human GRX gene promoter in H9c2 cells. The cells were transiently transfected with the GRX promoter-luciferase gene fusion plasmids. After the transfection, luciferase activity was assayed with cellular extracts as described under "Materials and Methods." Each value represents the mean of at least three independent experiments, and the S.D. was always within 10% of the mean. *, $p < 0.05$ compared with control.

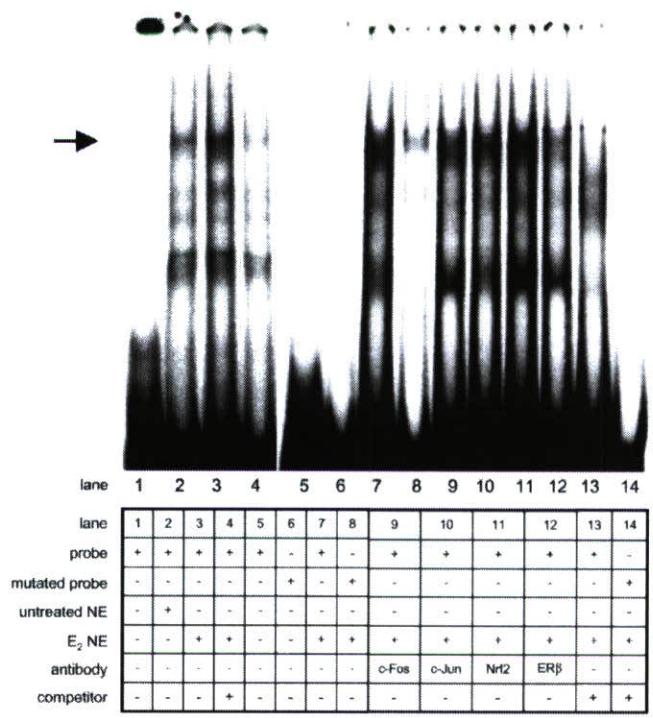

FIGURE 8. **The EpRE-like 1 element is responsive to E_2 in electrophoretic mobility shift assays.** H9c2 cells were incubated with 100 nM E_2 for 18 h, and the nuclear extracts were prepared as described under "Materials and Methods." ^{32}P-Labeled oligonucleotides specific to EpRE-like elements 1 and 2 of the GRX gene promoter were prepared and incubated with each nuclear extract and then subjected to a 5% nondenatured PAGE. In *lanes 1*, *5*, and *6*, the nuclear extract (*NE*) was free. In *lanes 6*, *8*, and *14*, ^{32}P-labeled mutant oligonucleotides were used. In *lanes 9–12*, *+Ab*, specific antibodies were added to the reaction mixture during the binding reaction for the supershift assay. *Arrowhead*, protein-DNA complex.

Important Role of ERβ in Other Cells—To further confirm the role of ERβ in protection against oxidative stress through redox regulation of Akt, we employed human breast cancer cells, SK-BR-3 and MDA-MB-231 cells. As shown in Fig. 9*A*, an RT-PCR analysis revealed that these cells mainly expressed ERβ mRNA. A stimulatory effect of E_2 on the activity of Akt was observed in these cells (Fig. 9, *B* and *C*). However, ICI182,780 abolished the protective effect of E_2 (Fig. 9, *B* and *C*). E_2 induced the expression of GRX (Fig. 9, *D* and *E*). The results suggested that the cytoprotective effect of E_2 is mediated through redox regulation of Akt activity in ERβ-expressing cells.

DISCUSSION

ERβ-mediated Cytoprotection against Oxidative Stress—Estrogenic hormones are required for the growth and differentiation of female

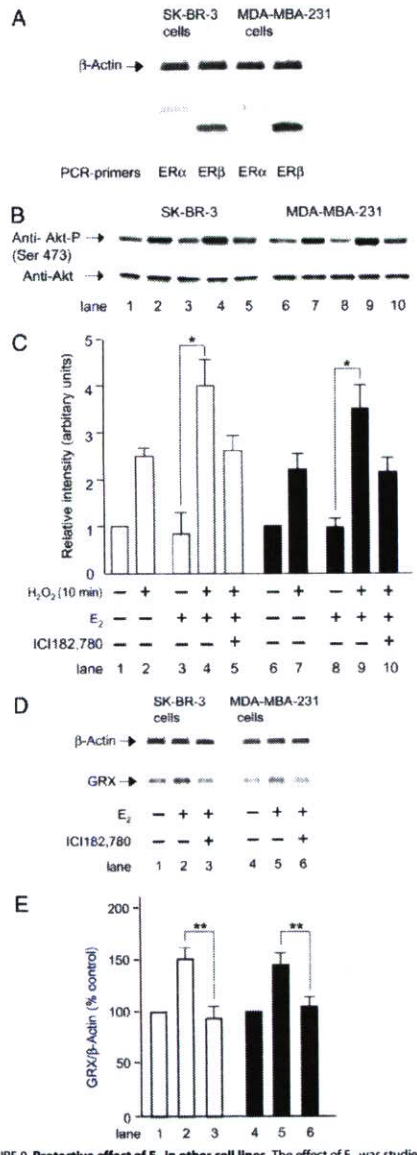

FIGURE 9. **Protective effect of E_2 in other cell lines.** The effect of E_2 was studied using ERβ-expressing human breast cancer SK-BR-3 cells and MDA-MB-231 cells. *A*, expression of ERs. The gene expression of ERs was estimated by RT-PCR analysis as described in the legend to Fig. 1. *B*, phosphorylation of Akt. The effect of E_2 on the phosphorylation of Akt under oxidative stress was estimated by immunoblot analysis using specific antibodies as described under "Materials and Methods." *C*, band intensity was estimated densitometrically, and the phosphorylation rates are expressed as the relative intensity of phosphorylated Akt to total Akt (*Akt-p/Akt*). The data are the mean ± S.D. of three independent analyses (*B* and *D*). *D*, gene expression of GRX. The effect of E_2 on levels of the GRX was estimated as described under "Materials and Methods." *E*, band intensity was estimated densitometrically and expressed as the intensity of GRX/β-actin. Each datum is a mean ± S.D. of three independent analyses. *, $p < 0.05$ compared with cells with H_2O_2 without E_2; **, $p < 0.05$ compared with cells with E_2 without ICI182,780.

reproductive tissues, contribute to male fertility, and play a role in maintaining cardiovascular, skeletal, and neural cell functions (9). Estrogen has been widely used to regulate fertility, relieve postmenopausal symptoms, and decrease the incidence and recurrence of mammary tumors. The ERs were the first members of the nuclear receptor family to be identified. ERα has been well characterized and plays a major role in E_2-mediated genomic actions in both reproductive and nonreproductive tissues. ERα-mediated cytoprotection against oxidative stress-induced cell damage has been reported in neurological cells (33, 34) and breast cancer cells (35). On the other hand, the role of ERβ is not well understood. A report using microarray analyses showed that most of the genes regulated by ERβ are distinct from those regulated by ERα in response to E_2 and selective estrogen receptor modulators (36). ERβ regulates plasminogen activator inhibitor-1 in endothelial cells, and a clinical evaluation of ERβ was suggested as a prognostic or predictive factor of drug resistance in breast cancer (37). These results suggest a significant role for ERβ in the regulation of cellular function, although the function of ERβ and its precise mechanism are still unclear (3). Thus, this is the first report aimed at the significant role of ERβ-mediated signals of E_2 in redox regulation in response to oxidative stress.

Involvement of Akt in the Cytoprotection of E2 Mediated by ERβ—The importance of Akt has been suggested in the cytoprotective effect of E_2 against oxidative stress. This effect of E_2 was rapid and nongenomic in neurological cells (38), vascular endothelial cells (39), and ovarian cancer cells (40). On the other hand, Stoica *et al.* (41) reported that ERα-mediated signals up-regulated the expression of Akt in ERα-positive MCF-7 breast cancer cells. They also demonstrated that Akt-mediated signals up-regulated the expression of ERα in these cells, suggesting that Akt plays a central role in the growth and survival of breast cancer cells; however, the mechanism by which Akt is activated by E_2 was not fully characterized.

In the present study, we were interested in the possible involvement of Akt signals in the ERβ-mediated anti-apoptotic effect against oxidative stress. We employed H9c2 cells that apparently express only ERβ (Fig. 1). We found that 1) H_2O_2-induced apoptosis was prevented when the cells were incubated with E_2 for over 18 h; 2) the anti-oxidative effect of E_2 was mediated by a genomic pathway through ERβ; and 3) E_2 retained the level of phosphorylated Akt in response to H_2O_2 via the GSH/GRX system.

Role of the GSH/GRX System in ERβ-mediated Akt Signals—We reported previously a role for the GRX/GSH system in the regulation of Akt phosphorylation (19). Akt is a Ser/Thr protein kinase with anti-apoptotic and oncogenic activities. Akt is activated through a growth factor receptor-mediated activation of the phosphatidylinositol 3-kinase pathway (21). The unphosphorylated form of Akt is virtually inactive, and phosphorylation at Thr^{308} and Ser^{473} stimulates its activity. Inactivation of Akt also occurs via dephosphorylation of the two phosphorylation sites by PP2A (23, 24). The activation of Akt contributes to the survival of H_2O_2-treated cells (25). H_2O_2 induces oxidation of Akt at Cys^{297} and Cys^{311}, and the oxidized form of Akt can be dephosphorylated by PP2A (19). PP2A is a major Ser/Thr phosphatase implicated in the regulation of many cellular processes, including the regulation of different signal transduction pathways, cell cycle progression, DNA replication, gene transcription, and protein translation (42). Yasukawa *et al.* have reported that Akt is also inactivated by *S*-nitrosylation at Cys^{224} in NO donor-treated cells (43). Furthermore, we recently reported that the phosphorylation of Akt is down-regulated by cytoplasmic calcium (32). Calcium induced the expression of the PP2A catalytic subunit mediated by cAMP via the cAMP-response element. In the present study, the activity and the expression of the anti-PP2A catalytic C subunit did not change upon treatment with E_2 in H9c2 cells (Fig. 4*H*), suggesting that the modulation of calcium levels may not be involved. Inactivation by ROS of protein phosphatases, such as protein-tyrosine phosphatase 1B (44), mitogen-activated protein kinase (MAPK) phosphatases (45), and PP2A (46), has been reported. In the present study, the activity of PP2A was not changed by H_2O_2 (Fig. 4*H*), suggesting that inactivation of PP2A by ROS is not involved. The redox state of Akt is regulated by GSH/GRX (19). Oxidation of Akt at Cys^{297} and Cys^{311} facilitates the association of PP2A, leading to the dephosphorylation of Akt. However, the activity of Akt is not affected by the oxidation. In the present study, oxidation of Akt was observed in the medium with 0.5% fetal calf serum in the absence of H_2O_2, and after the treatment with H_2O_2, the oxidation of Akt continued for 60 min. In such conditions, E_2 maintained Akt in the reduced form (Fig. 5). This suggested that E_2 potentiates the functions of the GSH/GRX system. The GSH/GRX system regulates many signals, such as ASK-1, NF1, PTP1B, protein kinase C, and protein kinase A (49). The present study indicates for the first time that ERβ-mediated signaling via E2 up-regulates the activity of the GSH/GRX system to stimulate Akt and protects cells against oxidative stress.

Up-Regulation of γ-GCS and GRX by E_2—The ERα-mediated expression of antioxidants in response to oxidative stress has been reported. Genomic effects on the expression of antioxidant enzymes reported were Mn-SOD (4, 6), Cu,Zn-SOD (6), COX-1 (47), and COX-2 (5). Induction of GRX expression by E_2 was reported in bovine aortic endothelial cells (48) and in female mice (34). These reports suggested a potential contribution of TRX and GRX to the protection of cells against oxidative stress. As to ERβ, the expression of γ-GCS induced by E_2 was reported to be mediated by ERβ (7) in breast epithelial cell lines.

In the present study, we found that the expression of both GRX and γ-GCS is up-regulated by E_2 in ERβ-expressing cells. Data on the induction of the γ-GCS heavy subunit (Fig. 6, *B* and *C*) together with an increase in the level of GSH obtained here (Fig. 6*A*) is consistent with such a contribution. Furthermore, E_2 up-regulated the expression of GRX (Fig. 6, *D* and *E*). Elevated levels of both GSH and GRX were necessary to retain the reduced form of Akt. BSO abolished the effect of E_2 on the phosphorylation of Akt (Fig. 5*B*), and cadmium also abolished the effect of E_2 (Fig. 5*C*). The up-regulation of γ-GCS as well as GRX expression by E_2 was abolished by ICI182,780 (Fig. 6, *A–E*), suggesting involvement of the ERβ-mediated genomic effect of E_2. The possible role of ERβ in the cytoprotection against oxidative stress was supported by the results obtained using other ERβ-expressing cells (Fig. 9). Although involvement of ERα in the cytoprotective effect of E_2 cannot be ruled out in these cells, it is suggested that the GRX/GSH system is involved in the cytoprotective and genomic effects of E_2 on the redox state of Akt, a pathway that is mediated, at least in part, by ERβ. This mechanism may also play an antiapoptotic role in cancer cells during carcinogenesis or chemotherapy. A difference in the distribution of ERα and ERβ was reported (3, 27, 50, 51). ERα and ERβ differ in the distribution in tissue cells and how they regulate cell proliferation and apoptosis, which may provide some insight into the tissue-specific functions and interplay between the two receptors.

The role of the GSH/GRX redox system in the antiapoptotic effect of E_2 was studied further. In the present study, we found that the induction of GRX expression by E_2 is mediated by an EpRE-like 1 element (Figs. 7 and 8). The human GRX promoter employed here possessed no apparent ERE or EpRE but had two EpRE-like sites. Interestingly, one of these sites, EpRE-like 1, bound to ERβ and promoted the transcriptional activity of GRX. Transcription of the GRX gene was increased by E_2 but decreased by anti-ERβ antibody. However, EpRE-like 1 did not bind to Nrf-2 or AP-1. This element may be a novel kind of ERE. In summary, E_2 has a cytoprotective effect against oxidative stress in H9c2 cells expressing ERβ. The genomic effect of E_2 on the GSH/GRX redox system potentiates Akt activity, a mechanism that may also play an antiapoptotic role in cancer cells during carcinogenesis or chemotherapy.

Acknowledgment—We are grateful to Takaaki Kohno for excellent technical assistance.

REFERENCES

1. Berlett, S. B., and Stadtman, E. R. (1997) *J. Biol. Chem.* **272,** 20313–20316
2. Finkel, T., and Holbrook, N. J. (2000) *Nature* **408,** 239–247
3. Yang, S. H., Liu, R., Perez, E. J., Wen, Y., Stevens, S. M., Jr., Valencia, T., Brun-Zinkernagel, A. M., Prokai, L., Will, Y., Dykens, J., Koulen, P., and Simpkins, J. W. (2004) *Proc. Natl. Acad. Sci. U. S. A.* **101,** 4130–4135
4. Baba, T., Shimizu, T., Suzuki, Y., Ogawara, M., Isono, K., Koseki, H., Kurosawa, H., and Shirakawa, T. (2005) *J. Biol. Chem.* **280,** 16417–16426
5. Egan, K. M., Lawson, J. A., Fries, S., Koller, B., Rader, D. J., Smyth, E. M., and Fitzgerald, G. A. (2004) *Science* **306,** 1954–1957
6. Strehlow, K., Rotter, S., Wassmann, S., Adam, O., Grohe, C., Laufs, K., Bohm, M., and Nickenig, G. (2003) *Circ. Res.* **93,** 170–177
7. Montano, M. M., Deng, H., Liu, M., Sun, X., and Singal, R. (2004) *Oncogene* **23,** 2442–2453
8. Beato, M., Herrlich, P., and Schutz, G. (1995) *Cell* **83,** 851–857
9. Schultz, J. R., Petz, L. N., and Nardulli, A. M. (2005) *J. Biol. Chem.* **280,** 347–354
10. Foster, C., Keitz, S., Hultenby, K., Warner, M., and Gustafsson, J. A. (2004) *Proc. Natl. Acad. Sci. U. S. A.* **101,** 14234–14239
11. Holmgren, A. (1989) *J. Biol. Chem.* **264,** 13963–13966
12. Meister, A. (1973) *Science* **180,** 33–39
13. Holmgren, A. (1976) *Proc. Natl. Acad. Sci. U. S. A.* **73,** 2275–2279
14. Gan, Z.-R., and Wells, W. W. (1986) *J. Biol. Chem.* **261,** 996–1001
15. Gravina, S. A., and Mieyal, J. J. (1993) *Biochemistry* **32,** 3368–3376
16. Song, J. J., Rhee, J. G., Suntharalingam, M., Walsh, S. A., Spitz, D. R., and Lee, Y. J. (2002) *J. Biol. Chem.* **277,** 46566–46575
17. Song, J. J., and Lee, Y. J. (2003) *Biochem. J.* **373,** 845–853
18. Murata, H., Ihara, Y., Nakamura, H., Yodoi, J., Sumikawa, K., and Kondo, T. (2003) *J. Biol. Chem.* **278,** 50226–50233
19. Huang, X., Begley, M., Morgenstern, K. A., Gu, Y., Rose, P., Zhao, H., and Zhu, X. (2003) *Structure (Camb.)* **11,** 21–30
20. Brazil, D. P., and Hemmings, B. A. (2001) *Trends Biochem. Sci.* **26,** 657–664
21. Franke, T. F., Hornik, C. P., Segev, L., Shostak, G. A., and Sugimoto, C. (2003) *Oncogene* **22,** 8983–8998
22. Luikenhuis, S., Perrone, G., Dawes, I. W., and Grant, C. M. (1998) *Mol. Biol. Cell* **9,** 1081–1091
23. Andjelkovic, M., Jakubowicz, T., Cron, P., Ming, X. F., Han, J. W., and Hemmings, B. A. (1996) *Proc. Natl. Acad. Sci. U. S. A.* **93,** 5699–5704
24. Pham, F. H., Sugden, P. H., and Clerk, A. (2000) *Circ. Res.* **86,** 1252–1258
25. Hayashi, S., Hajiro-Nakanishi, K., Makino, Y., Eguchi, H., Yodoi, J., and Tanaka, H. (1997) *Nucleic Acids Res.* **25,** 4035–4040
26. Goto, S., Kamada, K., Soh, Y., Ihara, Y., and Kondo, T. (2002) *Jpn. J. Cancer Res.* **93,** 1047–1056
27. Tamaru, N., Hishikawa, Y., Ejima, K., Nagasue, N., Inoue, S., Muramatsu, M., Hayashi, T., and Koji, T. (2004) *Lab. Invest.* **84,** 1460–1471
28. Kobayashi, T., Kishigami, S., Sone, M., Inokuchi, H., Mogi, T., and Ito, K. (1997) *Proc. Natl. Acad. Sci. U. S. A.* **94,** 11857–11862
29. Iida, T., Kijima, H., Urata, Y., Goto, S., Ihara, Y., Oka, M., Kohno, S., Scanlon, K. J., and Kondo, T. (2001) *Cancer Gene Ther.* **8,** 803–814
30. Sambrook, J., Fritsch, E. F., and Maniatis, T. (1989) *Molecular Cloning: A Laboratory Manual*, 2nd Ed., Cold Spring Harbor Laboratory, Cold Spring Harbor, NY
31. Padilla, C. A., Bajalica, S., Lagercrantz, J., and Holmgren, A. (1996) *Genomics* **32,** 455–457
32. Yasuoka, C., Ihara, Y., Ikeda, S., Miyahara, Y., Kondo, T., and Kohno, S. (2004) *J. Biol. Chem.* **279,** 51182–51192
33. Prokai, L., Prokai-Tatrai, K., Perjesi, P., Zharikova, A. D., Perez, E. J., Liu, R., and Simpkins, J. W. (2003) *Proc. Natl. Acad. Sci. U. S. A.* **100,** 11741–11746
34. Kenchappa, R. S., Diwakar, L., Annepu, J., and Ravindranath, V. (2004) *FASEB J.* **18,** 1102–1104
35. Fernando, R. I., and Wimalasena, J. (2004) *Mol. Biol. Cell* **15,** 3266–3284

36. Tee, M. K., Rogatsky, I., Tzagarakis-Foster, C., Cvoro, A., An, J., Christy, R. J., Yamamoto, K. R., and Leitman, D. C. (2004) *Mol. Biol. Cell* **15,** 1562–1572
37. Smith, L. H., Coats, S. R., Coats, S. R., Qin, H., Petrie, M. S., Covington, J. W., Su, M., Eren, M., and Vaughan, D. E. (2004) *Circ. Res.* **95,** 269–275
38. Yu, X., Rajala, R. V., McGinnis, J. F., Li, F., Anderson, R. E., Yan, X., Li, S., Elias, R. V., Knapp, R. R., Zhou, X., and Cao, W. (2004) *J. Biol. Chem.* **279,** 13086–13094
39. Lu, Q., Pallas, D. C., Surks, H. K., Baur, W. E., Mendelsohn, M. E., and Karas, R. H. (2004) *Proc. Natl. Acad. Sci. U. S. A.* **101,** 17126–17131
40. Mabuchi, S., Ohmichi, M., Kimura, A., Nishio, Y., Arimoto-Ishida, E., Yada-Hashimoto, N., Tasaka, K., and Murata, Y. (2004) *Endocrinology* **145,** 49–58
41. Stoica, G. E., Franke, T. F., Moroni, M., Mueller, S., Morgan, E., Iann, M. C., Winder, A. D., Reiter, R., Wellstein, A., Martin, M. B., and Stoica, A. (2003) *Oncogene* **22,** 7998–8011
42. Janssens, V., Goris, J., and Van Hoof, C. (2005) *Curr. Opin. Genet. Dev.* **15,** 34–41
43. Yasukawa, T., Tokunaga, E., Ota, H., Sugita, H., Martyn, J. A., and Kaneki, M. (2005) *J. Biol. Chem.* **280,** 7511–7518
44. Salmeen, A., Andersen, J. N., Myers, M. P., Meng, T. C., Hinks, J. A., Tonks, N. K., and Barford, D. (2003) *Nature* **423,** 769–773
45. Kamata, H., Honda, S., Maeda, S., Chang, L., Hirata, H., and Karin, M. (2005) *Cell* **120,** 649–661
46. Rao, R. K., and Clayton, L. W. (2002) *Biochem. Biophys. Res. Commun.* **293,** 610–616
47. Gibson, L. L., Hahner, L., Osborne-Lawrence, S., German, Z., Wu, K. K., Chambliss, K. L., and Shaul, P. W. (2005) *Circ. Res.* **96,** 518–525
48. Ejima, K., Nanri, H., Araki, M., Uchida, K., Kashimura, M., and Ikeda, M. (1999) *Eur. J. Endocrinol.* **140,** 608–613
49. Shelton, M. D., Chock, P. B., and Mieyal, J. J. (2005) *Antioxid. Redox Signal.* **7,** 348–366
50. Helguero, L. A., Fauld, M. H., Guslafsson, J. A., and Haldosen, L. A. (2005) *Oncogene* **24,** 6605–6616
51. Connor, E. E., Wood, D. L., Sonstegard, T. S., da Mota, A. F., Bennet, G. L., and Williams, J. L. (2005) *J. Endocrinol.* **185,** 593–603

Histochem Cell Biol (2006) 126: 111–123
DOI 10.1007/s00418-005-0141-6

ORIGINAL PAPER

**Keiko Shukuwa · Shin-ichi Izumi · Yoshitaka Hishikawa
Kuniaki Ejima · Satoshi Inoue · Masami Muramatsu
Yasuyoshi Ouchi · Takashi Kitaoka · Takehiko Koji**

Diethylstilbestrol increases the density of prolactin cells in male mouse pituitary by inducing proliferation of prolactin cells and transdifferentiation of gonadotropic cells

Accepted: 20 December 2005 / Published online: 9 February 2006

Abstract Diethylstilbestrol (DES) has been implicated in mammalian abnormalities. We examined the effects of DES on follicle-stimulating hormone (FSH), luteinizing hormone (LH), and prolactin (PRL) cells in the pituitaries of male mice treated with various doses of DES for 20 days. DES reduced the density of FSH and LH cells in a dose-dependent manner, but increased that of PRL cells. When the expression of estrogen receptor (ER) α and β was assessed, an induction of ERβ by DES was found predominantly in PRL cells. However, since these effects were abolished in ERα knockout mice, DES appears to act primarily through ERα. When the expression of Ki-67 and Pit-1 in PRL cells was examined at various time-points after DES treatment, some PRL cells became Ki-67 positive at 10–15 days, and Pit-1-positive cells were increased at 5–15 days. Furthermore, some FSH and LH cells became Pit-1 positive, and co-localized with PRL at 5–10 days. Our results indicate that DES increases PRL cells by inducing proliferation of PRL cells and transdifferentiation of FSH/LH cells to PRL cells.

Keywords Diethylstilbestrol · Pituitary · Prolactin · Estrogen receptors · Pit-1

K. Shukuwa · Y. Hishikawa · K. Ejima · T. Koji (✉)
Division of Histology and Cell Biology,
Department of Developmental and Reconstructive Medicine,
Nagasaki University Graduate School of Biomedical Sciences,
1-12-4 Sakamoto, 852-8523 Nagasaki, Japan
E-mail: tkoji@net.nagasaki-u.ac.jp
Tel.: +81-95-8497025
Fax: +81-95-8497028

S. Izumi
Division of Oral Cytology and Cell Biology,
Department of Developmental and Reconstructive Medicine,
Nagasaki University Graduate School of Biomedical Sciences,
852-8588 Nagasaki, Japan

T. Kitaoka · K. Shukuwa
Department of Ophthalmology and Visual Sciences,
Nagasaki University Graduate School of Biomedical Sciences,
852-8501 Nagasaki, Japan

S. Inoue · Y. Ouchi
Department of Geriatric Medicine, Graduate School of Medicine,
The University of Tokyo, 113-8655 Tokyo, Japan

M. Muramatsu
Research Center for Genomic Medicine, Saitama Medical School,
350-1241 Saitama, Japan

Introduction

Diethylstilbestrol (DES), a stilbene estrogen analogue acting as an agonist of estrogen, causes structural abnormalities in reproductive organs, infertility, and neoplasia in mammals (McLachlan et al. 1980). In the pituitary, it is known that treatment with DES causes pituitary hyperplasia followed by the development of prolactinomas (Walker and Kurth 1993), and DES increased the prolactin (PRL) cell population in rodent pituitaries (Cauwenberge et al. 2001; Matsubara et al. 2001). However, the precise mechanism of DES effect on pituitary cells remains unclear.

Estrogens play various roles in the pituitary, affecting the states of proliferation of certain cell populations (Hashi et al. 1996) and their hormone production (Scully et al. 1997). The effects of estrogens are mediated through estrogen receptors (ERs), ligand-dependent transcription regulatory factors (Osborne et al. 2000). ERs bind to estrogen responsive element (ERE) in the promoter region of some genes, such as follicle-stimulating hormone (FSH), luteinizing hormone (LH), and PRL (Maurer and Notides 1987; Shupnik and Rosenzweig 1991), and regulate their expression (Osborne et al. 2000). Currently, ER is categorized into two subtypes, ERα and β. The classical ER, ERα, is distributed in various reproductive organs as well as pituitary (McClellan et al. 1984; Greene et al. 1984; Koji and Brenner 1993; Friend et al. 1994). Furthermore, ERβ, a newly identified ER, was cloned in the rat prostate and ovary (Kuiper et al. 1996). Much attention has been

recently paid to the analysis of expression of both ERs in various tissues, including reproductive organs (Pelletier and El-Alfy 2000; Tsurusaki et al. 2003), and intestine (Kawano et al. 2004). In the rodent pituitary, ERα is distributed in many anterior pituitary cell types, including FSH, LH, and PRL cells (Mitchner et al. 1998), and plays a critical role in transcription of these genes (Scully et al. 1997). On the other hand, there is still a controversy about the localization and characterization of ERβ (Mitchner et al. 1998; Nishihara et al. 2000). Since ERs bind to ERE as homodimers or heterodimers (Petterson et al. 1997), a different pattern of gene regulation might be raised.

The expression of PRL gene is also regulated by a pituitary-specific transcription factor, referred to as Pit-1 (Ingraham et al. 1988; Crewshaw et al. 1989). Since Pit-1 can bind to PRL, growth hormone (GH), and thyroid-stimulating hormone (TSH) gene promoters, it is responsible for the transcriptional activation of genes for these hormones (Fox et al.1990; Lloyd and Osamura 1997). In mouse PRL gene promoter, Pit-1 binds to four sites within the distal enhancer and further four sites within the proximal region, thereafter activates the cell-type specific expression of PRL gene (Crewshaw et al. 1989). Therefore, the cellular analysis of Pit-1 expression would provide useful information on the promotion of PRL cell differentiation. However, our knowledge of the affection of estrogens on the PRL cell differentiation is still largely limited.

In the present study, we first investigated the effect of DES on the expression of sex-related pituitary hormones and its correlation with ERs in wild-type and ERα knockout (ERαKO) male mice. For this purpose, we quantitatively measured the effects of in vivo treatment of various doses of DES on the density of pituitary cells positive for these hormones and ERs. Second, to gain further insight into the kinetics of PRL cells, we examined the expression of Ki-67, which is regarded as a marker of the proliferative activity, and Pit-1 at various time-points after DES treatment by immunohistochemistry and Southwestern histochemistry, respectively. The results indicated that DES actions are mediated through ERα, and that DES increased the density of PRL cells by enhancing their proliferation and induction of transdifferentiation of FSH/LH cells to PRL cells.

Materials and methods

Chemicals and biochemicals

DES was purchased from ICN Biomedical (Aurora, OH, USA). Sodium dodecyl sulfate-polyacrylamide gel electrophoresis (SDS-PAGE) reagents were purchased from Daiichi Pure Chemicals (Tokyo, Japan). Immobilon, polyvinylidene difluoride membrane, was purchased from Millipore (Bedford, MA, USA). Lima bean trypsin inhibitor was purchased from Worthington Biochemical (Freehold, NJ, USA). The protein assay kit was purchased from Bio-Rad Laboratories (Hercules, CA, USA). Tris[hydroxymethyl]aminomethane (Tris), sodium molybdate, phenylmethylsulfonylfluoride (PMSF), bovine serum albumin (BSA; minimum 98%, γ-globulin free), 2-mercaptoethanol, Triton X-100, Brij 35, yeast transfer RNA, and salmon testis DNA were purchased from Sigma Chemical (St Louis, MO, USA). Paraformaldehyde (PFA) was purchased from Merck (Darmstadt, Germany). Ethylenediaminetetraacetic acid disodium salt dihydrate (EDTA) and 3,3′-diaminobenzidine–4 HCl (DAB) were purchased from Dojin Chemicals (Kumamoto, Japan). 4-Cl-1-naphthol was from Tokyo Kasei Kogyo (Tokyo, Japan). All other reagents used in this study were purchased from Wako Pure Chemicals (Osaka, Japan) and were of analytical grade.

Antibodies

Specific rabbit polyclonal antisera against mouse FSH (1:400), LH (1:1,000), PRL (1:800), GH (1:1,600), and TSH (1:400) were purchased from Biogenesis (Bournemouth, UK). Each antiserum did not cross-react with other pituitary hormones including adreno-corticotropic hormone (ACTH), according to the data provided by the company and previous study (Nishihara et al. 2000). A mouse monoclonal antibody against ERα (ER88; 1:160, 0.7 μg/ml) was purchased from BioGenex (San Ramon, CA, USA). For the detection of ERβ, a rabbit polyclonal antiserum against rat ERβ (1:400) was generated as described previously (Nishihara et al. 2000). A mouse monoclonal antibody against Ki-67 (MIB-5; 1:50, 4.0 μg/ml) was purchased from Immunotech (Marseille, France), and a mouse monoclonal antibody against β-actin (AC-15; 1:6,400, 0.45 μg/ml) was purchased from Sigma. Horseradish peroxidase (HRP)-conjugated goat anti-mouse IgG was purchased from Chemicon International (Temecula, CA, USA). HRP-conjugated goat anti-rabbit IgG was purchased from MBL (Nagoya, Japan). HRP-conjugated mouse monoclonal anti-thymine-thymine (T–T) IgG (1:80) was from Kyowa Medex (Tokyo, Japan). Normal goat IgG and normal mouse IgG were purchased from Sigma. Normal rabbit IgG was purchased from DAKO (Glostrup, Denmark).

Animals

Adult male and female ICR (Crj: CD-1), male C57BL/6J, and male ERαKO mice (6 weeks old) were used in the present study. ICR and C57BL/6J mice were purchased from Charles River Japan (Kanagawa, Japan), and ERαKO mice from a background of C57BL/6J were purchased from Taconic (Germantown, NY, USA). The experimental protocols (# 0112100012 and 0202200048) were approved by the Biochemical Research Center, Center for Frontier Life Sciences, Nagasaki University. Three mice were housed per cage in an air-conditioned and light-controlled room at the animal facility of

Nagasaki University. In the beginning of experiments, the male mice were injected subcutaneously with DES [1 ng, 10 ng, 100 ng, 1 μg, 10 μg, 100 μg, 1 mg, or 20 mg/kg body weight (BW)] dissolved in corn oil containing 5% ethanol or with the vehicle alone as a control, every 5 days as described previously (Libbus and Schuetz 1980; Kondo et al. 2002) ($n = 3$ in each group). In fact, the maximum injection dose of DES was determined based on the previous studies in mice (Marselos and Tomatis 1992; Walker and Kurth 1993). In physiological conditions, the blood level of estradiol was 10–60 pg/ml in adult male mammals (Wada et al. 1996), and so the doses of DES around 10–100 ng/kg BW would be regarded as physiological conditions in male animals. In the present study, we used a wide range of doses of physiological and pharmacological DES. Later, we concentrated on the analysis of specimens treated with 100 ng, 100 μg, and 20 mg/kg BW DES, in which significant differences in the density of positive cells for various pituitary hormones, as compared to the control group, were observed. On day 20, all animals were sacrificed, and their pituitary glands were removed. Normal female ICR mice at the estrous stage ($n = 5$) were also used as positive controls for ERs. The estrous cycle phase was estimated in each mouse by examination of vaginal cell smears. In the experiment designed to investigate time-course changes in cell kinetics of pituitaries of DES-treated mice, male ICR mice were treated with 20 mg/kg BW DES or the vehicle alone for 0, 5, 10, 15, and 20 days ($n = 3$ for each time-point).

Tissue preparation

Pituitaries, uteri, ovaries, and livers were divided into several pieces. Some pieces of the tissues were quickly frozen, stored at −80°C and later used for Western blotting. The other pieces were fixed in 4% PFA in phosphate-buffered saline (PBS; pH 7.2) at room temperature (RT) for about 20 h and embedded in paraffin using a standard procedure.

Western blot analysis of ERα and ERβ

Tissues were homogenized in a lysis buffer containing 50 mM Tris–HCl buffer (pH 7.5), 150 mM NaCl, 5 mM EDTA, 0.1 mM PMSF, 20 mM sodium molybdate, and 50 μg/ml lima bean trypsin inhibitor, as described previously (Nishihara et al. 2000; Kawano et al. 2004). After centrifugation of the homogenate at 13,000× g for 10 min at 4°C, the supernatant was collected and stored at −80°C. The protein concentration in each preparation was determined using a kit from Bio-Rad Laboratories according to the method of Bradford (1976), using BSA as a standard. An aliquot (30 μg) of sample lysates was mixed with the loading buffer (200 mM Tris–HCl, pH 8.0, 0.5 M sucrose, 5 mM EDTA, 0.01% bromophenol blue, 2.5% SDS, and 10% 2-mercaptoethanol), boiled for 5 min, and separated by SDS-PAGE with a 4–20% gradient gel according to the method of Laemmli (1970), and electrophoretically transferred onto polyvinylidene difluoride membranes. After blocking with 10% nonfat dry milk in Tris-buffered saline (TBS) for 1 h, blots were incubated overnight at 4°C with mouse anti-ERα (1:80) or rabbit anti-ERβ (1:200) in TBS/0.05% Triton X-100 buffer. The membranes were washed three times for 10 min each time with TBS/0.05% Triton X-100 buffer. Each membrane was reacted with HRP-goat anti-mouse IgG (1:400) or anti-rabbit IgG (1:200) in 10% nonfat dry milk in TBS for 1 h at RT and was again washed six times, 15 min each, with TBS/0.05% Triton X-100 buffer. The bands were visualized with DAB, Ni, Co, and H_2O_2 according to the method of Adams (1981). To confirm that the applied protein amounts were the same in each lane, the membranes were further reacted with mouse anti-β-actin (1:6,400) for 1 h, and with HRP-goat anti-mouse IgG (1:1,600). These were visualized as described above.

Immunohistochemistry for ERα, ERβ, FSH, LH, PRL, GH, TSH, and Ki-67

Immunohistochemical staining was performed using the methods described previously (Kawano et al. 2004; An et al. 2005). Paraffin-embedded tissues were cut into 5-μm thick sections and placed onto silane-coated glass slides. For ERα, ERβ, and Ki-67, the sections were deparaffinized with toluene, and rehydrated with serial ethanol solutions, and then autoclaved at 120°C for 15 min in 10 mM citrate buffer (pH 6.0) (Ehara et al. 1995). After inhibition of endogenous peroxidase activity with 0.3% H_2O_2 in methanol for 15 min at RT, they were preincubated with 500 μg/ml normal goat IgG and 1% BSA in PBS for 1 h at RT to block nonspecific binding of antibodies. Sections were then reacted with the primary antibodies overnight at RT. After washing with 0.075% Brij 35 in PBS, they were reacted with HRP-goat anti-mouse IgG (1:100) or HRP-goat anti-rabbit IgG (1:200) for 1 h at RT. After washing in 0.075% Brij 35 in PBS, the sites of HRP were visualized with DAB, Ni, Co, and H_2O_2. For FSH, LH, PRL, GH, and TSH detection, sections were similarly processed as described above, except for omitting the autoclave step. Sections were reacted with the primary antibodies for 1 h at RT. After washing, they were incubated with HRP-goat anti-rabbit IgG (1:100) for 1 h at RT. The sites of HRP were visualized with DAB and H_2O_2. As a negative control, normal mouse or rabbit IgG was used at the same dilution instead of the primary antibodies in every run.

Preparation of oligo-DNA probes for Pit-1

We synthesized double-stranded oligo-DNA containing the consensus sequence of Pit-1 binding domain (Pit-1

(+): 5′-CCCTATACATTTATTCATGGC-3′, Pit-1 (-): 5′-GCCATGAATAAATGTATAGGG-3′) (−89 to −69) of mouse GH gene promoter, which can bind to and activate mouse PRL gene promoter (Ingraham et al. 1988; Izumi et al. 2005). For a negative control probe, we synthesized the mutated Pit-1 (mPit-1 (+): 5′-CCCTATACATTTAggtggtGC-3′, mPit-1 (-): 5′-GCaccaccTAAATGTATAGGG-3′), with a six-base mutation indicated by the small letters (Ingraham et al. 1988; Izumi et al. 2005). Ingraham et al. (1998) revealed that the mutated Pit-1 oligo-DNA, which was mutated only one consensus Pit-1 element, did not compete for binding with Pit-1 probe, suggesting that the mutated Pit-1 probe could not bind to Pit-1. These oligo-DNAs were added with three repeats of adenine-thymine-thymine at the 3′-end for T–T dimers (Koji et al. 1994; Koji and Nakane 1996). We conducted a computer-assisted search (GenBank nucleic acid sequence database release 142) of the above Pit-1 oligo-DNA sequences and found 100% homology with these sequences. These oligo-DNAs were haptenized by introducing T–T dimers by UV irradiation using a dose of 12,000 J/m^2, as described previously (Koji et al. 1994; Koji and Nakane 1996).

Southwestern histochemistry for Pit-1

Southwestern histochemistry for Pit-1 of mouse pituitaries was performed, as described previously (Koji et al. 1994). Briefly, paraffin sections were deparaffinized, rehydrated, and autoclaved. Slides were immersed in 50 mM Tris–HCl buffer (pH 7.4) containing 5% nonfat dry milk, 150 mM NaCl, and 1 mM EDTA (TMSE) for 1 h at RT. They were incubated with TMSE solution, including T–T dimerized probe DNA at 2.0 μg/ml overnight at RT. Sections were washed in TMSE solution twice, 0.075% Brij 35 in PBS three times, and immersed in 500 μg/ml normal mouse IgG, 100 μg/ml salmon testis DNA, 100 μg/ml yeast transfer RNA, and 5% BSA in PBS for 1 h at RT. They were reacted overnight with HRP-mouse anti-T–T antibody (1:80) at RT. After washing in 0.075% Brij 35 in PBS, they were visualized with DAB, Ni, Co, and H_2O_2. To confirm the specificity of Pit-1 signals, mutated Pit-1 and non-probe were used as a negative control.

Simultaneous detection of PRL and Ki-67, identification of cell type of Pit-1-positive cells, and simultaneous detection of PRL and gonadotropins or GH.

For simultaneous detection of PRL and Ki-67, we performed double staining, as described previously (Kawano et al. 2004; An et al. 2005). Briefly, the sections were stained with anti-PRL antiserum, and HRP sites were visualized with DAB and H_2O_2. Then the sections were immersed in PBS and autoclaved. The slides were immersed in 0.1 M glycine–HCl buffer (pH 2.2) three times for 30 min each. After washing with Milli-Q water once and with PBS three times, the sections were reacted with anti-Ki-67 antibody. HRP sites were visualized with 4-Cl-1-naphthol and H_2O_2 solution. To identify Pit-1-positive cells, we also performed double staining for PRL, FSH, or LH and Pit-1 processed similarly, as described above. PRL, FSH, or LH signal was first visualized with DAB and H_2O_2, and Pit-1 signal was visualized with 4-Cl-1-naphthol and H_2O_2 solution. For simultaneous detection of PRL and FSH, LH, or GH, sections were similarly processed, except for omitting the autoclave step. PRL signal was first visualized with DAB and H_2O_2, and FSH, LH, or GH signal was visualized with 4-Cl-1-naphthol and H_2O_2 solution.

Quantitative analysis

The results of immunohistochemistry were graded as positive or negative, compared with that of negative control. For each section, the numbers of cell nuclei were counted in more than 2,000 nuclei in randomly selected fields at 400× magnification. Cell counts were performed in a blind fashion by three individuals. The number of positive cells was expressed as the percentage of cells with positive nuclei per total number of counted nuclei. The counting error from the cell size could be reduced by counting the cell nuclei (Davies et al. 1974). In the case of Pit-1-positive cells, red color was given to the positive cells by a computer-assisted image analyzer (DAB analysis system; Carl Zeiss, Göttingen, Germany) before counting. Positive cells were evaluated based on the staining density over the level of staining with the mutated probe. The signal intensity of pituitary hormones was measured by an image analyzer (DAB analysis system). We calculated the optical density of each cell in the pituitary as the sum of the gray values of all pixels corresponding to the cell.

Statistical analysis

All data were expressed as mean ± SD. Differences between groups were examined for statistical significance using the unpaired Student's *t*-test. A P value less than 0.05 denoted the presence of a statistically significant difference. All analyses were performed with a statistical software package (StatView, version 5.0; Abacus Concepts, Berkeley, CA).

Results

Effects of DES on FSH, LH, and PRL expression in pituitary glands

We examined the effects of DES on the expression of FSH, LH, and PRL in male mouse pituitaries by immunohistochemstry. These hormones were detected in the cytoplasm of anterior pituitary cells (Fig. 1). Quantitative analysis revealed that DES reduced the population density of FSH and LH cells in a dose-dependent manner, but increased that of PRL cells (Table 1). The

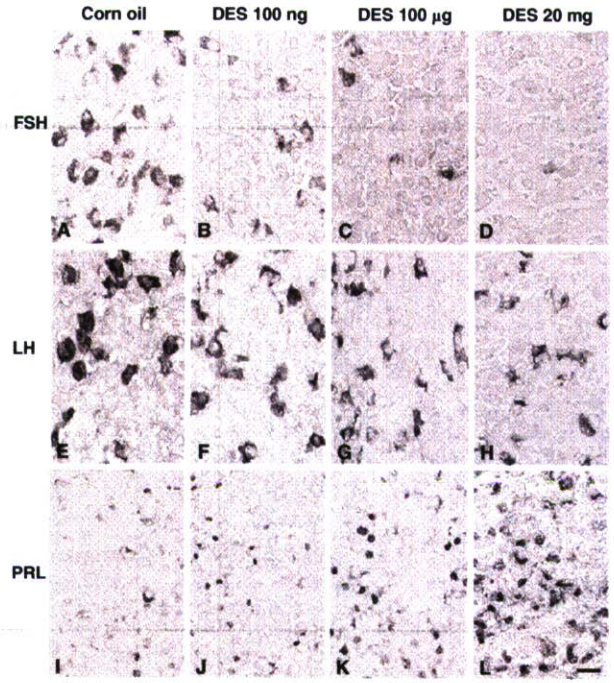

Fig. 1 Immunohistochemical localization of FSH (**a–d**), LH (**e–h**), and PRL (**i–l**) cells in paraffin sections of male mouse pituitaries treated with corn oil or DES at 100 ng, 100 μg, or 20 mg/kg BW. Magnification, 400×. Scale bar, 20 μm

percentage of PRL-positive cells at 20 mg/kg BW DES was four times higher than the value of control group injected with corn oil (Table 1). In parallel with the changes in the cell density, we confirmed similar DES effects on the signal intensities of the same hormones by image analysis (Fig. 2). The sections reacted with normal rabbit IgG at the same dilution instead of the specific antibody as a negative control showed no staining (data not shown).

Effects of DES on ERα and β expression in pituitary glands

First, we performed Western blot analysis of pituitary tissue extracts from wild-type male mice, and liver tissue extracts from ERαKO male mice to confirm the expression of ERα and β. We used extracts from the uterus and ovaries of normal female mice at the estrous stage as positive controls for ERα and β, respectively. A

Table 1 Percentage of positive cells in male mouse pituitaries

Positive cells	Treatment (dose/kg BW)			
	Corn oil	DES 100 ng	DES 100 μg	DES 20 mg
FSH	13.7 ± 0.4	6.3 ± 0.2*	4.2 ± 0.3**	1.9 ± 0.5**
LH	12.6 ± 0.5	10.4 ± 0.4	6.2 ± 1.2*	4.5 ± 0.8**
PRL	10.6 ± 0.4	12.2 ± 0.6	20.8 ± 1.2**	40.5 ± 2.5**
ERα	44.6 ± 1.3	37.3 ± 0.6*	25.4 ± 1.1**	17.6 ± 0.8**
ERβ	0.2 ± 0.5	0.3 ± 0.6	8.0 ± 0.7*	15.1 ± 0.5**
ERα alone in PRL[a]	80.2 ± 2.0	ND	ND	27.3 ± 1.3
ERβ alone in PRL[b]	ND	ND	ND	20.2 ± 0.9
ERα and β in PRL[c]	ND	ND	ND	36.4 ± 1.5
PRL in ERβ[d]	ND	ND	ND	89.6 ± 1.2

Data represent mean ± SD (%). *ND* not determined. *$P < 0.05$, **$P < 0.01$, compared with corn oil
[a]ERα alone-positive cells in PRL cells
[b]ERβ alone-positive cells in PRL cells
[c]ERα and β-positive cells in PRL cells
[d]PRL cells in ERβ-positive cells

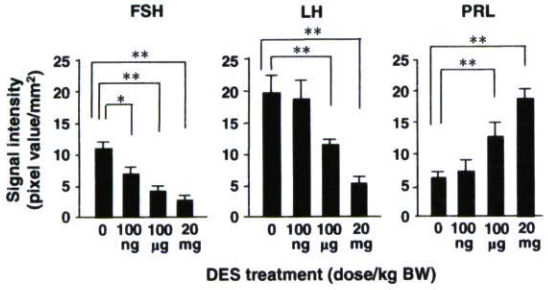

Fig. 2 Quantitative analysis of the signal intensity of FSH (*left panel*), LH (*middle panel*), and PRL (*right panel*). Data represent mean ± SD. $^{*}P < 0.05$, $^{**}P < 0.01$

66-kDa band for ERα was detected in the control pituitary, but no band for ERβ was detected (Fig. 3). The pituitary extracts from mice treated with DES at 20 mg/kg BW showed weaker 66-kDa ERα band and the appearance of a 55-kDa band for ERβ. In the liver extracts from ERαKO mice treated with corn oil, the 66-kDa band for ERα was not detected. In addition, the 42-kDa β-actin band confirmed the loading of equivalent amounts of protein.

In the next step, we analyzed the effect of DES treatment on the population of ERα- and β-positive cells in the pituitary by immunohistochemistry. ERα was detected in the nuclei of many pituitary cells in the control, whereas DES markedly decreased the percentage of ERα-positive cells (Fig. 4a–d; Table 1). In contrast, ERβ signal was detected in the nuclei of some anterior lobe cells at DES doses higher than 100 µg/kg BW, although it was not detected in the control or at lower DES doses (Fig. 4e–h; Table 1). The sections reacted with normal mouse or rabbit IgG as a negative control showed no staining (data not shown).

To clarify the correlation between ER expression and PRL cell counts, we performed immunohistochemical analysis of ERs and PRL by the combined use of adjacent and mirror sections. Most of the PRL cells were positive for ERα alone in the control (Table 1), while PRL cells positive for ERβ alone, or both ERα and β were induced in mice treated with DES at 20 mg/kg BW (Fig. 5; Table 1). In addition, ERβ expression was predominantly in PRL cells (Table 1).

Effect of DES on Ki-67 labeling of PRL cells in pituitary glands

To investigate the underlying mechanism of the increase in the percentage of PRL cells, we examined the expression of Ki-67 (a marker for the proliferative activity) by immunohistochemistry at 0, 5, 10, 15, and 20 days after treatment with 20 mg/kg BW DES. Then we also performed double staining for Ki-67 and PRL in the same sections. Ki-67 was detected in the nuclei of only a few anterior pituitary cells at 0 day (Fig. 6a), and Ki-67-positive cells were increased by DES (Fig. 6b). The percentage of Ki-67-positive PRL cells was significantly increased at 10–15 days after DES treatment (Fig. 6c; Table 2).

Effect of DES on Pit-1 expression in pituitary glands

Since Pit-1 expression is regarded as a marker of enhanced PRL cell differentiation (Ingraham et al. 1988; Crewshaw et al. 1989), we next examined the expression of Pit-1 by Southwestern histochemistry at 0, 5, 10, 15 and 20 days after DES treatment. As shown in Fig. 7, Pit-1 was specifically detected in the nuclei of anterior pituitary cells, and the DES treatment increased Pit-1-positive cells. The sections reacted with mutated Pit-1 probe at the same concentration, or without probes as a negative control, showed no signals. As can be seen in Fig. 8a–c, double-positive cells of Pit-1 and PRL were increased by DES treatment. Quantitative analysis revealed that the percentage of Pit-1-positive PRL cells was significantly increased at 5–15 days (Table 2). DES treatment did not significantly change the percentage of GH and TSH cells in the pituitary, but reduced those of FSH and LH cells (Table 2). Double-positive cells of Pit-1 and FSH or LH were found at 5–10 days, although such cells were not found at 0 day (Fig. 8d–i; Table 2).

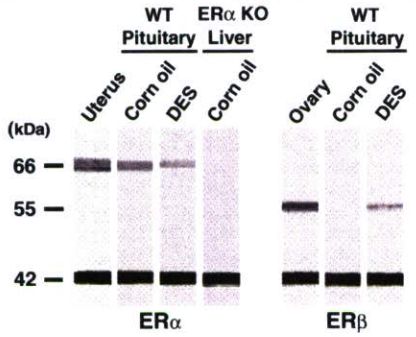

Fig. 3 Western blot analysis of ERα and ERβ. Thirty micrograms of the extracts from pituitaries of wildtype (WT) mice and livers of ERα knockout mice (ERαKO) treated with corn oil or 20 mg/kg BW DES (and uterus and ovary at estrous as a positive control) were subjected to SDS-PAGE. Western blotting was performed using monoclonal antibody ER 88 for ERα (66-kDa) and a polyclonal antibody for ERβ (55-kDa). The membranes were further reacted with monoclonal antibody for β-actin (42-kDa) as a loading control

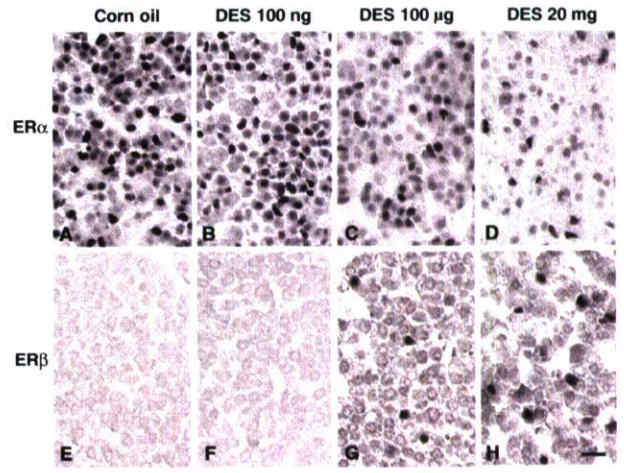

Fig. 4 Immunohistochemical localization of ERα (**a**–**d**) and ERβ (**e**–**h**) in male mouse pituitaries treated with corn oil or DES at 100 ng, 100 µg, or 20 mg/kg BW. Magnification, 400×. Scale bar, 20 µm

Appearance of PRL- and FSH-, or LH-double positive cells by DES treatment

To identify the type of cells that differentiate to PRL cells, we examined the co-expression of PRL and gonadotropins or GH. As shown in Fig. 9a–f, double positive cells of PRL and FSH or LH were found at 5 days after DES treatment. Quantitative analysis revealed that the percentage of PRL-positive FSH cells and PRL-positive LH cells was significantly increased at 5–10 days (Table 3). On the other hand, only a few PRL- and GH-double positive cells were detected (about 2%) through the experiment (Fig. 9g–i; Table 3).

Effects of DES on expression of sex-related hormones and ERβ in pituitaries of ERαKO mice

To gain insight into the roles of ERα and β in the effect of DES on the expression of sex-related hormones, we conducted the same set of experiments on the pituitaries of ERαKO mice. DES had no effect on the population density of cells positive for these hormones in ERαKO mice (Fig. 10). While ERβ-positive cells were detected in the pituitaries of corn oil-treated ERαKO mice, their density did not change by DES treatment. In addition, there were no significant differences in the expression of these hormones and ERs between the pituitaries of ICR and C57BL/6 wild-type mice (data not shown).

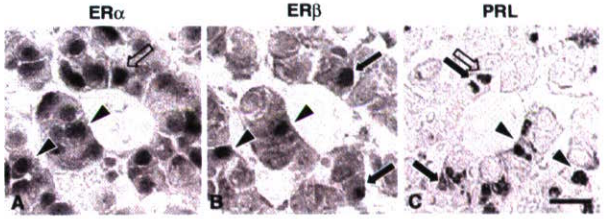

Fig. 5 Co-localization of ERs and PRL in pituitaries of mice treated with DES at 20 mg/kg BW. Pituitary sections were immunostained for ERα (**a**), ERβ (**b**), and PRL (**c**) by the combined use of adjacent and mirror sections treated with DES. *Open arrows* indicate PRL cells positive for ERα alone, *solid arrows* indicate PRL cells positive for ERβ alone, and *arrowheads* indicate PRL cells positive for both receptors. Magnification, 400×. Scale bar, 20 µm

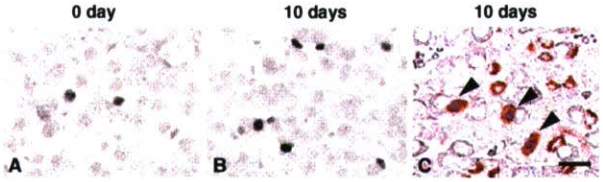

Fig. 6 Expression of Ki-67 in pituitaries of mice treated with 20 mg/kg BW DES. **a** and **b** Immunohistochemical localization of Ki-67 at 0 day (**a**) and 10 days (**b**) after DES treatment. **c** Double staining for Ki-67 and PRL in pituitaries of DES-treated mice at 10 days. Ki-67-positive cells are stained *blue*, and PRL-positive cells are *brown*. *Arrowheads* indicate double-positive cells. Magnification, 400×. Scale bar, 20 μm

Discussion

In the present study, we examined the effects of DES on the population of FSH-, LH-, and PRL-positive cells in male mouse pituitary, and found that DES reduced the density of FSH and LH cells in a dose-dependent manner, but conversely increased that of PRL cells. Interestingly, DES induced ERβ expression predominantly in PRL cells. Since these effects of DES were almost abolished in ERαKO mice, it is conceivable that ERα mediates the major action of DES. Although the role of ERβ expression in the PRL cell kinetics is unknown, our results strongly indicate that the increase of PRL cells by DES depends upon both enhanced proliferation of PRL cells and induction of transdifferentiation of FSH/LH cells to PRL cells.

It was surprising that ERβ-positive cells were increased while ERα-positive cells were decreased in parallel with the increase in the density of PRL cells after DES treatment. A change in the major population of ER subtypes is known to occur around the day of birth in the rat pituitary (Nishihara et al. 2000); ERβ rather than ERα is predominantly expressed in the fetal pituitary,

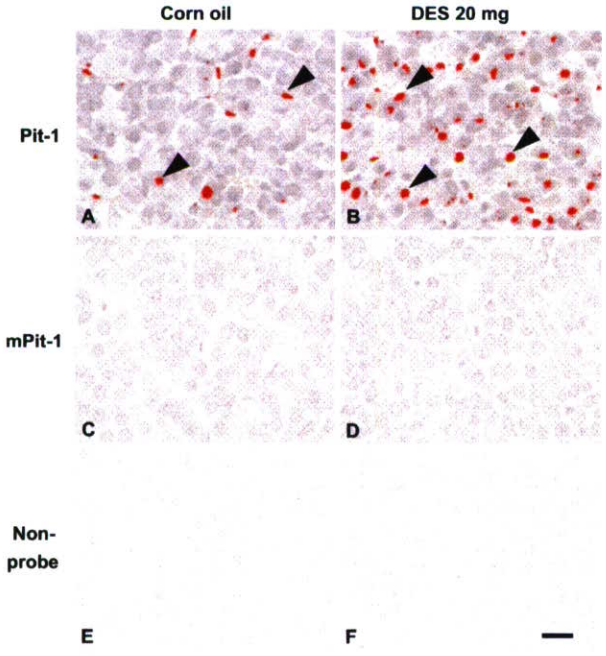

Fig. 7 Localization of Pit-1 in mouse pituitary by Southwestern histochemistry after 15-day-treatment with corn oil (**a**, **c**, **e**) or DES 20 mg/kg BW (**b**, **d**, **f**). The pituitary sections were reacted with T–T dimerized Pit-1 probe (**a**, **b**), T–T dimerized mutated Pit-1 (mPit-1) probe (**c**, **d**), or without probe (**e**, **f**). The *red color* represents positive cells as determined by image analysis (**a**–**f**). *Arrowheads* indicate positive cells. Magnification, 400×. Scale bar, 20 μm

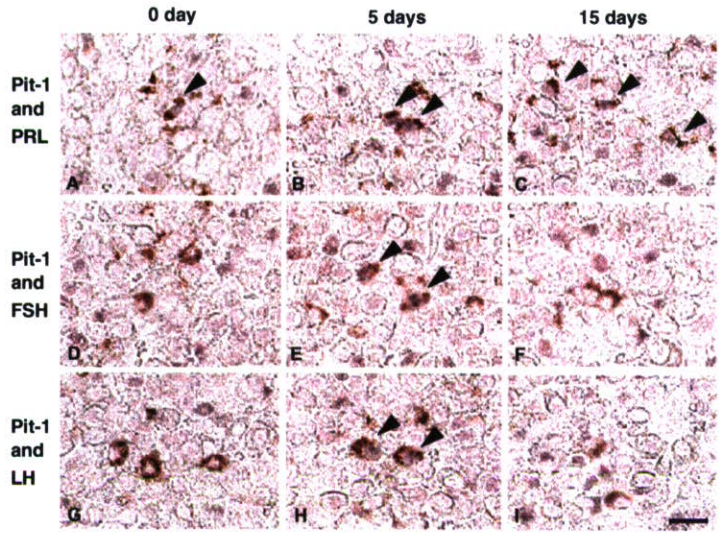

Fig. 8 Co-localization of Pit-1 and PRL or gonadotropins in pituitaries of mice treated with 20 mg/kg BW DES. Double staining for Pit-1 and PRL (**a**–**c**), Pit-1 and FSH (**d**–**f**), Pit-1 and LH (**g**–**i**) in pituitaries of mice at 0 day (**a**, **d**, **g**), 5 days (**b**, **e**, **h**), or 15 days (**c**, **f**, **i**) after DES treatment. Pit-1-positive cells are stained *blue*, and PRL-, FSH-, or LH-positive cells are *brown*. *Arrowheads* indicate double-positive cells. Magnification, 400×. Scale bar, 20 μm

but after birth the expression changes from ERβ to ERα, and ERβ almost disappears in adult mouse pituitary (Schreihofer et al. 2002). In accord, our study revealed the lack of ERβ-positive cells in the control group, but they appeared after treatment with a high-dose DES. In addition, the ERβ expression was almost limited to PRL cells. Considering that the DES effects were abolished in ERαKO mice, which maintain ERβ expression, DES seems to affect the pituitary at least primarily through ERα. However, the change of ER subtypes in PRL cells by DES might be related to the enhanced expression of protooncogene, such as *c-fos* (Allen et al. 1997). Since the DES-ERβ complex may function as a negative regulator of genes controlled by activating protein-1 (AP-1) element, which was activated by binding of Fos/Jun protein complex (Paech et al. 1997), the switching of ER subtype from ERα to ERβ may suggest that the pituitary becomes more resistant to DES exposure.

Recently, similar effects of DES on the population of FSH, LH, and PRL cells have been reported in male

Table 2 Percentage of positive cells in mouse pituitaries treated with DES 20 mg/kg BW

Positive cells	DES treatment (days)				
	0	5	10	15	20
PRL	11.2 ± 0.5	19.4 ± 1.7*	32.1 ± 1.0**	41.8 ± 1.5**	41.1 ± 0.5**
Ki-67	1.3 ± 0.2	4.1 ± 0.2	10.0 ± 0.3*	8.8 ± 0.3*	4.9 ± 0.2
Ki-67 in PRL[a]	1.2 ± 0.7	4.4 ± 1.6	16.4 ± 1.2**	15.7 ± 1.2**	5.8 ± 1.3
Pit-1	6.5 ± 0.8	19.4 ± 0.3**	26.8 ± 0.4**	37.1 ± 1.7**	10.8 ± 1.4
Pit-1 in PRL[b]	16.5 ± 0.5	33.4 ± 1.6**	61.0 ± 1.0**	76.7 ± 2.4**	20.2 ± 2.1
PRL in Pit-1[c]	24.1 ± 0.6	32.5 ± 2.5*	52.2 ± 2.1**	74.5 ± 0.9**	67.2 ± 1.1**
GH	44.8 ± 1.0	44.7 ± 1.1	43.8 ± 1.5	42.8 ± 1.0	42.7 ± 0.7
TSH	9.0 ± 0.5	8.6 ± 0.2	9.1 ± 0.2	8.7 ± 0.6	8.9 ± 0.4
FSH	11.4 ± 1.2	9.7 ± 0.3	5.5 ± 0.4*	2.9 ± 0.3**	2.5 ± 0.5**
Pit-1 in FSH[d]	0.2 ± 0.1	33.2 ± 1.0**	29.1 ± 0.9**	1.9 ± 0.2	0.4 ± 0.2
LH	10.6 ± 1.1	8.4 ± 0.3	6.4 ± 0.7*	4.0 ± 0.7**	3.6 ± 0.4**
Pit-1 in LH[e]	0.4 ± 0.3	31.6 ± 0.5**	27.9 ± 0.7**	1.3 ± 0.2	0.3 ± 0.1

Data represent mean ± SD (%). The percentage of Ki-67- or Pit-1-positive cells in the pituitaries of corn oil-treated mice was 1.2 ± 0.3, 6.2 ± 0.8%, respectively, and no changes were noted during this period. *$P < 0.05$, **$P < 0.01$, compared with 0 day

[a]Ki-67-positive cells in PRL cells
[b]Pit-1-positive cells in PRL cells
[c]PRL cells in Pit-1-positive cells
[d]Pit-1-positive cells in FSH cells
[e]Pit-1-positive cells in LH cells

Table 3 Percentage of positive cells in mouse pituitaries treated with DES 20 mg/kg BW

Positive cells	DES treatment (days)				
	0	5	10	15	20
PRL in FSH[a]	0.3 ± 0.3	25.0 ± 4.0*	26.3 ± 3.2*	0.7 ± 0.5	0.3 ± 0.2
PRL in LH[b]	0.6 ± 0.5	26.4 ± 3.1*	28.3 ± 1.5*	1.0 ± 0.4	0.4 ± 0.2
PRL in GH[c]	1.7 ± 0.6	1.8 ± 0.5	1.6 ± 0.4	1.7 ± 0.2	1.6 ± 0.3

Data represent mean ± SD (%). *$P < 0.01$, compared with 0 day
[a]PRL-positive cells in FSH cells
[b]PRL-positive cells in LH cells
[c]PRL-positive cells in GH cells

Syrian hamster pituitary (Cauwenberge et al. 2001). The DES-induced reduction of FSH and LH cells could be explained as an estrogen function of DES, through the negative feedback mechanism (Scully et al. 1997). Estrogens are also known to stimulate PRL synthesis and secretion (Scully et al. 1997), and PRL cell proliferation (Hashi et al. 1996). Therefore, the effects of DES on FSH, LH, and PRL cells in the present study may be largely ascribed to the strong estrogen function of DES.

In the present study, we examined the expression of functional Pit-1 by Southwestern histochemistry. In the control pituitary, only 16.5% of PRL cells were Pit-1 positive. If Pit-1 is a prerequisite for the transcription of mRNA for PRL, all PRL cells should be positive for Pit-1. Therefore, it may be suggested that PRL cells, once fully differentiated, would not require the continuous presence of Pit-1 at an enough amount to be detected by Southwestern histochemistry. In contrast, the percentage of Pit-1-positive PRL cells was significantly increased at 5–15 days after DES treatment. Since Pit-1 expression is regarded as a marker of enhanced PRL cell differentiation, DES may promote the differentiation of PRL cells, particularly at the early stage of DES treatment.

Our study also revealed that the DES treatment did not significantly change the population density of GH and TSH cells among pituitary cells, but decreased that of FSH and LH cells. Considering that double-positive cells for Pit-1 and FSH or LH were detected at 5–10 days, and also that double-positive cells for PRL and FSH or LH were found at the same time, these results strongly indicate that the transdifferentiation of FSH/LH cells to PRL cells was activated by DES. Actually, in the differentiation of pituitary cells, two pathways may be possible; differentiation of stem cells into mature cells or transdifferentiation of certain type of cells to another cell type. The present results seem to support, at least, the latter case. In this context, it should be noted that bihormonal cells, which might be an intermediate stage of transdifferentiation (Horvath et al. 1990), have been

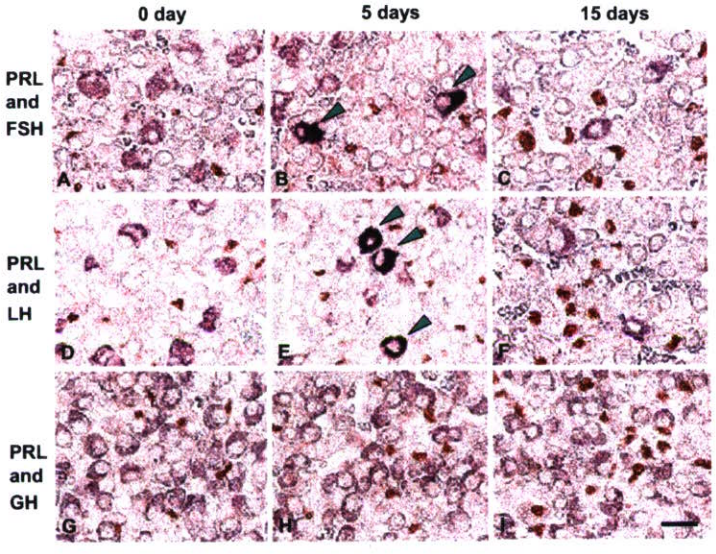

Fig. 9 Co-localization of PRL and gonadotropins or GH in pituitaries of mice treated with DES 20 mg/kg BW. Double staining for PRL and FSH (**a**–**c**), PRL and LH (**d**–**f**), and PRL and GH (**g**–**i**) in pituitaries of mice at 0 day (**a**, **d**, **g**), 5 days (**b**, **e**, **h**), or 15 days (**c**, **f**, **i**) after DES treatment. PRL-positive cells are stained *brown*, and FSH-, LH-, or GH-positive cells are *blue*. *Arrowheads* indicate double-positive cells. Magnification, 400×. Scale bar, 20 μm

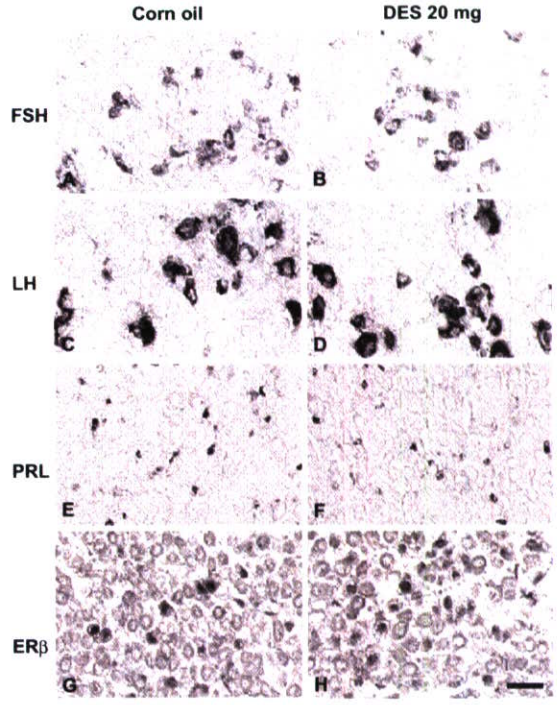

Fig. 10 Immunohistochemical localization of FSH (**a**, **b**), LH (**c**, **d**), PRL (**e**, **f**), and ERβ (**g**, **h**) in pituitaries of ERα knockout mice treated with corn oil (**a**, **c**, **e**, and **g**) or DES 20 mg/kg BW (**b**, **d**, **f**, and **h**). Magnification, 400×. Scale bar, 20 μm

observed in the pituitaries of mammals (Childs et al. 1994; Goth et al. 1996), and pituitary adenomas (Senovilla et al. 2004). In fact, that long-term estrogen treatment induced mammosomatotrophs, which are interconvertible between PRL cells and GH cells (Goth et al. 1996), though this may not be in the present case, because only a few double-positive cells for PRL and GH were detected in the DES-treated pituitary. Moreover, co-expression of Pit-1 and FSH or LH was also observed in pregnant rats (Vidal et al. 1998) and prolactinomas induced by estrogen (Mukdsi et al. 2004). Since it is known that PRL and GH cells belong to the Pit-1 lineage, whereas FSH and LH cells belong to another lineage (Hauspie et al. 2003), these results may indicate that the specification of the different lineages in the pituitary is made less stringent by DES or estrogens, and then transdifferentiation of FSH/LH cells to PRL cells might be induced. In addition, although the expression of Pit-1 was stimulated by DES in this study, we could not find either ERE or AP-1 sequence in the Pit-1 gene and its promoter region by computer-based searching (data not shown). Therefore, DES-induced Pit-1 expression might occur through an indirect pathway, and is an important subject that needs to be clarified in the future.

In conclusion, the present study indicated that DES affects the population density of FSH, LH, and PRL cells through ERα in male mouse pituitary, and also induces the expression of ERβ predominantly in PRL cells. Moreover, our results indicate that DES increases the population density of PRL cells by inducing proliferation of PRL cells and transdifferentiation of FSH/LH cells to PRL cells. Further studies are needed to elucidate the differential roles of ERα and ERβ in the regulation of PRL cell kinetics under the influence of DES.

Acknowledgments This study was supported in part by a Grant-in-Aid for Scientific Research from the Japanese Ministry of Education, Science, Sports, and Culture (nos. 1247003, 15390058, and 16659047 to T. Koji) and by a grant from the Japanese Environment Agency (to T. Koji). We thank Dr. Tetsuo Shukuwa (Division of Dermatology, National Nagasaki Medical Center) for his helpful advice and excellent technical support in this work.

References

Adams JC (1981) Heavy metal intensification of DAB-based HRP reaction product. J Histochem Cytochem 29:775
Allen DL, Mitchner NA, Uvegas TE, Nephew KP, Khan S, Ben-Jonathan N (1997) Cell-specific induction of c-*fos* expression in the pituitary gland by estrogen. Endocrinology 138:2128–2135

An S, Hishikawa Y, Koji T (2005) Induction of cell death in rat small intestine by ischemia reperfusion: differential roles of Fas/Fas ligand and Bcl-2/Bax systems depending upon cell types. Histochem Cell Biol 123:249–261

Bradford MM (1976) A rapid and sensitive method for the quantitation of microgram quantities of protein utilizing the principle of protein-dye binding. Anal Biochem 72:248–254

Cauwenberge AV, Nonclerq D, Laurent G, Zanen J, Beckers JF, Alxandre H, Heuson-Stiennon JA, Toubeau G (2001) Immunohistochemistry of the golden hamster pituitary during chronic administration of diethylstilbestrol: a quantitative analysis using confocal laser scanning microscopy. Histochem Cell Biol 115:169–178

Crewshaw EB III, Kalla K, Simmons DM, Swanson LW, Rosenfeld MG (1989) Cell-specific expression of the prolactin gene in transgenic mice is controlled by synergistic interactions between promoter and enhancer elements. Genes Dev 3:959–972

Childs GV, Unabia G, Rougeau D (1994) Cells that express luteinizing hormone (LH) and follicle-stimulating hormone (FSH) β-subunit messenger ribonucleic acids during the estrous cycle: the major contributors contain LHβ, FSHβ, and/or growth hormone. Endocrinology 134:990–997

Davies AG, Courot M, Gresham P (1974) Effects of testosterone and follicle-stimulating hormone on spermatogenesis in adult mice during treatment with oestradiol. J Endocrinol 60:37–45

Ehara H, Koji T, Deguchi T, Yoshii A, Nakano M, Nakane PK, Kawada Y (1995) Expression of estrogen receptor in diseased human prostate assessed by non-radioactive in situ hybridization and immunohistochemistry. Prostate 27:304–313

Fox SR, Jong MT, Casanova J, Ye ZS, Stanley F, Samuels HH (1990) The homeodomain protein, Pit-1/GHF-1, is capable of binding to and activating cell-specific elements of both the growth hormone and prolactin gene promoters. Mol Endocrinol 4:1069–1080

Friend KE, Chiou YK, Lopes MB, Laws ER Jr, Hughes KM, Shupnik MA (1994) Estrogen receptor expression in human pituitary: correlation with immunohistochemistry in normal tissue, and immunohistochemistry and morphology in macroadenomas. J Clin Endocrinol Metab 78:1497–1504

Goth MI, Lyons CE Jr, Ellwood MR, Barrett JR, Thorner MO (1996) Chronic estrogen treatment in male rats reveals mammosomatotropes and allows inhibition of prolactin secretion by somatostatin. Endocrinology 137:274–280

Greene GL, Sobel NB, King WJ, Jensen EV (1984) Immunochemical studies of estrogen receptors. J Steroid Biochem 20:51–56

Hauspie A, Seuntjens E, Vankelecom H, Denef C (2003) Stimulation of combinatorial expression of prolactin and glycoprotein hormone α-subunit genes by gonadotropin-releasing hormone and estradiol-17β in single rat pituitary cells during aggregate cell culture. Endocrinology 144:388–399

Hashi A, Mazawa S, Chen SY, Yamakawa K, Kato J, Arita J (1996) Estradiol-induced diurnal changes in lactotroph proliferation and their hypothalamic regulation in ovariectomized rats. Endocrinology 137:3246–3252

Horvath E, Lloyd RV, Kovacs K (1990) Propylthiouracyl-induced hypothyroidism results in reversible transdifferentiation of somatotrophs into thyroidectomy cells. A morphologic study of the rat pituitary including immunoelectron microscopy. Lab Invest 63:511–520

Ingraham HA, Chen R, Mangalam HJ, Elsholts HP, Flynn SE, Lin CR, Simmons DM, Swanson L, Rosenfeld MG (1988) A tissue-specific transcription factor containing a homeodomain specifies a pituitary phenotype. Cell 55:519–529

Izumi S, Koji T, Nakane PK (2005) Southwestern histochemistry: a method for localization of transcription factors. In: Hacker GW, Tubbs RR (eds) Molecular morphology in human tissues: techniques and applications. CRC Press, Washington, pp. 133–146

Kawano N, Koji T, Hishikawa Y, Murase K, Murata I, Kohno S (2004) Identification and localization of estrogen receptor α- and β-positive cells in adult male and female mouse intestine at various estrogen levels. Histochem Cell Biol 121:399–405

Koji T, Brenner RM (1993) Localization of estrogen receptor messenger ribonucleic acid in rhesus monkey uterus by nonradioactive in situ hybridization with digoxigenin-labeled oligodeoxynucleotides. Endocrinology 132:382–392

Koji T, Komuta K, Nozawa M, Yamada S, Nakane PK (1994) Localization of cyclic adenosine 3',5'-monophosphate-responsive element (CRE)-binding proteins by southwestern histochemistry. J Histochem Cytochem 42:1399–1405

Koji T, Nakane PK (1996) Recent advances in molecular histochemical techniques: in situ hybridization and southwestern histochemistry. J Electron Microsc 45:119–127

Kondo T, Goto S, Ihara Y, Urata Y, Ikeda S, Hishikawa Y, Izumi S, Shin M, Koji T (2002) Diethylstilbestrol attenuates antioxidant activities in testis from male mice. Free Radic Res 36:957–966

Kuiper GG, Enmark E, Pelto-Huikko M, Nilsson S, Gustafsson JA (1996) Cloning of a novel estrogen receptor expressed in rat prostate and ovary. Proc Natl Acad Sci USA 93:5925–5930

Laemmli UK (1970) Cleavage of structural proteins during the assembly of the head of bacteriophage T4. Nature 227:680–685

Libbus BL, Schuetz AW (1980) Gonadotrophin-induced reinitiation of meiosis in testes of oestradiol-treated prepubertal rats. J Reprod Fertil 60:1–6

Lloyd RV, Osamura RY (1997) Transcription factors in normal and neoplastic pituitary tissue. Microsc Res Tech 39:168–181

Marselos M, Tomatis L (1992) Diethylstilbestrol: II, pharmacology, toxicology and carcinogenicity in experimental animals. Eur J Cancer 29(A):149–155

Matsubara M, Harigaya T, Nogami H (2001) Effects of diethylstilbestrol on the cytogenesis of prolactin cells in the pars distalis of the pituitary gland of the mouse. Cell Tissue Res 306:301–307

Maurer RA, Notides AC (1987) Identification of an estrogen-responsive element from the 5'-flanking region of the rat PRL gene. Mol Cell Biol 7:4247–4254

McClellan MC, West NB, Tacha DE, Greene GL, Brenner RM (1984) Immunocytochemical localization of estrogen receptors in the macaque reproductive tract with monoclonal antiestrophilins. Endocrinology 114:2002–2014

McLachlan JA, Newbold RR, Bullock BC (1980) Long-term effects on the female mouse genital tract associated with prenatal exposure to diethylstilbestrol. Cancer Res 40:3988–3999

Mitchner NA, Garlick C, Ben-Jonathan N (1998) Cellular distribution and gene regulation of estrogen receptors α and β in the rat pituitary gland. Endocrinology 139:3976–3983

Mukdsi JH, De Paul AL, Munoz S, Aoki A, Torres AI (2004) Immunolocalization of Pit-1 in gonadotroph nuclei is indicative of the transdifferentiation of gonadotroph to lactotroph cells in prolactinomas induced by estrogen. Histochem Cell Biol 121:453–462

Nishihara E, Nagayama Y, Inoue S, Hiroi H, Muramatsu M, Yamashita S, Koji T (2000) Ontogenetic changes in the expression of estrogen receptor α and β in rat pituitary gland detected by immunohistochemistry. Endocrinology 141:615–620

Osborne CK, Zhao HH, Fuqua SAW (2000) Selective estrogen receptor modulators: structure, function, and clinical use. J Clin Oncol 18:3172–3186

Paech K, Webb P, Kuiper GG, Nilsson S, Gustafsson J-A, Kushner PJ, Scanlan TS (1997) Differential ligand activation of estrogen receptors ERα and ERβ at AP1 sites. Science 277:1508–1510

Pelletier G, El-Alfy M (2000) Immunocytochemical localization of estrogen receptors alpha and beta in the human reproductive organs. J Clin Endocrinol Metab 85:4835–4840

Petterson K, Grandien K, Kuiper GG, Gustafsson JA (1997) Mouse estrogen receptor β forms estrogen response element-binding heterodimers with estrogen receptor α. Mol Endocrinol 11:1486–1496

Schreihofer DA, Rowe DF, Rissman EF, Scordalakes EM, Gustafsson J-A, Shupnik MA (2002) Estrogen receptor-α (ERα), but not ERβ, modulates estrogen stimulation of the ERα-truncated varient, TERP-1. Endocrinology 143:4196–4202

Scully KM, Gleiberman AS, Lindzey J, Lubahn DB, Korach KS, Rosenfeld MG (1997) Role of estrogen receptor-α in the anterior pituitary gland. Mol Endocrinol 11:674–681

Senovilla L, Nunez L, de Campos JM, de Luis DA, Romero E, Sanchez A, Garcia-Sancho J, Villalobos C (2004) Multifunctional cells in human pituitary adenomas: implications for paradoxical secretion and tumorigenesis. J Clin Endocrinol Metab 89:4545–4552

Shupnik MA, Rosenzweig BA (1991) Identification of an estrogen-responsive element in the rat LHβ gene. J Biol Chem 266:17084–17091

Tsurusaki T, Aoki D, Kanetake H, Inoue S, Muramatsu M, Hishikawa Y, Koji T (2003) Zone-dependent expression of estrogen receptors α and β in human benign prostatic hyperplasia. J Clin Endocrinol Metab 88:1333–1340

Vidal S, Román A, Oliveria MC, De La Cruz L, Moya L (1998) Simultaneous localization of Pit-1 protein and gonadotropins on the same cell type in the anterior pituitary glands of the rat. Histochem Cell Biol 110:183–188

Wada O, Okubo A, Nagata N, Yazaki Y (1996) Clinical management of laboratory data in medical practice, vol. 2, 1st edn. Bunkodo, Tokyo, pp 486–487

Walker BE, Kurth LA (1993) Pituitary tumors in mice exposed prenatally to diethylstilbestrol. Cancer Res 53:1546–1549